



TECHNISCHE UNIVERSITÄT MÜNCHEN

TUM School of Medicine and Health

Exploring the Role of ALDH1A3 in RSL3-triggered Ferroptosis in Glioblastoma

Yang Wu

Vollständiger Abdruck der von der TUM School of Medicine and Health der Technischen Universität München zur Erlangung eines

Doctor of Philosophy (Ph.D.)

genehmigten Dissertation.

Vorsitz: Prof. Dr. Thomas Korn

Betreuer: Prof. Dr. Jürgen Schlegel

Prüfende der Dissertation:

1. Priv.-Doz. Dr. Friederike Liesche-Starnecker
2. Prof. Dr. Friederike Schmidt-Graf

Die Dissertation wurde am 27.03.2024 bei der TUM School of Medicine and Health der Technischen Universität München eingereicht und durch die TUM School of Medicine and Health am 04.06.2024 angenommen.

Abstract

Glioblastoma is the deadliest brain tumor. It arises within the brain and spreads rapidly, exhibiting its invasive behavior. Glioblastomas are highly heterogeneous, which rises significant challenges for therapy efficiency. Until now, glioblastoma remains difficult to treat and has a poor prognosis. Ferroptosis is defined as a regulated cell death triggered by radical oxygen species (ROS) accretion and the progress of lipid peroxidation. Different research groups explored ferroptosis as a potential therapeutic strategy in cancer treatment, aiming to breed the selective death of cancer cells undergoing aberrant metabolism. The present study demonstrated that RSL3-induced lipid peroxidation and the subsequent initiation of ferroptosis exhibit differential responses in malignant glioma cell lines, with some being sensitive and others resistant to RSL3-induced ferroptosis. Intriguingly, this sensitivity to RSL3 correlates significantly with ALDH1a3 expression levels. Inhibiting ALDH1a3 activity by chemical inhibition and gene Knock-out confers protection to glioblastoma against RSL3-triggered ferroptotic cell death. Further investigations into the underlying mechanisms revealed that ALDH1a3 contributes to ferroptosis by facilitating the essential release of iron through ferritinophagy. Furthermore, in an experiment to investigate the response of TMZ-resistant cells to the ferroptosis inducer RSL3, LN229 clones resistant to TMZ also exhibited resistance to ferroptosis induction, despite the evident lipid peroxidation triggered by RSL3. Further exploration revealed that the ALDH1A3 gene was downregulated in TMZ-resistant LN229 cells. Most intriguingly, only those clones that up-regulated ALDH1A3 expression following TMZ withdrawal displayed re-sensitization to ferroptosis induction. In addition, ALDH1A3 expression appeared to be associated by the EGFR-dependent PI3K pathway activation. Akt phosphorylation was notably observed exclusively in ALDH1A3-high expressing clones. The blockade of the EGFR signaling pathway over

EGFR inhibitor AG1478 led to a reduction in ALDH1A3 expression. Together, these findings demonstrate a potential new therapy target for glioblastoma treatment.

Table of Content

Summary.....	4
Zusammenfassung	6
Publications:.....	8
Introduction.....	9
Glioblastoma	9
Ferroptosis	14
EGFR Pathway	18
Autophagy.....	21
Acetaldehyde dehydrogenase.....	23
Objective.....	27
Materials and Method	29
Results and Discussion	37
1 RSL3 trigger the induction of Ferroptosis in glioblastoma.....	38
2 Glioblastoma cells presenting high-ALDH1A3 expression are sensitive to Ferroptosis.....	39
3 Autophagy supports ferroptosis in glioblastoma and is influenced by the expression of ALDH1a3	41
4 TMZ induced lipid droplets formation and peroxidation in glioblastoma.....	42
5 TMZ-resistant cells exhibit resistance to the ferroptosis inducer RSL3, resulted from the suppression of ALDH1A3.	43
6 EGFR pathway is suppressed under TMZ long-term treatment and associated with ALDH1A3 expression.	45
7 Could RSL3 treatment and ALDH1A3-targetting be new therapy strategies in glioblastoma?.....	46
Conclusion	47
Abbreviations:	49
Acknowledgement.....	53
Reference:	54
Appendix:	61

Summary

Glioblastoma: The deadliest form of brain tumor, glioblastoma, is classified by the World Health Organization (WHO) as IDH-wildtype-only adult-type diffuse gliomas, molecularly characterized by TERT mutation, chromosome 7/10 deletion, and EGFR abnormality. Despite various approaches, therapies for glioblastoma remain limited.

The primary treatments for glioblastoma involve maximal safe resection combined with radiotherapy and chemotherapy. Patients with poor performance status may receive hyperfractionated radiotherapy and adjuvant Temozolomide (TMZ), or TMZ alone.

Treatment resistance is a significant obstacle in glioblastoma management, and two key mechanisms contribute to this issue: the methylation of MGMT promoter and the existence of Glioblastoma stem cells. DNA repair enzyme MGMT can reverse the DNA damage induced by TMZ, causing resistance. Patients with MGMT promoter methylation respond better to TMZ therapy due to reduced MGMT activity. Glioblastoma Stem Cells (GSCs) are resilient, possessing enhanced DNA repair capabilities and oxidative stress tolerance, making them resistant to conventional therapies. These cells within the tumor are factors leading to therapy resistance and tumor recurrence.

Ferroptosis, as an iron-dependent regulated cell death related to the quantity of reactive oxygen species (ROS) and peroxidized lipid, has recently gained prominence as a possible therapeutic solution in glioblastoma. In glioblastoma, ferroptosis assumes a pivotal role in modulating oxidative stress and influencing responses to chemotherapy. Emerging evidence suggests that targeting ferroptosis holds considerable potential for increasing the potency of glioblastoma treatments. Recent researches have highlighted the susceptibility of Glioblastoma Stem Cells

(GSCs) to ferroptosis, shedding light on ferroptosis as a potential and novel therapeutic target to cure glioblastoma.

Overcoming these intricate mechanisms of resistance is paramount for effective glioblastoma therapy. Innovative approaches targeting these challenges directly hold the key to improving outcomes for this relentless disease. The urgency to address these issues underscores the importance of ongoing research and clinical trials in the quest for more effective treatments.

Within this thesis, I have encapsulated findings that I published previously as first author in two scientific papers (refer to the 'Publications' section, publication 1 and 2), and provided a more comprehensive background introduction and engaged in a deeper discussion. These studies delve into the role of ALDH1A3 in triggering ferroptosis in glioblastoma and predicting the sensitivity of ferroptosis-induced cell death in TMZ-resistant glioblastoma cell lines. Through these investigations, our aim is to unravel the hidden mechanisms contributing to therapy resistance and to unveil novel therapeutic avenues for glioblastoma.

Zusammenfassung

Die tödlichste Form von Hirntumoren, das Glioblastom, wird von der Weltgesundheitsorganisation (WHO) als IDH-wildtypische adulte diffuse Gliome klassifiziert, molekular charakterisiert durch TERT-Mutation, Deletion der Chromosomen 7/10 und Auffälligkeiten im EGFR. Trotz verschiedener Ansätze bleiben Therapien für das Glioblastom begrenzt.

Die Hauptbehandlungen für das Glioblastom umfassen maximale sichere Resektion in Kombination mit Strahlentherapie und Chemotherapie. Patienten mit schlechtem Allgemeinzustand können eine hyperfraktionierte Strahlentherapie und adjuvante Temozolomid (TMZ) oder nur TMZ erhalten.

Die Behandlungsresistenz ist ein erhebliches Hindernis in der Glioblastomtherapie, und zwei Hauptmechanismen tragen zu diesem Problem bei: die Methylierung des MGMT-Promotors und das Vorhandensein von Glioblastom-Stammzellen. Das DNA-Reparaturenzym MGMT kann die durch TMZ verursachten DNA-Schäden umkehren und somit zu Resistenz führen. Patienten mit MGMT-Promotormethylierung sprechen aufgrund reduzierter MGMT-Aktivität besser auf die TMZ-Therapie an. Glioblastom-Stammzellen (GSCs) sind widerstandsfähig, da sie verbesserte DNA-Reparaturfähigkeiten und Toleranz gegenüber oxidativem Stress besitzen und daher resistent gegenüber konventionellen Therapien sind. Diese Zellen im Tumor sind Faktoren, die zu Therapieresistenz und Tumorrezidiv führen.

Ferroptose, als eine eisenabhängige regulierte Zelltodform im Zusammenhang mit der Menge an reaktiven Sauerstoffspezies (ROS) und peroxidierter Lipide, hat in letzter Zeit als mögliche therapeutische Lösung für das Glioblastom an Bedeutung gewonnen. In Glioblastomen nimmt die Ferroptose eine Schlüsselrolle bei der Modulation von oxidativem Stress und der Beeinflussung von Reaktionen auf die Chemotherapie ein. Neue Erkenntnisse legen nahe, dass die gezielte Bekämpfung der Ferroptose

erhebliches Potenzial hat, die Wirksamkeit von Glioblastom-Behandlungen zu erhöhen. Aktuelle Forschungen haben die Anfälligkeit von Glioblastom-Stammzellen (GSCs) für die Ferroptose hervorgehoben und somit die Ferroptose als potenzielles und neuartiges therapeutisches Ziel zur Heilung des Glioblastoms ins Licht gerückt.

Die Überwindung dieser komplexen Resistenzmechanismen ist entscheidend für eine effektive Glioblastomtherapie. Innovative Ansätze, die diese Herausforderungen direkt angehen, sind der Schlüssel zur Verbesserung der Ergebnisse bei dieser unerbittlichen Krankheit. Die Dringlichkeit, diese Probleme anzugehen, unterstreicht die Bedeutung laufender Forschung und klinischer Studien auf der Suche nach wirksameren Behandlungen.

In dieser Arbeit habe ich Erkenntnisse zusammengefasst, die ich zuvor als Erstautor in zwei wissenschaftlichen Arbeiten veröffentlicht habe (siehe Abschnitt 'Veröffentlichungen', Veröffentlichung 1 und 2), und eine umfassendere Hintergrundinformation geboten sowie eine tiefere Diskussion geführt. Diese Studien untersuchen die Rolle von ALDH1A3 bei der Auslösung von Ferroptose im Glioblastom und prognostizieren die Empfindlichkeit gegenüber durch Ferroptose induziertem Zelltod in TMZ-resistenten Glioblastom-Zelllinien. Durch diese Untersuchungen möchten wir die verborgenen Mechanismen, die zur Therapieresistenz beitragen, aufdecken und neue therapeutische Wege für das Glioblastom enthüllen.

Publications:

1. **Yang Wu**, Helena Kram, Jens Gempt, Friederike Liesche-Starnecker, Wei Wu and Jürgen Schlegel. **ALDH1-Mediated Autophagy Sensitizes Glioblastoma Cells to Ferroptosis.** *Cells* 2022. <https://doi.org/10.3390/cells11244015>.
2. **Yang Wu**, Sophie Franzmeier, Friederike Liesche-Starnecker, Jürgen Schlegel. **Enhanced Sensitivity to ALDH1A3-dependent Ferroptosis in TMZ-Resistant Glioblastoma Cells.** *Cells* 2023. <https://doi.org/10.3390/cells12212522>
3. Kram Helena, Prokop Georg, Haller Bernhard, Gempt Jens, **Wu Yang**, Schmidt-Graf Friederike, Schlegel Jürgen, Conrad Marcus, Liesche-Starnecker Friederike. **Glioblastoma Relapses Show Increased Markers of Vulnerability to Ferroptosis.** *Front. Oncol.*, 21 April 2022. Volume 12 – 2022. <https://doi.org/10.3389/fonc.2022.841418>.
4. Wei Wu, **Yang Wu**, Karoline Mayer, Charlotte von Rosenstiel, Johannes Schecker, Sandra Baur, Sylvia Würstle, Friederike Liesche-Starnecker, Jens Gempt, Jürgen Schlegel, **Lipid Peroxidation Plays an Important Role in Chemotherapeutic Effects of Temozolomide and the Development of Therapy Resistance in Human Glioblastoma,** *Translational Oncology*, Volume 13, Issue 3, 2020, 100748, ISSN 1936-5233. <https://doi.org/10.1016/j.tranon.2020.100748>.
5. Wei Wu, Jessica L. Klockow, Michael Zhang, Famyrah Lafortune, Edwin Chang, Linchun Jin, **Yang Wu**, Heike E. Daldrup-Link, **Glioblastoma multiforme (GBM): An overview of current therapies and mechanisms of resistance,** *Pharmacological Research*, Volume 171, 2021, 105780, ISSN 1043-6618, <https://doi.org/10.1016/j.phrs.2021.105780>.

Introduction

Glioblastoma

Glial cells

Glial cells or neuroglia, which are non-neuronal cells, found in both the central nervous system (CNS) and the peripheral nervous system (PNS). Glial cells are not able to provoke electrical impulses, but play essential roles in supporting and protecting of neurons. In the central nervous system, glial cells encompass various types such as oligodendrocytes, astrocytes, ependymal cells, and microglia, while in the peripheral nervous system, they consist of Schwann cells and satellite cells (1).

Glia possesses the ability to undergo cell division even in adulthood, a feature that sets them apart from terminally differentiated neurons, which generally lose this capacity. This distinction is rooted in the limited ability of the mature nervous system to replace neurons following injuries like strokes or trauma, often resulting in a significant proliferation of glial cells near or at the damaged site (2).

Glioblastoma

Glioma, as a sort of primary brain tumors, originates from glial cells. Gliomas have traditionally been classified based on their histological appearance into astrocytic, oligodendroglia, or ependymal tumors. Based on the 2021 WHO classification, glioblastoma (GBM) is categorized as a diffuse astrocytic glioma without mutations in IDH or histone H3 genes. It is distinguished by distinctive features including microvascular proliferation, necrosis, and specific molecular markers such as TERT promoter mutations, EGFR amplification, and alterations in chromosomes +7/-10(3).

Glioblastomas are identified by their histological features, showcasing a prevalence of highly atypical glial cells characterized by abnormal shapes, sizes, and nuclei, along with heightened mitotic activity. Necrosis is frequently observed in the central region of the tumor. In addition to histological diagnosis, molecular characteristics serve as another crucial marker for diagnosis. Telomerase Reverse Transcriptase (TERT) encodes the telomerase enzyme, takes a leading role in synthesizing the absent 3' end of a DNA strand during replication. Mutations in the promoter of TERT gene lead to elevated the activity of telomerase and the continuation of telomeres. TERT mutations can be found in around 80% of glioblastoma cases (4). Epidermal Growth Factor Receptor (EGFR) pathway is a demanding signaling cascade governing cell growth, proliferation, and survival (5). Dysregulation of EGFR pathway, often through EGFR amplification, mutation, or other genetic alterations, is crucial in the formation and spread of glioblastomas. These tumors represent a complex interplay of genetic changes, with EGFR abnormalities present in a substantial percentage of cases. Understanding the intricacies of the EGFR pathway and its impact on GBM provides valuable insights for potential therapeutic interventions and underscores its central role in the genetic landscape of these aggressive brain tumors.

Therapeutic methods in glioblastoma

Surgery

Gross total resection (GTR) is the guiding principle for glioblastoma surgery, often followed by radiotherapy and chemotherapy. GTR improves survival outcomes and may increase progression-free survival (PFS) when using fluorescence-guided 5-ALA during surgery. GTR is also considered for recurrent cases, as it can improve the patient's quality of life. However, performing GTR, with or without guidance, requires specialized equipment,

and the uptake of fluorescence varies among patients. Often, technical and brain-functional issues limit the extent of tumor removal (6).

Radiotherapy

Conventional radiotherapy post-surgery delivers 60 Gy in 2-Gy fractions over 6 weeks, combined with temozolomide. Radiotherapy provides benefit over supportive care alone. However, patients in poor condition or advanced age may derive limited benefit from conventional radiotherapy. Hypo fractionated radiotherapy, involving lower doses over a shorter timeframe, yields similar outcomes (7).

Chemotherapy

Alkylating agent temozolomide (TMZ) is a major part of glioblastoma standard chemotherapy. Alkylating agents are a class of highly reactive compounds with potent chemical properties, categorized as anticancer compounds and alternatively referred to bio-alkylating agents. These agents have the ability to create carbon cations or other extremely reactive electrophilic groups within the body. These compounds then form covalent bonds with electron-rich moieties (amino, thiol, hydroxyl, carboxyl, and phosphate groups) present in biological macromolecules within cells, such as DNA, RNA and enzymes. This binding results to DNA strand breakage, ultimately causing the death of tumor cells (8).

Standard chemotherapy involves 6 cycles of TMZ (150-200 mg/m² on days 1-5 every 28 days), preceded by daily TMZ at 75 mg/m² during radiotherapy. TMZ, an alkylating agent, induces DNA damage in cancer cells. Methylation status of the O-6-methylguanine-DNA methyltransferase (MGMT) promoter indicates TMZ treatment effectiveness, as MGMT repairs damaged DNA, leading to chemotherapy resistance (9). Additionally, TMZ resistance and tumor relapse can occur due to mechanisms unrelated to MGMT, such as the presence of glioblastoma

stem cells (GSCs). Further discussion of chemotherapy resistance will be presented later.

Novel Therapies

Novel techniques inhibiting Poly (ADP ribose) polymerase (PARP), such as veliparib (10) and Olaparib (11) exert cytotoxic effects and synergize with TMZ, although they don't significantly improve progression-free survival (PFS). Protein kinase inhibitors, such as EGFR inhibitors Erlotinib (12) and Gefitinib (13), exhibit limited efficacy in glioblastoma patients, despite their significance in other cancer types. Immunotherapy treatments are being investigated in clinical trials, but current outcomes are not yet satisfactory (14).

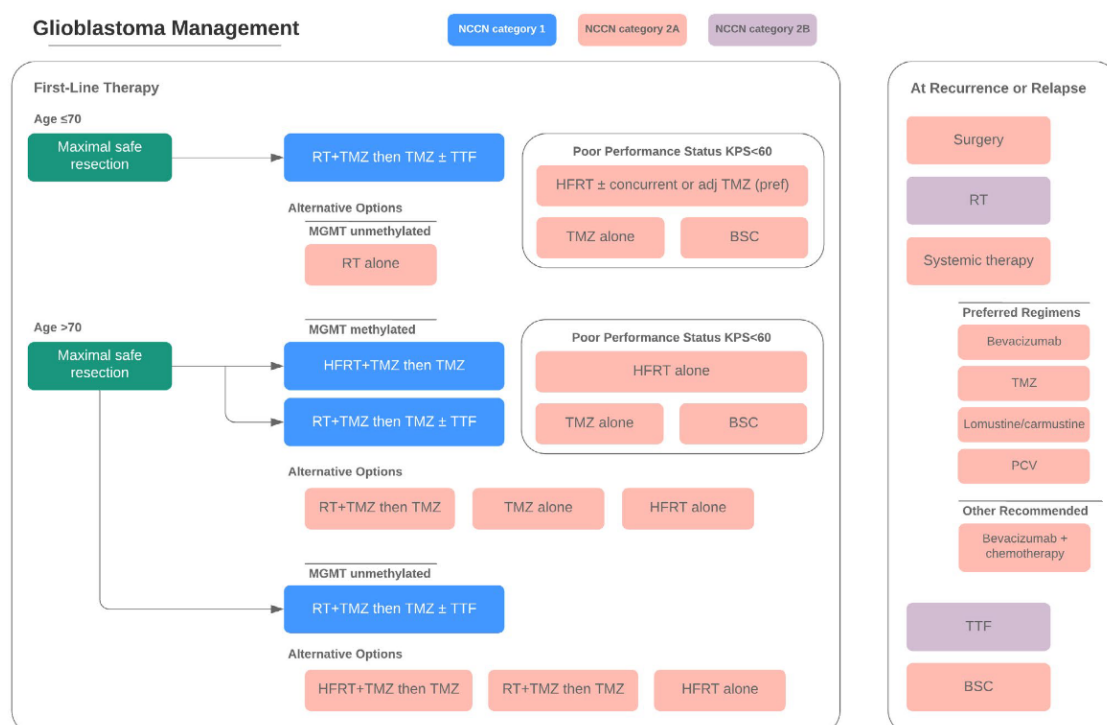


Figure 1. Treatment Algorithm for Glioblastoma. From Aaron C. Tan et al(15). The comprehensive approach to treating glioblastoma in patients involves a multi-step procedure. Following the confirmation of diagnosis, the focus is on achieving maximal safe tumor removal through surgical resection. Following is administering Temozolomide concurrently with radiation as maintenance therapy. TMZ treatment is exclusive in MGMT unmethylated patient. In relapse patient, surgery, radiotherapy and

standard TMZ treatment are still first line treatments. ± Indicates presence or absence; other abbreviations see section Abbreviation.

Chemotherapy resistance

One of the significant challenges in glioblastoma treatment is its tendency to recur despite the limited available therapies. Several crucial mechanisms underlie the development of treatment resistance, which further complicates the management of this aggressive brain tumor.

a) MGMT Status:

Temozolomide operates by transferring methyl groups onto DNA, using DNA damage and subsequently triggering cell death. A primary mechanism of resistance to Temozolomide treatment involves the DNA repair enzyme O-6-methylguanine-DNA methyltransferase (MGMT). This enzyme is accountable for repairing the alkylation damage induced by Temozolomide, ultimately leading to resistance against the treatment. Patients who were diagnosed with MGMT promoter methylation, however, tend to respond better to Temozolomide therapy due to the diminished activity of MGMT (9).

b) Glioblastoma Stem Cells (GSCs):

Glioblastoma stem cells (GSCs) are intricately linked to therapy resistance in glioblastoma and contribute to disease relapse (16). These cells possess the remarkable ability to differentiate into various cell types and have a high potential to serve as the seeds for tumor regrowth. Classical GSC biomarkers such as CD133 and ALDH1a3 identify these cells (17, 18). Cells expressing these biomarkers exhibit enhanced DNA repair capabilities and increased tolerance to oxidative stress. This intrinsic resilience contributes to their resistance against conventional therapies.

Ferroptosis

Ferroptosis, a lately characterized regulated cell death, is frequently conceptualized as a cell damage process influenced by iron imbalance and lipid over-peroxidation. Mitochondrial has been proved to plays an important role to activate ferroptosis. Treatments targeting mitochondrial drives Reactive oxygen species (ROS) generation, induces DNA stress, initiates lipid peroxidation and finally triggers ferroptosis.

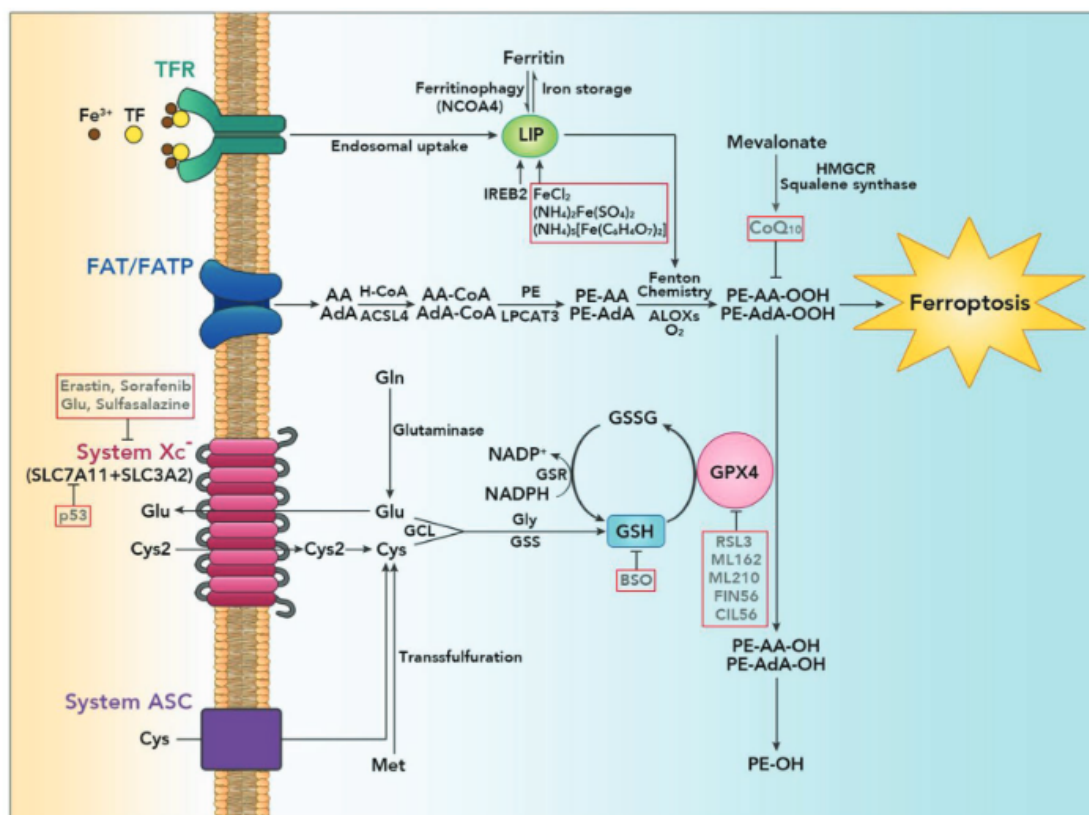


Figure 2. Ferroptosis regulatory mechanisms. From Chen Liang et al. (19) The labile iron pool (LIP) is central, sourced from transferrin receptor-mediated endocytosis or ferritinophagy. Increased LIP catalyzes Fenton-like reactions, inducing ferroptosis. Cysteine (Cys) and reduced glutathione (GSH) metabolism play pivotal roles. Cysteine uptake via system Xc⁻ initiates ferroptosis, while reducing conditions allow direct cysteine import. GSH, a key intracellular antioxidant, is synthesized from glutamate, cysteine, and glycine. Phosphatidylethanolamines (PEs) containing arachidonoyl (AA) or adrenoyl (AdA) moieties undergo oxidation, contributing to ferroptosis. The

mevalonate pathway, central in ferroptosis, generates anti-ferroptotic biomolecules. Glutathione peroxidase 4 (GPX4) is a pivotal regulator, transforming toxic PE-AA-OOH/PE-AdA-OOH into non-toxic alcohols. Oxidized GSH (GSSG) is reduced to GSH, crucial for combating lipid peroxidation. Representative ferroptosis inducers include ALOXs, BSO, CoQ10, Gln, HMGCR, IREB2, NCOA4, and TF.

Reactive Oxygen Species (ROS)

ROS is produced by various mechanisms, including the mitochondrial electron transport chain (ETC), the cell membrane-damaging effects of ionizing radiation, and as byproducts of cellular oxidation and reduction processes. ROS acts as a key regulator in orchestrating metabolic equilibrium, particularly in specific environments like hypoxia. Nonetheless, an excessive accumulation of ROS can lead to DNA damage and initiate the process of carcinogenesis. The build-up of ROS can be constrained through mechanisms such as the factor-erythroid 2-related factor 2 (Nrf2) pathway and the oxidation-reduction system involving glutathione (GSH) and glutathione disulfide (GSSG). As a major anti-oxidation pathway, redox stress inhibits ubiquitylation and degradation by Kelch-like ECH-associated protein 1 (KEAP1), consequently release nrf2 into nuclear and activate the transcript of down-stream genes for detoxification. An additional reduction system utilized to curtail ROS is the glutathione redox system. In its reduced state as GSH, glutathione serves as a robust antioxidant. By donating electrons, it effectively scavenges and neutralizes reactive oxygen species (ROS). As GSH furnishes electrons to counterbalance ROS, it undergoes oxidation and establishes a disulfide linkage with another GSH molecule. This transformation gives rise to glutathione disulfide (GSSG), recognized as the oxidized configuration of glutathione.

Glutathione peroxidase 4 (GPX4) has been recognized as a central enzyme tasked with catalyzing the reduction of GSSG to GSH, thereby mitigating lipid peroxidation. The manipulation of GPX4 using small molecules like RSL3 ((1S,3R)-RSL3) disrupts the glutathione redox system, culminating in the initiation of ferroptosis.

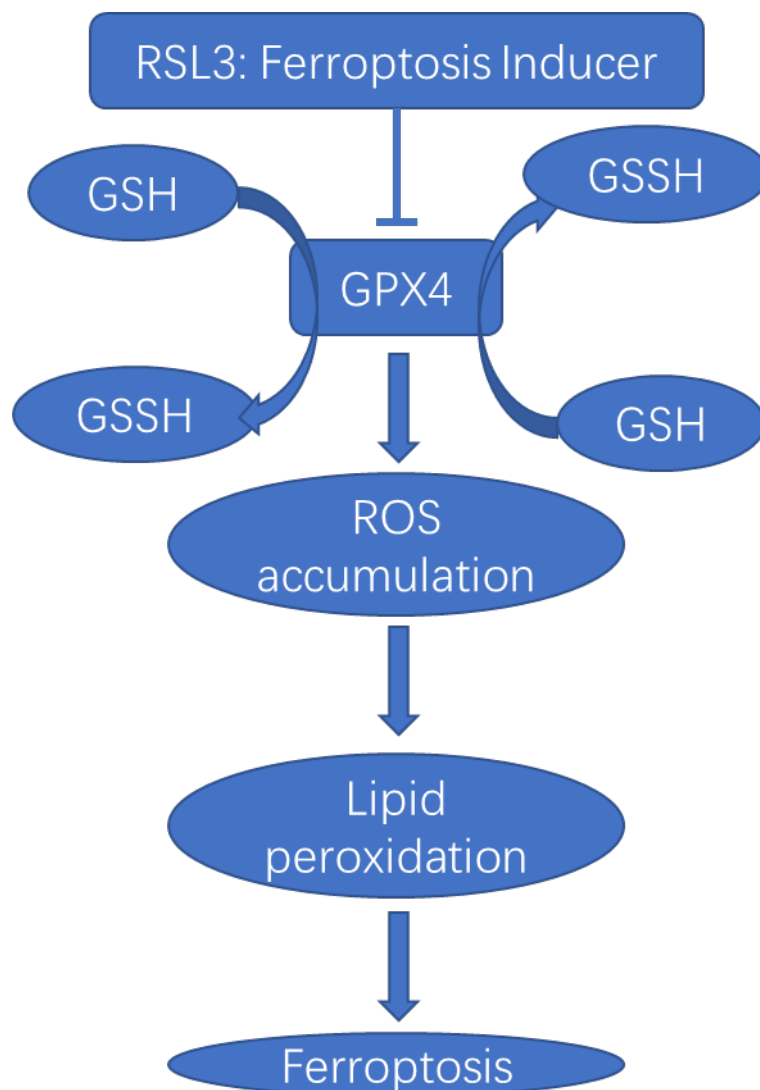


Figure 3. The mechanism of RSL3 inducing ferroptosis. RSL3 directly inhibit glutathione peroxidase 4 (GPX4). GPX4 reduce lipid hydroperoxides to their corresponding alcohols, thereby preventing the accumulation of oxidative damage to cell membranes. RSL3 disrupts the cellular antioxidant defense system by inhibiting GPX4, leading to lipid peroxide and increased susceptibility to ferroptosis. This process involves the accumulation of reactive oxygen species (ROS) and lipid

radicals, ultimately culminating in oxidative damage to cell membranes and subsequent cell death.

Lipid Peroxidation

After ROS accumulation, polyunsaturated fatty acids (PUFAs) in cellular membranes become affected to peroxidation. The process initiates when $\bullet\text{OH}$ radicals extract hydrogen atoms from PUFAs, forming PUFA radicals. This radical can further react with molecular oxygen to produce a lipid peroxy radical ($\text{LOO}\bullet$). The $\text{LOO}\bullet$ radical, in turn, can initiate a chain reaction by adding hydrogen atoms from neighboring PUFAs, leading to the formation of lipid hydroperoxides (LOOH). These hydroperoxides are unstable and can decompose into highly reactive and toxic aldehydes, such as malondialdehyde (MDA) and 4-hydroxynonenal (4-HNE), contributing to cellular damage (20, 21).

Iron in cellular and iron-storage protein Ferritin

Iron in cells primarily functions as an oxygen transporter within heme, essential for the proper functioning of enzymes involved in various vital cellular processes (22). Additionally, Iron ions involve in the Fenton reaction, resulting in the generation of superoxide radicals (23). This process can also disrupt pH balance and dysregulate ATP synthesis within cancer cells (24, 25).

Ferritin, an iron storage protein, significantly increased in glioblastoma patient (26). Fe(II) can be transported into cells through iron-transport proteins on the cellular membrane. Once inside, ferritin converts Fe(II) to Fe(III) and stores it within the ferritin mineral core. Proteasome mediate Ferritin degradation and subsequently release iron into cellular (27, 28).

EGFR Pathway

The Epidermal Growth Factor Receptor (EGFR) pathway, a pivotal cellular signaling cascade, involves cell growth, proliferation, and survival. The EGFR pathway is activated when epidermal growth factors (EGF) bind to EGFR on the cell surface and trigger receptor dimerization, subsequently phosphorylates specific tyrosine residues within the cytoplasmic domain, and recruit downstream signaling molecules. These molecules, often part of the PI3K-Akt and Ras-Raf-MAPK pathways, transmit the signal inward, leading to gene expression changes that influence various cellular processes (29). Dysregulation of the EGFR pathway, for example EGFR abnormal amplification, EGFR mutation, has been implicated in numerous diseases, particularly cancer, making it an important target for therapeutic interventions aimed at modulating cell behavior and combating disease progression. EGFR amplification emerges as a prevalent occurrence in glioblastomas (GBMs). Alongside amplification, there are instances of EGFR mutation, rearrangement, and modified splicing. Collectively, these diverse genetic alterations encompass a substantial 57% of GBM cases. This comprehensive spectrum of changes underscores the intricate role of EGFR in GBM and highlights its pervasive involvement in the genetic landscape of these tumors.

EGFR gene is situated at chromosome 7p12, and amplified in around 40% of glioblastoma patients (30). Epidermal Growth Factor Receptor wild-type (wtEGFR) holds significant importance as a mediator of tumor cell invasion distinct from angiogenesis, within in vivo experiments. Through the induction of heightened expression of EGFR variant III (EGFRvIII) in GBM cell lines, there is a consistent activation of receptor phosphorylation, resulting in heightened tumorigenic

characteristics. This is primarily achieved by fostering an accelerated rate of proliferation while concurrently diminishing the occurrence of apoptosis. The activation of EGFR induces PI3K-AKT and MAPK pathways, and intricately modulate cellular apoptosis and manipulate tumor survival. After EGFR is activated and phosphorylated, it attracts PI3K to the cell membrane, resulting in the phosphorylation of phosphatidylinositol 4,5-bisphosphate (PIP2) and the formation of phosphatidylinositol (3,4,5)-trisphosphate (PIP3). Subsequently, AKT binds to PIP3, getting phosphorylated at Threonine 308 at phosphoinositide-dependent protein kinase-1 (PDK1) and at Serine 473 at the mammalian target of rapamycin complex 2 (mTORC2), thereby reaching its complete functional potential. The phosphatase and tensin homolog (PTEN) negatively regulates the PI3K/AKT pathway by dephosphorylating PIP3, leading to its dislodgment from the cellular membrane (31). This prompts the re-localization of AKT into the cytoplasm, rendering it inactive and impeding the possibility of reactivation. MAPK initiates in the phosphorylation of Jun, a nuclear transcriptional factor. Jun associates with various nuclear proteins, giving rise to the pivotal transcription factor activator protein 1 (AP-1). This transcription factor holds the responsibility for orchestrating the translation and transcription of proteins that play a crucial role in cell proliferation and replication.

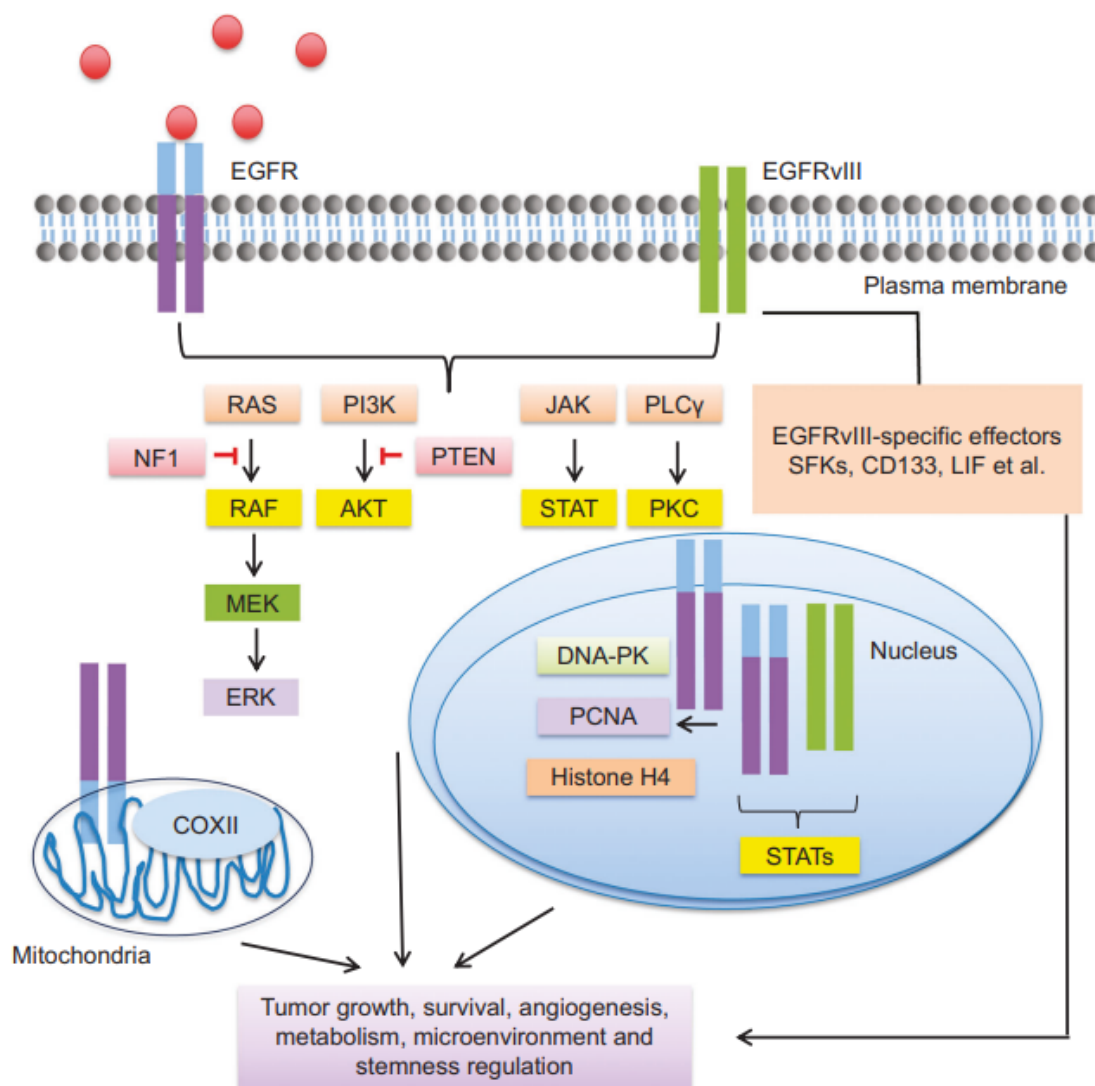


Figure 4. Signaling pathways mediated by EGFR/EGFRvIII. From An et al. (29).

Signaling pathways facilitated by EGFR/EGFRvIII are involved in transduce signals through classic receptor tyrosine kinase (RTK) pathways, the RAS/RAF/MEK/ERK pathway, the PI3K/AKT pathway, the JAK/STAT pathway, and the PKC pathway.

Autophagy

Autophagy is a cellular mechanism that degrades and recycles cellular damaged components (32). It's often referred to as "self-eating" because the cell digests its own components to maintain cellular homeostasis and adapt to different conditions. Autophagy is triggered in response to different stressors, for example nutrient deprivation, oxidative stress, or the accumulation of damaged cellular components. By recycling these components, the cell can generate energy and building blocks to adapt to the stress. During development, autophagy contributes to tissue remodeling and differentiation by eliminating redundant cells and cellular components, pivotal for shaping functional tissues. Moreover, autophagy also contributes to immune responses by assisting in the degradation of intracellular pathogens, such as bacteria or viruses.

Canonical autophagy pathway begins with the suppression of mammalian target of rapamycin 1 (mTOR) by the treatment of Rapamycin or nutrition deprivation, then activated autophagosome biosynthesis. After the initiation of autophagosome synthesis, UNC-51-like kinase 1 (ULK1) triggers the phosphorylation of the Beclin1 pathway in conjunction with autophagy-related genes (ATG), leading to the formation of the nucleation complex. The elongation of autophagosome membranes hinges on ubiquitin-like conjugation. Initially, ATG7 and ATG10 collaborate to link ATG12 with ATG5, and subsequently, the ATG12-ATG5 complex attaches membrane-bound ATG8 to phosphatidylethanolamine (PE), culminating in the transfer of microtubule-associated protein 1 light chain 3 (LC3). Consequently, the transition from LC3a to LC3b is recognized as a hallmark signifying the activation of autophagy.

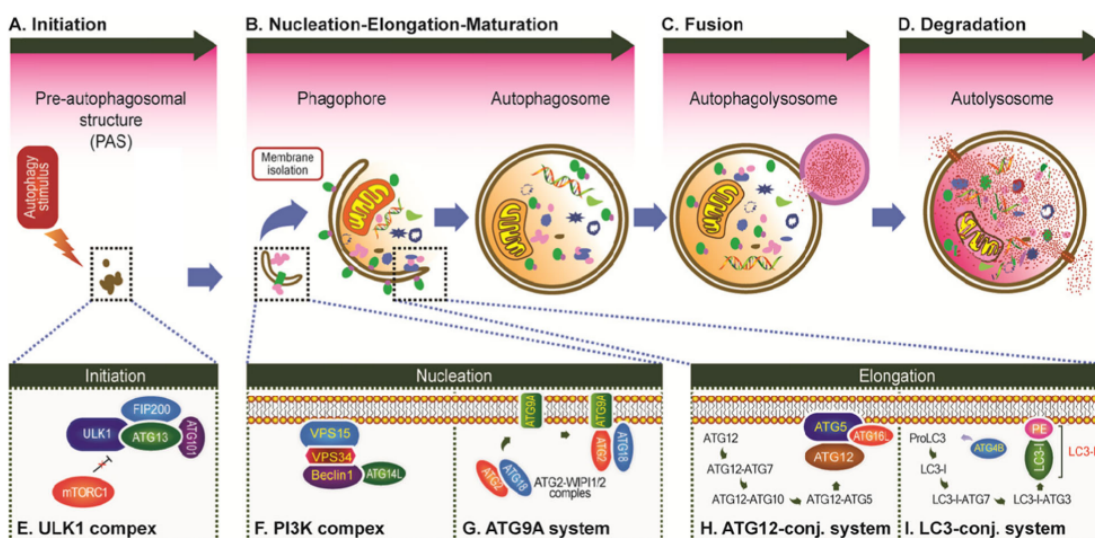


Figure 5. Schematic overview of autophagy. From Xiaohua Li, et al.(33). In the initiation phase (a), the ULK1 complex is activated, and various ATG proteins are engaged and accumulated to the pre-autophagosome structure (PAS). Following this, in the nucleation phase (b), ATG proteins and lipids assembled to form the phagophore, which then undergoes elongation. During elongation, the phagophore envelops cytoplasmic components and organelles. The maturation phase (b) involves the completion and transport of the autophagosome. Subsequently, in the fusion phase (c), autophagosome and lysosome blend together. In the degradation phase (d), the cargos within the autolysosome undergo degradation.

Autophagy involves in various aspects of cancer cells. Autophagy survives cancer cells by providing recycled metabolites essential for growth. It also exerts influence on mitochondrial function through mitophagy, and recent discoveries highlight its impact on tumor cell migration and invasion. This impact is achieved by regulating focal adhesion turnover and facilitating the secretion of cytokines that promote cell migration. Recently, autophagy has been proved to assist cancer stem cells (CSCs) to survive and preserve stemness. The most pertinent focus within this dissertation on autophagy centers around the activation of autophagy react to oxidative stress. Oxidative stress, which has been proved to induce autophagy in contexts such as starvation and

ischemia/reperfusion scenarios. When confronted with oxidative stress, which produced by reactive oxygen species (ROS), encompassing free radicals such as superoxide, hydroxyl radicals, and hydrogen peroxide, increases significantly, causing to cellular damage and eventual cell death. Research indicated that the oxidative stress involved in the activation of the extracellular signal-regulated kinase 1/2 (ERK1/2) pathway (34). Inhibiting the ERK1/2 pathway led to suppression of autophagy and induction of apoptosis (35). In turn, suppression of autophagy decreased mitochondrial superoxide levels and protected cells from death by preventing the translocation of Apoptosis Inducing Factor (AIF) from mitochondria to nuclei (36). To sum up, oxidative stress triggers autophagy activation, and in turn, autophagy moderates oxidative stress while influencing the regulation of cell death.

Recently, emerging research focus on the crosstalk between autophagy and ferroptosis. The ferroptosis inducer RSL3 activate autophagy in glioma depending on dosages, and RSL3 induced cell death could be reversed by inhibiting autophagy (37). Autophagy mediated ferroptosis is named ferritinophagy (38). Activated ferroptosis leads to the induction of autophagy, resulting in the subsequent degradation of ferritin, an iron storage protein, and the ferritinophagy cargo receptor NCOA4 (39, 40). Furthermore, one of the critical steps in ferroptosis, ROS accumulation, depends on the activation of autophagy (38).

Acetaldehyde dehydrogenase

The Acetaldehyde dehydrogenase (ALDH) superfamily comprises enzymes responsible for metabolizing aldehydes in the human body. The human ALDH family contains 19 members: ALDH1s (1A1, 1A2, 1A3, 1B1, 1L1, and 1L2), ALDH2, ALDH3s (3A1, 3A2, 3B1, and 3B2), ALDH4A1,

ALDH5A1, ALDH6A1, ALDH7A1, ALDH8A1, ALDH9A1, ALDH16A1, and ALDH18A1 (41). ALDH superfamily mainly participate in embryo development, body growth, cell proliferation and differentiation. ALDH1A family of enzymes plays a central role in retinoic acid (RA) synthesis (42). The process involves two oxidative steps: Retinol Oxidation: Retinol is oxidized into retinaldehyde (retinal) by enzymes such as retinol dehydrogenases. Retinaldehyde Oxidation: retinaldehyde is further oxidized into RA by the ALDH1A family, which includes ALDH1A1, ALDH1A2, and ALDH1A3. RA acts on various cellular processes, such as regulating genes expression, cell development and differentiation (43). Additionally, the expression of ALDHs is highly correlated with progenitor cells, for example cord blood cells and bone marrow (44, 45). For these reasons, ALDH family, especially ALDH1As, are considered as a stem cells marker. ALDHs facilitate the conversion of aldehydes into their respective carboxylic acids through oxidation, using NADP⁺ (Nicotinamide adenine dinucleotide phosphate) as a cofactor (46). This enzymatic reaction converts toxic aldehydes into less harmful carboxylic acids, which can be readily metabolized or excreted by the body. By detoxifying aldehydes, ALDHs play a crucial role in maintaining cellular health and resisting cellular damage induced by ROS (47). Aldehydes can induce the generation of ROS, which potentially inducing oxidative stress and other forms of cellular damage, including DNA damage and lipid peroxidation (48). Dysfunction or deficiency of ALDH enzymes can lead to the accumulation of toxic aldehydes, which has been implicated in various diseases, including alcohol-related liver damage and neurodegenerative disorders (49, 50).

ALDH in cancers

ALDH1 has emerged as a recognized marker for cancer stem cells (CSCs) across various cancers and has been associated with unfavorable

prognoses (51, 52). Moreover, the presence of ALDH1-positive (ALDH+) cell populations has demonstrated implications in the context of chemotherapy and radiotherapy resistance in specific cancer types (53, 54). For instance, in breast cancer stem cells, ALDH+ cells contribute to radiotherapy resistance by modulating the Nrf2-KEAP1 axis (55). Inhibiting ALDH in ovarian cancer stem cells improve cell death with chemotherapy (54). In summary, the prevalence of ALDH+ cells are closely intertwined with the realm of CSCs, reflecting their significance in cancer biology and therapy outcomes. ALDHs play an important role in glioma and should not be underestimated. ALDH1A1 exhibited frequent overexpression in high-grade glioma patients, and tumor cells expressing ALDH1A1 were found to be more concentrated in the border of tumor, indicative of potentially heightened invasiveness (51). This overexpression of ALDH1A1 was significantly linked to poor differentiation and an unfavorable prognosis. ALDH inhibitors gossypol and phenformin combined decrease invasiveness, cell viability and stemness in glioblastoma (56). In glioblastoma, it is ALDH1A3, rather than ALDH1A1, that serves as the primary functional acetaldehyde dehydrogenase, and playing a significant role in contributing to resistance against temozolomide (TMZ) treatment (18). Through whole-genome transcriptome microarray and mRNA sequencing analysis, it was distinctly observed that ALDH1A3 exhibited heightened expression in the Mesenchymal subtype of gliomas. Notably, the targeted suppression of ALDH1A3 expression resulted in a notable reduction in glioma invasion (57, 58).

ALDH1A3

ALDH1A3, a member of the ALDH superfamily, has garnered attention due to its high expression and related to poor-outcome in various cancers (59-61). ALDH1A3 overexpression closely related to tumor progression and therapy resistance (53, 62, 63), making it a potent

therapeutic target. In glioma and glioblastoma, ALDH1A3 strongly associates with mesenchymal phenotype maintenance (57, 64-66) and cell invasion. Within the realm of CSC markers, ALDH1A3 has come to the forefront in GBM. The role of ALDH1A3 in GBM extends beyond its enzymatic function. ALDH1A3 confers resistance to apoptosis and enhances DNA repair mechanisms, rendering GBM cells resilient to chemotherapy and radiotherapy (18, 67, 68). Furthermore, ALDH1A3-mediated metabolic reprogramming supports the high energy demands of proliferating cancer cells, ensuring their survival in the hostile tumor microenvironment (69). Genetic mutations or alterations in these transcriptional regulators can dysregulate ALDH1A3 expression, contributing to the aberrant stemness observed in cancer cells. Cell signaling pathways, such as the NF κ B pathway, can upregulate ALDH1A3 expression at the transcriptional level (70). Epigenetic modifications, including DNA methylation and histone acetylation, intricately modulate ALDH1A3 expression (71, 72). ALDH1A3 might undergo post-transcriptional regulation, potentially through mechanisms such as protein ubiquitination and microRNA-mediated silencing (67, 73).

Objective

Glioblastoma stands out as the most significant challenges in oncology due to its high fatality rates, limited therapeutic options, and bleak prognoses. Among the primary modalities for glioblastoma treatment, chemotherapy, particularly Temozolomide (TMZ), faces pervasive resistance across the patient population. Growing research suggest that ALDH1A3 plays a crucial part in bestowing resistance to TMZ, along with its impact on the autophagic pathway. Recent studies have emphasized a potential role of ALDH1A3 in detoxifying aldehydes produced by TMZ in glioblastoma and is associated with ROS metabolism. For this reason, ferroptosis activation appears to be a promising novel therapeutic strategy in the context of glioblastoma.

Therefore, the primary goal of this thesis was to explore the role of ALDH1A3 in glioblastoma and to seek out innovative therapeutic approaches aimed at inducing ferroptosis in glioblastoma to overcome therapy resistance.

This thesis aimed to address:

- a) Inducing ferroptosis in glioblastoma cell lines by RSL3 treatment.
- b) Discovering the mechanism underlying RSL3-triggered ferroptosis in glioblastoma.
- c) Investigating the efficacy of RSL3 in TMZ-resistance glioblastoma cell lines.

Experimental Procedure:

To investigate the objective of this thesis, the following experiments have been done:

- a) Established proper glioblastoma cell lines (Patient-derived glioblastoma cell lines, TMZ lone term treated cell lines)
- b) Investigated the Lipid peroxidative state and cell viability after RSL3 treatment.
- c) Investigated the RSL3-induced cell death in ALDH1A3 wildtype, Knock-out and over-expression cell lines.
- d) Discovered the mechanism of ALDH1A3 sensitizing glioblastoma to RSL3 treatment by immunoprecipitation assay and autophagy markers read-out.

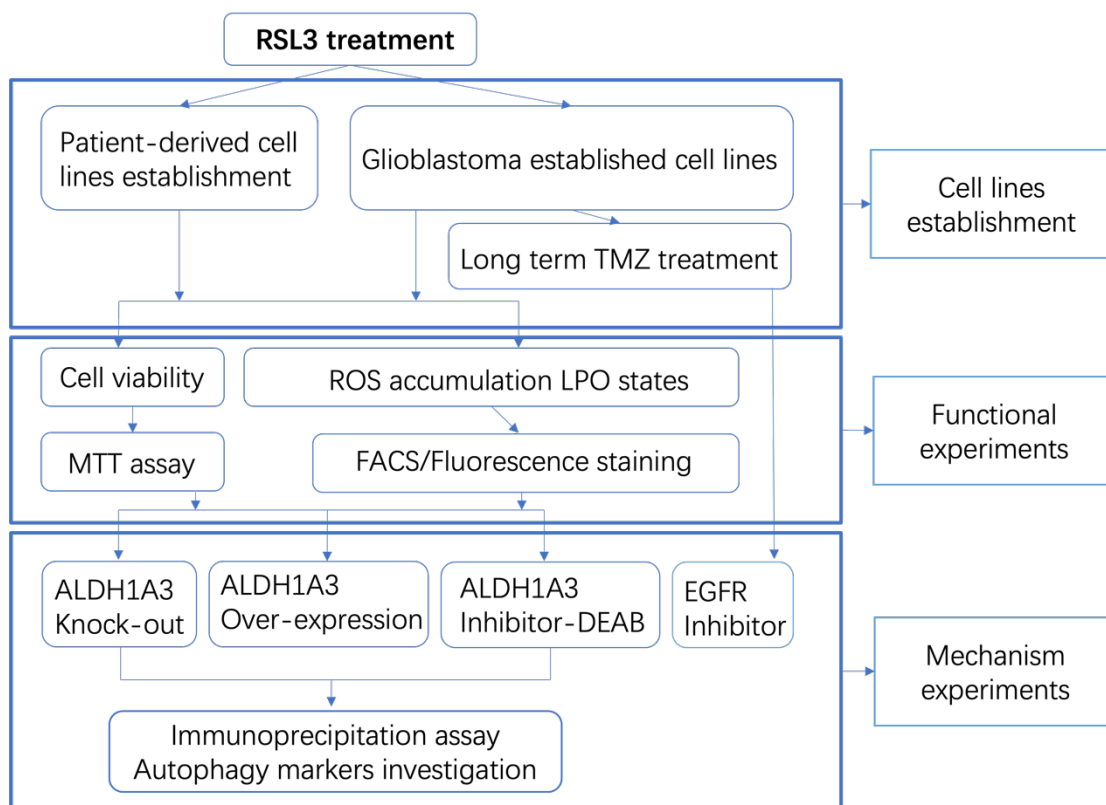


Figure 6. Flowchart of Experimental Procedures.

Materials and Method

1. Glioblastoma primary cell lines

Glioblastoma specimens were sourced from the Neurosurgery Department at Klinikum rechts der Isar, Technical University of Munich, following the acquisition of informed consent from participating patients. The ethical clearance for the collection and utilization of patient-derived tumor samples was granted by the regional ethics committee. Tissue specimens underwent washing in PBS (use 1% Penicillin-Streptomycin for bacteria elimination) and were subsequently dissected into fragments using surgical blades. These tissue fragments were subjected to a 30-minute incubation with 5ml Papain (with 500ul DNase) to facilitate the isolation of single cells or cell groups. The digestive process was arrested by the addition of 5ml Ovocuid (with 500ul DNase) for 5 minutes. Isolated cells were centrifuged to collected and subsequently cultured in primary cell culture medium, with specific samples designated as PDCL#9 (female, 86 years), PDCL#13 (male, 67 years), and PDCL#17 (female, 63 years).

Table 1. Primary Cell Culture Medium Recepte.

Product	Volume
RPMI-1640 (Gibco, Dreieich, Germany)	500ml
B27 (Gibco, Dreieich, Germany)	10ml
N2 Supplement (Gibco, Dreieich, Germany)	5ml
Nonessential amino acids (Gibco, Dreieich, Germany)	5ml
L-glutamine (Gibco, Dreieich, Germany)	10ml
Fibroblast growth factor 2 (Peprotech, Hamburg, Germany)	10 µg
Transforming growth factor beta 2 (Peprotech, Hamburg, Germany)	150ng
Epidermal growth factor (Peprotech, Hamburg, Germany)	1 µg

2. Cell viability assays

LN229, U87MG, and T98G cells were plated in 96-well plates at a density of 5000 cells per well. After a 24-hour incubation, various concentrations of treatments were applied, while control cells were exposed to 0.5% DMSO alone. Cell viability was determined using the 3-(4,5-dimethylthiazol-2-yl)-2,5-diphenyltetrazolium bromide (MTT) assay, in accordance with the guidelines provided by the manufacturer (Sigma, Munich, Germany). Absorbance measurements were taken using an Infinite F200 pro Microplate Absorbance Reader (Tecan, Maennedorf, Switzerland).

3. LDH release assay

Cell death detection encompassed the quantification of lactate dehydrogenase (LDH) release, a widely employed marker for cellular damage and cytotoxicity. This assessment was conducted utilizing the Cytotoxicity Detection (LDH) Kit (Roche #11644793001, Darmstadt, Germany), adhering closely to the guidelines outlined by the manufacturer. The method involved the measurement of absorbance at the wavelength of 490nm, a key parameter indicating LDH activity. This analysis was carried out using an advanced Infinite F200 pro Microplate Absorbance Reader, which ensured accurate and reliable readings for a comprehensive evaluation of cellular responses to various treatments or experimental conditions.

4. Lipid peroxidation assays

Cells were plated on cover slides and treated 24 hours before conducting lipid peroxidation assays. After treatment, cells were stained with BODIPY® 581/591 C11-Reagent (Thermo Fisher, Bremen, Germany) for

30 minutes and then washed with PBS. Subsequently, cells were either fixed with 30% PFA for fluorescence imaging or trypsinized into single cells for fluorescence-activated cell sorting (FACS). Fluorescence images were captured using a Zeiss fluorescence microscope (Zeiss, Munich, Germany) and analyzed with Image J software (National Institutes of Health, Bethesda, MD, USA). FACS parameters were configured based on the guidance provided with the BODIPY® 581/591 C11-Reagent kit, and each experimental group included 20,000 cells analyzed through the flow cytometer. Compensation settings were adjusted as follows: FL1-0.8%FL2; FL2-29.8%FL1; FL2-0.0%FL3; FL3-19.3%FL2; FL3-0.0%FL4; FL4-16.4%FL3. Fluorescence images for FACS were captured using a Zeiss LSM780 fluorescence microscope (Zeiss, Munich, Germany) and analyzed with Image J software (National Institutes of Health, Bethesda, MD, USA). FACS results were further analyzed using FlowJo software (FlowJo Inc., OH, USA).

5. Immunoprecipitation assay

LN229 and T98G glioblastoma cell lines were subjected to treatment and harvested after 24 hours in lysis buffer. A 30µg protein aliquot was extracted from each cell lysate as the input sample. For immunoprecipitation, antibodies were individually added to the lysates (each containing 30µg protein) and incubated overnight at 4°C. Subsequently, 2mg protein-G-Sepharose beads were introduced into each immunoprecipitation sample and incubated for 3 hours at 4°C. Following thorough washing, Sepharose beads were collected, diluted with SDS sample buffer, and heated at 100°C for 5 minutes. Both the input sample and immunoprecipitation samples underwent fractionation through 10% SDS-page gels and were subsequently analyzed by western blotting using anti-LC3b (NB100-2220, Novus Bio, Munich, Germany).

6. Sphere formation assay

Cells are cultured in non-adherent conditions, typically in serum-free medium supplemented with growth factors and other necessary nutrients. The non-adherent environment prevents cells from attaching to the surface and promotes the formation of three-dimensional structures known as spheres or spheroids. Spheres are typically quantified by counting the number of spheres formed or measuring the size of the spheres. Pictures were taken after 7 days by Nikon microscopy (Melville, NY, America).

7. ALDH1a3 stable transfection

The ALDH1a3 plasmid was sourced from OriGENE (MG222097). In a concise process, PDCL#9 cells, initially lacking ALDH1a3 expression, underwent transfection with the ALDH1a3 plasmid using Lipofectamine 2000 (Invitrogen, Carlsbad, CA, USA). Following a 48-hour incubation, clones overexpressing ALDH1a3 were selectively established through a two-week treatment with G418 (Merck, Germany, Munich, 50mg/mL in H₂O).

Table 2. Technical devices

Device	Model	Producer
CO ₂ Incubator	HERAcells 150i	Thermo Fisher Scientific Inc, Waltham, MA, USA
Centrifuge	5417R	Eppendorf AG, Hamburg, Germany
Flow cytometer	FACS Calibur™	Becton Dickinson, Heidelberg, Germany
Heater mixer	53355	Eppendorf AG, Hamburg, Germany

Spectrophotometer	NanoDrop 2000c	Thermo Fisher Scientific Inc, Waltham, MA, USA
-------------------	----------------	---

Table 3. Chemicals and reagents

Substance	Catalogue	Producer
Diamidino-phenylindole (DAPI)	D1306	ThermoFisher, Karlsruhe, Germany
Dimethylsulfoxide (DMSO)	A994.2	Carl Roth GmbH, Karlsruhe, Germany
Lipofectamine™ 2000	L200008	ThermoFisher, Karlsruhe, Germany
Page Ruler	26619	ThermoFisher, Karlsruhe, Germany
Protease Phosphatase Inhibitor Cocktail	5872	CST, Frankfurt am Main, Germany
Protein G sepharose	10246735	GE Healthcare, Munich, Germany
Thiazolyblue (MTT)	4022.1	Roth, Karlsruhe, Germany

Table 3. Software

Software	Producer
Adobe	Adobe Systems incorporated, San Jose, CA, USA
Axiovision Rel	Carl Zeiss Microscopy, LLC, NY, USA
FlowJo	Tree Star, Inc., Ashland, OR, USA
GraphPad Prism	GraphPad Software, La Jolla, CA, USA
NIS Elements	Nikon Instruments Inc, Melville, NY, USA

8. Cells migration assay

After a 24-hour serum-free incubation, three thousand cells were cultured and subsequently seeded onto a transwell chamber. The transwell chamber was placed in a 24-well plate for an additional 24 hours. Following this incubation period, the cells on the lower side of the chamber were stained with crystal violet to facilitate the visualization and quantification of cell attachment and migration. For each transwell chamber, five photographs were captured, each focusing on different areas of the cells on the bottom side.

9. Oil Red O staining assay

Oil Red O stain (1320-06-5, Sigma, Munich, Germany) was prepared 10 minutes prior to experiments. Cells were seeded into a 6-well plate for 24 hours, cleaned with PBS and 100% isopropanol and subjected to Oil Red staining for 1 minute, followed by washing with 60% isopropanol for 15 seconds. Images were captured using a Nikon microscope (Melville, NY, USA).

10. RNA isolation and Rt-PCR assay

RNA extraction was carried out using Trizol Reagent (15596026, Thermofisher, USA, MA) and chloroform, followed by purification with isopropanol and ethanol precipitation. The resultant purified RNA was then eluted in nuclease-free water. For the RT-PCR assay, total RNA isolated from LN229 parental and TMZ-resistant cell lines served as the starting material. Reverse transcription was conducted using the Takara reverse transcription kit (RR037B, Takara, Saint-Germain-en-Laye, France).

Amplification and data analysis were performed using the Zytomed instrument.

Table 5. Primers sequences

Primer	Sequence
ALDH1A3 forward	CACCTTCCAC-GGCCCCGTTAGCGG
ALDH1A3 reverse	AAACCCGCTAACGGGGCCGTGGAA
B-actin forward	GAGCTACGAGCTGCCTGACG
B-actin reverse	GTAGTTTCGTGGATGCCACAGGAC

11. Western blotting

Cells were lysed in RIPA buffer containing phosphatase inhibitors (5 mM sodium orthovanadate), and the resulting protein lysates were subjected to separation through a 10% SDS-PAGE gel, followed by transfer onto a PVDF membrane. After blocking with 5% BSA, the membrane was incubated with primary antibodies overnight at 4 °C. Subsequently, the membrane underwent three 5-minute washes in Tris-buffered saline containing 1% Tween-20 (TBST). Following the washes, the membrane was exposed to peroxidase-conjugated goat anti-rabbit IgG (7074P2, CST, Leiden, Germany) and visualized using the Super ECL detection reagent.

Table 6. Antibodies.

Antibody	Resource	Specie
Anti-ALDH1A3	ab129815, Berlin, Germany	Rabbit
Anti-p-AKT	Cell Signaling Technology, #4060	Rabbit
Anti-AKT	Cell Signaling Technology, 5112s	Rabbit
Vinculin	abcam, ab129002	Rabbit

12. Colony formation assay

LN229 glioblastoma cells were plated in 10cm dishes at a sparse density of 500 cells per well and allowed to incubate for 14 days. After this incubation period, cells were gently washed with phosphate-buffered saline (PBS) and fixed with 4% paraformaldehyde for 15 minutes at room temperature. Following fixation, the cells underwent staining with a crystal violet solution (0.5% crystal violet in 20% methanol) for 10 minutes. Excess stain was meticulously washed off with distilled water, and the plates were left to air-dry. Capturing the visual representation of the cells was achieved using a smartphone equipped with a lens of 26mm and a pixel pitch of 1.7 μ m.

Results and Discussion

Glioblastoma stands out as one of the worldwide most fatal cancers, characterized by its limited treatment options and exceptionally short survival rates. Given the challenging landscape related with glioblastoma, there is an urgent requirement for novel therapeutic approaches. Temozolomide stands as the primary pharmaceutical intervention employed in the treatment of glioblastoma within the framework of standard care. Nonetheless, the emergence of resistance to Temozolomide is a pervasive phenomenon, manifesting in nearly all cases. Therefore, research groups are actively exploring novel strategies, with a strong emphasis on inducing ferroptosis—a newly characterized form of programmed cell death—within glioblastoma cells. This pursuit target not only unlock new avenues for therapeutic intervention but also to enhance the effectiveness of combination treatments alongside conventional therapeutic modalities.

As an increasing body of research elucidates ferroptosis in the context of disease and therapeutic responses, it has solidified its position as a promising novel treatment approach within the realm of glioblastoma. Distinguished by the buildup of reactive oxygen species (ROS) and peroxidized lipid, ferroptosis is critical in the oxidative stress response within glioblastoma. The GPX4 inhibitor RSL3 disrupts the glutathione redox system, thereby triggering the initiation of ferroptosis. RSL3 activates the NF- κ B pathway, results to the downregulation of GPX4, ATF4, and SLC7A11 expression in glioblastoma cells. This downregulation ultimately induces cell death through ferroptosis (74). Additional evidence supports the notion that RSL3 treatment triggers autophagic cell death via the disruption of glycolysis function (37). Nonetheless,

there remain additional mechanisms and regulatory pathways yet to be unveiled and fully comprehended.

Temozolomide (TMZ) treatment exhibits multifaceted connections with ferroptosis in glioblastoma. In the study performed by Song et al., it was demonstrated that temozolomide (TMZ) activates ferroptosis through Nrf2/HO1 pathway, and the process of ferroptosis induced by TMZ treatment was reversed upon blocking DMT1, a pivotal gene within the Nrf2/HO1 pathway (75). Activation of TRIM25, which involved in the Nrf2 pathway, releases cells from ferroptotic cell death, and resulting in TMZ resistance (76). Suppressing autophagy activates ferroptosis, enhancing the susceptibility of glioblastoma stem cells to chemo-treatment (77).

Our earlier findings suggest that one of the underlying mechanisms of TMZ resistance in glioblastoma is linked to the detoxification role of ALDH1A3 (78). Moreover, TMZ triggers autophagy and down-regulates the expression of ALDH1A3. Existing evidence supports the notion that ALDH1A3 might, in turn, regulate autophagy processes.

1 RSL3 trigger the induction of Ferroptosis in glioblastoma.

To investigate the impact of RSL3-triggered cell death in glioblastoma, cell viability assays were conducted on seven glioblastoma cell lines, consisting of four established cell lines and three primary cell lines. Four cell lines (T98G, PDCL#9, PDCL#13, and X01) exhibited resistance to RSL3, where a high dose of RSL3 (6.4 μM) resulted in approximately 50% cell death. Conversely, three RSL3-sensitive cell lines (LN229, U87, and PDCL#17) displayed susceptibility to RSL3-induced cell death, with a median dose of RSL3 ranging from 0.8 to 1.6 μM leading to approximately

50% cell death. In all the tested cell lines, RSL3-induced cell death was reversible by the treatment with both a ferroptosis inhibitor, Ferrostatin, and an iron chelator, DFO. Additionally, BODIPY staining was employed to assess lipid peroxidation levels, which were found to increase following RSL3 treatment in the tested cell lines. Notably, this elevation in lipid peroxidation was effectively reversed when cells were treated with Ferrostatin and DFO. This suggests that the observed cell death in glioblastoma triggered by RSL3 was linked to ferroptosis, a process that involves lipid peroxidation and is able to be prevented by inhibiting ferroptosis or removing excess iron with DFO.

The GPX4 inhibitor RSL3 acts by disrupting the glutathione redox system and thereby inducing ferroptosis across various cancer types. In a study by Sui et al., RSL3 was found to trigger ferroptosis by inhibiting GPX4 and generating reactive oxygen species (ROS) in colorectal cancer (79). Yang et al. further elucidated an additional function of RSL3, which involves the suppression of the Nrf2 pathway in KRAS-deficient colorectal cancer (80). Shintoku et al. conducted research demonstrating that RSL3 induces ferroptosis through the peroxidation activity of lipoxygenases (81). Treatment with RSL3 was shown to activate the NF- κ B pathway, inducing ferroptosis in glioma (74). Furthermore, RSL3 treatment induces autophagic cell death by disrupting glycolysis function (37).

2 Glioblastoma cells presenting high-ALDH1A3 expression are sensitive to Ferroptosis.

In the present study, the four RSL3-resistant cell lines exhibited low expression levels of ALDH1a3, whereas the three sensitive cell lines displayed high levels of ALDH1a3. To further validate this correlation, ALDH1a3 knockout cell lines were generated in both LN229 and T98G cell

lines, and subsequent treatment with RSL3 uncovered a significant variation in RSL3 sensitivity between the ALDH1a3 knockout and wildtype cell lines. Furthermore, it was observed that lipid peroxidation induced by RSL3 was effectively reversed by the application of an ALDH1 inhibitor, DEAB. To delve deeper into this phenomenon, experiments were conducted using over-expressed ALDH1a3 in the PDCL#9 cell line. The over-expression of ALDH1a3 led to a significant increase of sensitivity to RSL3 in the ALDH1a3 over-expressing cell line. This heightened sensitivity could once again be reversed by treatment with a combination of DEAB.

In our previous studies conducted by our research group, it was established that ALDH1a3 serves as a key mechanism for the resistance of TMZ, likely owing to its role in detoxifying aldehydes (78). Furthermore, our previous research demonstrated high-level expression of ALDH1a3 in glioblastoma relapse patient samples through immunohistochemistry analysis (82). These observations suggested that ALDH1a3 is essential in glioblastoma therapy resistance. However, the expression of ALDH1a3 is indeed correlated with ferroptosis sensitivity, and this relationship appears to be attributed to the enzymatic function of ALDH1a3, as have been shown in DEAB treatment experiments. These results suggest that targeting ALDH1a3 may have multifaceted implications in cancer therapy, impacting both drug resistance and ferroptosis-related pathways.

ALDH1a3 is commonly considered as a marker of glioblastoma stem cells. Therefore, tumor cells expressing high level of ALDH1a3 could be considered as cancer stem cells (CSCs). Recently, there has been a growing body of research focused on inducing ferroptosis in cancer stem cells. Iron transport proteins have been shown to be upregulated in CSCs (83), and there is accumulating evidence suggesting that CSCs exhibit a high demand for antioxidants (84). So far have not been addressed the role of ALDH1a3 in inducing ferroptosis, it is plausible that the enzymatic function of ALDH1a3 serves as the connecting link between glioblastoma

stem cells and their sensitivity to ferroptosis. Another plausible mechanism involves ALDH1a3's potential role in modulating the autophagic process, which will be discussed in the subsequent section.

3 Autophagy supports ferroptosis in glioblastoma and is influenced by the expression of ALDH1a3

Ferritinophagy, a type of autophagy-mediated ferroptosis, initiates with the degradation of the iron storage protein, ferritin(40). In the present findings, the induction of cell death by RSL3 could be reversed with Bafilomycin A1, a well-known autophagy inhibitor. This observation suggests that autophagy involved in the ferroptosis process. The inhibition of ROS accumulation further supports and confirms these results. Moreover, in ALDH1a3 wildtype cell lines, RSL3 treatment led to the LC3a to LC3b transversion, an autophagy marker, whereas this conversion did not occur in knockout cell lines. This observation suggests that the activation of autophagy is dependent on the expression of ALDH1a3. To further evaluate how ALDH1a3 is involved in autophagy, an immunoprecipitation assays has been done in LN229 and T98G ALDH1a3 wildtype cell lines. Under normal conditions and following RSL3 treatment, the ALDH1a3 antibody primarily captured LC3a and showed slight affinity for LC3b. However, when treated with a combination of DEAB, the ALDH1a3 antibody lost its capacity to bind to LC3a. While this result does not provide a comprehensive explanation of the mechanism by how ALDH1a3 modulates autophagy, it does indicate that the enzymatic function of ALDH1a3 is associated with the autophagy process.

As a downstream effect of autophagy, ferritin degradation occurred following RSL3 treatment in ALDH1a3 wildtype cell lines. Notably, both the inhibition of ALDH1 by DEAB and the knockout of ALDH1a3 were able to

reverse the expression of ferritin. These results strongly suggest that the consequence of ALDH1a3's modulation of autophagy is ferritin degradation and the potential release of iron.

In the previous research findings of our group, coexistence between ALDH1a3 and p62 under conditions of oxidative stress were identified (18). This finding is corroborated by the result of the present study that ALDH1a3 regulates autophagy. Interestingly, another member of the ALDH1 family, ALDH1a1, has been found to enhance the cytotoxicity of hydroxychloroquine and influenced autophagy flux in cancer cell lines by regulating helicase like transcription factor (HLTF) (85). Furthermore, the expression of ALDH1 correlated closely to LC3b expression in pancreatic cells, which further suggests the potential involvement of the ALDH1 family in the autophagy process (86). While these findings are not sufficient to conclusively demonstrate that ALDH1a3 directly regulates autophagy, there is a strong likelihood that ALDH1a3, a marker for GSCs, is involved in the autophagy process and can potentially trigger ferroptosis.

4 TMZ induced lipid droplets formation and peroxidation in glioblastoma.

The present findings discovered that cell lines resistant to TMZ displayed a substantial accumulation of LDs, and these LDs persisted even after the cessation of TMZ treatment. Furthermore, we noted an exacerbation in the state of lipid peroxidation following TMZ treatment. These cumulative results paint a vivid picture of glioblastoma cells undergoing a profound metabolic reprogramming in response to the stress imposed by TMZ treatment. The intricate relationship between LDs and GBM cells, particularly in the context of TMZ resistance, provides an insight for understanding the dynamics of this tumor type. While LDs initially

emerge as promising targets for ferroptosis induction, their role in buffering against oxidative stress signifies the adaptability and resilience of tumor cells.

In GBM, the presence of lipid droplets (LDs) has been strongly associated to the prognosis and treatment outcomes. Research conducted by Feng Gend et al. (15) demonstrated that LDs are highly accumulated in GBM cells, but not in normal brain tissue or low-grade gliomas. GBM cells have been observed to employ LDs as reservoirs for excess fatty acids and cholesterol, serving as a protective shield against lipotoxicity and endoplasmic reticulum (ER) stress. It has been established that LDs tend to accumulate in response to oxidative stress (16). This interesting finding implies that treatment with temozolomide (TMZ), a chemotherapy agent, induces the formation of LDs within GBM cells, making them potential targets for ferroptosis induction using RSL3.

5 TMZ-resistant cells exhibit resistance to the ferroptosis inducer RSL3, resulted from the suppression of ALDH1A3.

Considering prolonged TMZ treatment, one might expect TMZ-resistant cell lines to exhibit heightened sensitivity to ferroptosis inducers RSL3 for the reason of the accumulation of lipid peroxidation over time. However, contrary to this expectation, the present results revealed that TMZ-resistant cell lines exhibited a surprising tolerance to RSL3 treatment, which is designed to trigger ferroptosis. This paradox prompted a closer examination of the underlying mechanisms. Furthermore, these results unveiled a noteworthy observation related to ALDH1A3 expression. Following TMZ treatment, we observed a significant down-regulation of ALDH1A3, a phenomenon that aligns with the findings of Wu's results from our group (87). Wu's study reported a suppression of ALDH1A3 expression

during a 5-day TMZ treatment, followed by a rebound to higher levels after TMZ withdrawal. In this thesis, a consistent pattern emerges, wherein the suppression of ALDH1A3 expression is observed following TMZ treatment. Two out of five TMZ-resistant cell lines exhibit a significant recovery of ALDH1A3 expression within one month of TMZ withdrawal. Elevated ALDH1A3 expression levels are also identified in cases of relapsed glioblastoma. These findings suggest a dependency of ALDH1A3 recovery on the duration of TMZ withdrawal. During prolonged TMZ exposure, a drastic reduction in cell numbers occurs, leading to the survival of TMZ-resistant clones through selective single-cell-like proliferation. The intrinsic heterogeneity within glioblastoma cells becomes a critical consideration in this context, as it profoundly influences experimental reproducibility and result interpretation. Therefore, acknowledging the existence of heterogeneity is imperative when drawing conclusions from the present findings.

These collective findings indicate that TMZ treatment exerts a suppressive effect on ALDH1A3 expression. Building upon the first published paper, which established a close relationship between ALDH1A3 expression and the sensitivity of RSL3, the expression levels of ALDH1A3 are potentially linked to the responsiveness to RSL3-induced ferroptosis. Remarkably, after TMZ withdrawal, the two cell lines that exhibited ALDH1A3 expression recovery also demonstrated heightened sensitivity to RSL3. These observations reinforce the hypothesis that the expression of ALDH1A3 plays a pivotal role in modulating the sensitivity to RSL3-induced ferroptosis.

6 EGFR pathway is suppressed under TMZ long-term treatment and associated with ALDH1A3 expression.

In this research, a suppression of EGFR pathway after long-term TMZ treatment in LN229 cells has been discovered, and a corresponding suppression of cell proliferation could be found accordingly. The EGFR pathway demonstrates aberrant activation in approximately 40% of glioblastoma patients, correlating with poor prognosis and tumor invasion (88). In a study conducted by Inaba et al., it was found that the inhibition of the EGFR pathway resulted in a slowdown of cell proliferation and did not augment sensitivity to TMZ treatment (89). According to the findings of Gong et al., EGFR deficiency appears to be a factor in glioblastoma's resistance to chemotherapy (90). These studies support the present findings, suggesting that the EGFR pathway may indeed be suppressed in TMZ-resistant cell lines. Moreover, Inhibition of EGFR using AG1498 decreases ALDH1A3 expression in wild-type LN229 and two ALDH1A3 recovered TMZ-resistance cell lines. This regulation appears to be associated with transcriptional control, as suggested by the RT-PCR results. Although existing research has not definitively established a direct regulatory link between the EGFR pathway and ALDH1A3 expression, several indicators suggest a relationship between EGFR pathway activity and the regulation of ALDH1. In high-grade ovarian carcinoma and triple negative breast cancer, the positive expression of ALDH1 is correlated with the up-regulated EGFR pathway (91, 92). These researches further indicate a correlation between EGFR pathway activation and high expression of ALDH1A3. To delve deeper into the regulation of ALDH1A3 by EGFR, extensive research needs to be conducted.

7 Could RSL3 treatment and ALDH1A3-targetting be new therapy strategies in glioblastoma?

My study delves into the intricate relationship between TMZ treatment, ALDH1A3 expression, and ferroptosis sensitivity in glioblastoma. While TMZ resistance might suggest increased susceptibility to ferroptosis due to lipid peroxidation, the observed tolerance to RSL3 in TMZ-resistant cell lines warrants further investigation. The dynamic regulation of ALDH1A3 expression in response to TMZ, coupled with its impact on ferroptosis, adds complexity to glioblastoma therapy resistance.

The previous findings from my first publication indicate that ALDH1A3-positive cells are sensitive to RSL3 (93), and the results from our research group showed relapsed glioblastoma cells often overexpress ALDH1A3 (82). Targeting ALDH1A3-positive glioblastoma with RSL3 emerges as a potential therapeutic approach. However, it's crucial to note that while our results provide valuable *in vitro* insights, comprehensive understanding of the underlying mechanisms is lacking. Moreover, RSL3 application is confined to *in vitro* studies, necessitating the development of effective *in vivo* delivery methods. In addition, the underlying mechanisms between lipid droplets formation under TMZ treatment, lipid re-programming and ALDH1A3 regulation are still under discovering. These findings underscore the need for ongoing research to unravel glioblastoma treatment resistance intricacies and identify therapeutic strategies.

In summary, targeting ALDH1A3-positive cells with RSL3 shows promise, but extensive research and development efforts are required for its clinical application.

Conclusion

In conclusion, this thesis is dedicated to glioblastoma therapy resistance, with a primary focus on the role of ALDH1A3 and the potential of ferroptosis as a novel treatment strategy. Through a series of experiments and analyses, it has shed light on several critical findings that may have implications in the field of glioblastoma research and treatment.

My investigations have unveiled the role of ALDH1A3, a key member of the ALDH enzyme superfamily, in the induction of ferroptosis within glioblastoma. The inhibition or genetic knockout of ALDH1A3 has been demonstrated to enhance the tolerance of glioblastoma cells to RSL3 treatment. Further mechanistic studies have illuminated ALDH1A3's involvement in autophagy and its contribution to ferritin degradation. These findings suggest that the increased sensitivity of ALDH1A3-positive cells to RSL3 treatment may result from its intricate involvement in autophagy processes, particularly the degradation of ferritin. The downregulation of ALDH1A3 following TMZ exposure and its subsequent rebound in expression upon TMZ withdrawal signify a dynamic regulatory mechanism that may contribute to further ferroptosis induction therapy in glioblastoma. Additionally, my research has uncovered a connection between the EGFR pathway and the expression of ALDH1A3 in glioblastoma, further unveiling the mechanism of ALDH1A3 regulation. This link suggests that targeting ALDH1A3 could enhance ferroptosis-based treatments for glioblastoma.

In summary, my study has deepened our understanding of how glioblastoma becomes resistant to therapy. Identifying ALDH1A3 as a key player in this resistance, its relation to ferroptosis sensitivity, and the way EGFR

pathway influences its expression offer valuable insights. These findings might lead to innovative treatments for glioblastoma. While challenges remain, the potential of targeting ALDH1A3 and utilizing ferroptosis offers hope for improving the prognosis and outcomes of glioblastoma patients. This research marks a step in overcoming the challenges posed by this aggressive brain tumor and brings hope for a better future in glioblastoma therapy.

Abbreviations:

AA	arachidonoyl
ACSL4	acyl-CoA synthetase long-chain family member 4
AdA	adrenoyl
adj	adjuvant
AKT	Protein kinase B (also known as PKB)
ALOXs	arachidonate lipoxygenases
ALOXs	arachidonate lipoxygenases
ASC	alanine/serine/cysteine transporter
ATG	Autophagy-related proteins
ATG10	Autophagy-related protein 10
ATG12	Autophagy-related protein 12
ATG14L	Autophagy-related protein 14-like
ATG16L	Autophagy-related protein 16-like
ATG2	Autophagy-related protein 2
ATG4	Autophagy-related protein 4
ATG5	Autophagy-related protein 5
ATG7	Autophagy-related protein 7
ATG9A	Autophagy-related protein 9A
Beclin1	Beclin 1
BSC	best supportive care

BSO	buthionine sulfoximine
CAR	chimeric antigen receptor
CoQ10	coenzyme Q10
Cys	cysteine
DC	dendritic cell
EGFR	epidermal growth factor receptor
FAT	fatty acid translocase
FATP	fatty acid transport protein
Ferritinophagy	ferritin degradation
FGFR	fibroblast growth factor receptor
FIP200	FAK-family Interacting Protein of 200 kDa
GBM	Glioblastoma multiforme
GCL	glutamate-cysteine ligase
Gln	glutamine
Gly	glycine
GPX4	Glutathione peroxidase 4
GRB2	Growth factor receptor-bound protein 2
GSH	reduced glutathione
GSR	glutathione-disulfide reductase
GSS	glutathione synthetase
GSSG	oxidized glutathione
HFRT	hyperfractionated radiotherapy

HMGCR	3-hydroxy-3-methylglutaryl-CoA reductase
IREB2	iron-responsive element binding protein 2
KPS	Karnofsky performance status
LC3	Microtubule-associated proteins 1A/1B light chain 3
LC3-I	LC3 isoform I
LC3-II	LC3 isoform II
LIP	labile iron pool
LPCAT3	lysophosphatidylcholine acyltransferase 3
Met	methionine
mTOR	mammalian target of rapamycin
NADP+	nicotinamide adenine dinucleotide phosphate
NADPH	reduced nicotinamide adenine dinucleotide phosphate
NCCN	National Comprehensive Cancer Network
NCOA4	Nuclear receptor coactivator 4
PAS	Phagophore assembly site
PCV	procarbazine, lomustine, and vincristine regimen
PE	Phosphatidylethanolamine
PI3K	Phosphoinositide 3-kinase
PI3K	Phosphoinositide 3-kinase
PIP2	Phosphatidylinositol 4,5-Bisphosphate
PIP3	Phosphatidylinositol (3,4,5)-trisphosphate

pref	preferred
ProLC3	Pro-form of LC3
PTEN	Phosphatase and Tensin Homolog
RT	radiotherapy
System Xc-	cystine uptake system
TF	transferrin receptor
TFR	transferrin receptor
TMZ	temozolomide
TTF	tumor-treating fields
ULK1	Unc-51-like kinase 1

Acknowledgement

My doctoral journey was initially challenging, but it turned out to be a profoundly enriching experience. At the culmination of this academic journey, I would like to extend my heartfelt gratitude to my supervisor, prof. Juergen Schlegel. Thank you for your helpful discussions, feedback, and the time you spent guiding me. In addition to your academic guidance, I'm immensely thankful for the invaluable mental support you provided during those moments when I faced personal challenges and almost fell into depression. Your mentorship extended far beyond academia, and for that, I am truly grateful. It has been an honor to learn under your guidance, and I am deeply appreciative of the opportunity to work with such an exceptional mentor.

I would also like to extend my gratitude to Priv.-Doz. Dr. med. Friederike Liesche-Starnecker, Prof. Dr. Friederike Schmidt-Graf, and Dr. Claire Ertelt-Delbridge for their invaluable assistance and support during the course of my study. Their kindness and willingness to lend a helping hand have been truly appreciated. I would like to say thanks to our secretary Mrs. Claudia Walter for supporting me with the lab organization.

I am also very grateful to Dr. rer. nat. Laura Steingruber, Sophie Franzmeier, Dr. Yuxiang Zhou and Jia Rao, who were not only colleagues but also friends. Without your company, my doctoral journey would have been dulling and bleak. I would like to thank my friend zuoyufan Yin, and may he find eternal peace.

Finally, I would like to express my heartfelt gratitude to my parents and my husband for their unconditional support. I love you.

Reference:

1. Fields RD, Araque A, Johansen-Berg H, Lim SS, Lynch G, Nave KA, Nedergaard M, Perez R, Sejnowski T, Wake H. Glial biology in learning and cognition. *Neuroscientist*. 2014;20(5):426-431.
2. Buffo A, Rite I, Tripathi P, Lepier A, Colak D, Horn AP, Mori T, Gotz M. Origin and progeny of reactive gliosis: A source of multipotent cells in the injured brain. *Proc Natl Acad Sci U S A*. 2008;105(9):3581-3586.
3. Smith HL, Wadhvani N, Horbinski C. Major Features of the 2021 WHO Classification of CNS Tumors. *Neurotherapeutics*. 2022;19(6):1691-1704.
4. Killela PJ, Reitman ZJ, Jiao Y, Bettegowda C, Agrawal N, Diaz LA, Jr., Friedman AH, Friedman H, Gallia GL, Giovannella BC, Grollman AP, He TC, He Y, Hruban RH, Jallo GI, Mandahl N, Meeker AK, Mertens F, Netto GJ, Rasheed BA, Riggins GJ, Rosenquist TA, Schiffman M, Shih Ie M, Theodorescu D, Torbenson MS, Velculescu VE, Wang TL, Wentzensen N, Wood LD, Zhang M, McLendon RE, Bigner DD, Kinzler KW, Vogelstein B, Papadopoulos N, Yan H. TERT promoter mutations occur frequently in gliomas and a subset of tumors derived from cells with low rates of self-renewal. *Proc Natl Acad Sci U S A*. 2013;110(15):6021-6026.
5. Liu F, Hon GC, Villa GR, Turner KM, Ikegami S, Yang H, Ye Z, Li B, Kuan S, Lee AY, Zanca C, Wei B, Lucey G, Jenkins D, Zhang W, Barr CL, Furnari FB, Cloughesy TF, Yong WH, Gahman TC, Shiau AK, Cavenee WK, Ren B, Mischel PS. EGFR Mutation Promotes Glioblastoma through Epigenome and Transcription Factor Network Remodeling. *Mol Cell*. 2015;60(2):307-318.
6. Lara-Velazquez M, Al-Kharboosh R, Jeanneret S, Vazquez-Ramos C, Mahato D, Tavanaiepour D, Rahmathulla G, Quinones-Hinojosa A. Advances in Brain Tumor Surgery for Glioblastoma in Adults. *Brain Sci*. 2017;7(12).
7. Gzell C, Back M, Wheeler H, Bailey D, Foote M. Radiotherapy in Glioblastoma: the Past, the Present and the Future. *Clin Oncol (R Coll Radiol)*. 2017;29(1):15-25.
8. Fu D, Calvo JA, Samson LD. Balancing repair and tolerance of DNA damage caused by alkylating agents. *Nat Rev Cancer*. 2012;12(2):104-120.
9. Hegi ME, Diserens AC, Gorlia T, Hamou MF, de Tribolet N, Weller M, Kros JM, Hainfellner JA, Mason W, Mariani L, Bromberg JE, Hau P, Mirimanoff RO, Cairncross JG, Janzer RC, Stupp R. MGMT gene silencing and benefit from temozolomide in glioblastoma. *N Engl J Med*. 2005;352(10):997-1003.
10. Sim HW, McDonald KL, Lwin Z, Barnes EH, Rosenthal M, Foote MC, Koh ES, Back M, Wheeler H, Sulman EP, Buckland ME, Fisher L, Leonard R, Hall M, Ashley DM, Yip S, Simes J, Khasraw M. A randomized phase II trial of veliparib, radiotherapy, and temozolomide in patients with unmethylated MGMT glioblastoma: the VERTU study. *Neuro Oncol*. 2021;23(10):1736-1749.
11. Hanna C, Kurian KM, Williams K, Watts C, Jackson A, Carruthers R, Strathdee K, Cruickshank G, Dunn L, Erridge S, Godfrey L, Jefferies S, McBain C, Sleigh R, McCormick

- A, Pittman M, Halford S, Chalmers AJ. Pharmacokinetics, safety, and tolerability of olaparib and temozolomide for recurrent glioblastoma: results of the phase I OPARATIC trial. *Neuro Oncol.* 2020;22(12):1840-1850.
12. Prados MD, Chang SM, Butowski N, DeBoer R, Parvataneni R, Carliner H, Kabuubi P, Ayers-Ringler J, Rabbitt J, Page M, Fedoroff A, Sneed PK, Berger MS, McDermott MW, Parsa AT, Vandenberg S, James CD, Lamborn KR, Stokoe D, Haas-Kogan DA. Phase II study of erlotinib plus temozolomide during and after radiation therapy in patients with newly diagnosed glioblastoma multiforme or gliosarcoma. *J Clin Oncol.* 2009;27(4):579-584.
 13. Rich JN, Reardon DA, Peery T, Dowell JM, Quinn JA, Penne KL, Wikstrand CJ, Van Duyn LB, Dancy JE, McLendon RE, Kao JC, Stenzel TT, Ahmed Rasheed BK, Tourt-Uhlig SE, Herndon JE, 2nd, Vredenburgh JJ, Sampson JH, Friedman AH, Bigner DD, Friedman HS. Phase II trial of gefitinib in recurrent glioblastoma. *J Clin Oncol.* 2004;22(1):133-142.
 14. Lim M, Xia Y, Bettegowda C, Weller M. Current state of immunotherapy for glioblastoma. *Nat Rev Clin Oncol.* 2018;15(7):422-442.
 15. Tan AC, Ashley DM, Lopez GY, Malinzak M, Friedman HS, Khasraw M. Management of glioblastoma: State of the art and future directions. *CA Cancer J Clin.* 2020;70(4):299-312.
 16. Prager BC, Bhargava S, Mahadev V, Hubert CG, Rich JN. Glioblastoma Stem Cells: Driving Resilience through Chaos. *Trends Cancer.* 2020;6(3):223-235.
 17. Beier D, Hau P, Proescholdt M, Lohmeier A, Wischhusen J, Oefner PJ, Aigner L, Brawanski A, Bogdahn U, Beier CP. CD133(+) and CD133(-) glioblastoma-derived cancer stem cells show differential growth characteristics and molecular profiles. *Cancer Res.* 2007;67(9):4010-4015.
 18. Wu W, Schecker J, Wurstle S, Schneider F, Schonfelder M, Schlegel J. Aldehyde dehydrogenase 1A3 (ALDH1A3) is regulated by autophagy in human glioblastoma cells. *Cancer Lett.* 2018;417:112-123.
 19. Liang C, Zhang X, Yang M, Dong X. Recent Progress in Ferroptosis Inducers for Cancer Therapy. *Adv Mater.* 2019;31(51):e1904197.
 20. Yang WS, Kim KJ, Gaschler MM, Patel M, Shchepinov MS, Stockwell BR. Peroxidation of polyunsaturated fatty acids by lipoxygenases drives ferroptosis. *Proc Natl Acad Sci U S A.* 2016;113(34):E4966-4975.
 21. Wu L, Xian X, Tan Z, Dong F, Xu G, Zhang M, Zhang F. The Role of Iron Metabolism, Lipid Metabolism, and Redox Homeostasis in Alzheimer's Disease: from the Perspective of Ferroptosis. *Mol Neurobiol.* 2023;60(5):2832-2850.
 22. Torti FM, Torti SV. Regulation of ferritin genes and protein. *Blood.* 2002;99(10):3505-3516.
 23. Winterbourn CC. Toxicity of iron and hydrogen peroxide: the Fenton reaction. *Toxicol Lett.* 1995;82-83:969-974.
 24. Sun H, Zhang C, Cao S, Sheng T, Dong N, Xu Y. Fenton reactions drive nucleotide and ATP syntheses in cancer. *J Mol Cell Biol.* 2018;10(5):448-459.
 25. Torti SV, Manz DH, Paul BT, Blanchette-Farra N, Torti FM. Iron and Cancer. *Annu Rev Nutr.* 2018;38:97-125.

26. Jaksch-Bogensperger H, Spiegl-Kreinecker S, Arosio P, Eckl P, Golaszewski S, Ebner Y, Al-Schameri R, Strasser P, Weis S, Bresgen N. Ferritin in glioblastoma. *Br J Cancer*. 2020;122(10):1441-1444.
27. De Domenico I, Vaughn MB, Li L, Bagley D, Musci G, Ward DM, Kaplan J. Ferroportin-mediated mobilization of ferritin iron precedes ferritin degradation by the proteasome. *EMBO J*. 2006;25(22):5396-5404.
28. Zhang Y, Mikhael M, Xu D, Li Y, Soe-Lin S, Ning B, Li W, Nie G, Zhao Y, Ponka P. Lysosomal proteolysis is the primary degradation pathway for cytosolic ferritin and cytosolic ferritin degradation is necessary for iron exit. *Antioxid Redox Signal*. 2010;13(7):999-1009.
29. An Z, Aksoy O, Zheng T, Fan QW, Weiss WA. Epidermal growth factor receptor and EGFRvIII in glioblastoma: signaling pathways and targeted therapies. *Oncogene*. 2018;37(12):1561-1575.
30. Ekstrand AJ, Sugawa N, James CD, Collins VP. Amplified and rearranged epidermal growth factor receptor genes in human glioblastomas reveal deletions of sequences encoding portions of the N- and/or C-terminal tails. *Proc Natl Acad Sci U S A*. 1992;89(10):4309-4313.
31. Mellinghoff IK, Cloughesy TF, Mischel PS. PTEN-mediated resistance to epidermal growth factor receptor kinase inhibitors. *Clin Cancer Res*. 2007;13(2 Pt 1):378-381.
32. Mizushima N. Autophagy: process and function. *Genes Dev*. 2007;21(22):2861-2873.
33. Li X, He S, Ma B. Autophagy and autophagy-related proteins in cancer. *Mol Cancer*. 2020;19(1):12.
34. Lee YJ, Cho HN, Soh JW, Jhon GJ, Cho CK, Chung HY, Bae S, Lee SJ, Lee YS. Oxidative stress-induced apoptosis is mediated by ERK1/2 phosphorylation. *Exp Cell Res*. 2003;291(1):251-266.
35. Fu J, Shao CJ, Chen FR, Ng HK, Chen ZP. Autophagy induced by valproic acid is associated with oxidative stress in glioma cell lines. *Neuro Oncol*. 2010;12(4):328-340.
36. Wang C, He C, Lu S, Wang X, Wang L, Liang S, Wang X, Piao M, Cui J, Chi G, Ge P. Autophagy activated by silibinin contributes to glioma cell death via induction of oxidative stress-mediated BNIP3-dependent nuclear translocation of AIF. *Cell Death Dis*. 2020;11(8):630.
37. Wang X, Lu S, He C, Wang C, Wang L, Piao M, Chi G, Luo Y, Ge P. RSL3 induced autophagic death in glioma cells via causing glycolysis dysfunction. *Biochem Biophys Res Commun*. 2019;518(3):590-597.
38. Gao M, Monian P, Pan Q, Zhang W, Xiang J, Jiang X. Ferroptosis is an autophagic cell death process. *Cell Res*. 2016;26(9):1021-1032.
39. Hou W, Xie Y, Song X, Sun X, Lotze MT, Zeh HJ, 3rd, Kang R, Tang D. Autophagy promotes ferroptosis by degradation of ferritin. *Autophagy*. 2016;12(8):1425-1428.
40. Park E, Chung SW. ROS-mediated autophagy increases intracellular iron levels and ferroptosis by ferritin and transferrin receptor regulation. *Cell Death Dis*. 2019;10(11):822.
41. Black WJ, Stagos D, Marchitti SA, Nebert DW, Tipton KF, Bairoch A, Vasiliou V. Human aldehyde dehydrogenase genes: alternatively spliced transcriptional variants and their suggested nomenclature. *Pharmacogenet Genomics*. 2009;19(11):893-902.

42. Kedishvili NY. Retinoic Acid Synthesis and Degradation. *Subcell Biochem.* 2016;81:127-161.
43. Duester G. Retinoic acid synthesis and signaling during early organogenesis. *Cell.* 2008;134(6):921-931.
44. Storms RW, Green PD, Safford KM, Niedzwiecki D, Cogle CR, Colvin OM, Chao NJ, Rice HE, Smith CA. Distinct hematopoietic progenitor compartments are delineated by the expression of aldehyde dehydrogenase and CD34. *Blood.* 2005;106(1):95-102.
45. Liu C, Chen BJ, Deoliveira D, Sempowski GD, Chao NJ, Storms RW. Progenitor cell dose determines the pace and completeness of engraftment in a xenograft model for cord blood transplantation. *Blood.* 2010;116(25):5518-5527.
46. Jackson B, Brocker C, Thompson DC, Black W, Vasiliou K, Nebert DW, Vasiliou V. Update on the aldehyde dehydrogenase gene (ALDH) superfamily. *Hum Genomics.* 2011;5(4):283-303.
47. Choi H, Tostes RC, Webb RC. Mitochondrial aldehyde dehydrogenase prevents ROS-induced vascular contraction in angiotensin-II hypertensive mice. *J Am Soc Hypertens.* 2011;5(3):154-160.
48. Singh S, Brocker C, Koppaka V, Chen Y, Jackson BC, Matsumoto A, Thompson DC, Vasiliou V. Aldehyde dehydrogenases in cellular responses to oxidative/electrophilic stress. *Free Radic Biol Med.* 2013;56:89-101.
49. Grunblatt E, Riederer P. Aldehyde dehydrogenase (ALDH) in Alzheimer's and Parkinson's disease. *J Neural Transm (Vienna).* 2016;123(2):83-90.
50. Wang W, Wang C, Xu H, Gao Y. Aldehyde Dehydrogenase, Liver Disease and Cancer. *Int J Biol Sci.* 2020;16(6):921-934.
51. Xu SL, Liu S, Cui W, Shi Y, Liu Q, Duan JJ, Yu SC, Zhang X, Cui YH, Kung HF, Bian XW. Aldehyde dehydrogenase 1A1 circumscribes high invasive glioma cells and predicts poor prognosis. *Am J Cancer Res.* 2015;5(4):1471-1483.
52. Douville J, Beaulieu R, Balicki D. ALDH1 as a functional marker of cancer stem and progenitor cells. *Stem Cells Dev.* 2009;18(1):17-25.
53. Wang S, Zhou X, Liang C, Bao M, Tian Y, Zhu J, Zhang T, Yang J, Wang Z. ALDH1A3 serves as a predictor for castration resistance in prostate cancer patients. *BMC Cancer.* 2020;20(1):387.
54. Guo F, Yang Z, Sehouli J, Kaufmann AM. Blockade of ALDH in Cisplatin-Resistant Ovarian Cancer Stem Cells In Vitro Synergistically Enhances Chemotherapy-Induced Cell Death. *Curr Oncol.* 2022;29(4):2808-2822.
55. Kamble D, Mahajan M, Dhat R, Sitasawad S. Keap1-Nrf2 Pathway Regulates ALDH and Contributes to Radioresistance in Breast Cancer Stem Cells. *Cells.* 2021;10(1).
56. Park J, Shim JK, Kang JH, Choi J, Chang JH, Kim SY, Kang SG. Regulation of bioenergetics through dual inhibition of aldehyde dehydrogenase and mitochondrial complex I suppresses glioblastoma tumorspheres. *Neuro Oncol.* 2018;20(7):954-965.
57. Zhang W, Liu Y, Hu H, Huang H, Bao Z, Yang P, Wang Y, You G, Yan W, Jiang T, Wang J, Zhang W. ALDH1A3: A Marker of Mesenchymal Phenotype in Gliomas Associated with Cell Invasion. *PLoS One.* 2015;10(11):e0142856.
58. Mao P, Joshi K, Li J, Kim SH, Li P, Santana-Santos L, Luthra S, Chandran UR, Benos PV, Smith L, Wang M, Hu B, Cheng SY, Sobol RW, Nakano I. Mesenchymal glioma stem cells

- are maintained by activated glycolytic metabolism involving aldehyde dehydrogenase 1A3. *Proc Natl Acad Sci U S A*. 2013;110(21):8644-8649.
59. Ni W, Xia Y, Luo L, Wen F, Hu D, Bi Y, Qi J. High expression of ALDH1A3 might independently influence poor progression-free and overall survival in patients with glioma via maintaining glucose uptake and lactate production. *Cell Biol Int*. 2020;44(2):569-582.
 60. Motomura H, Nozaki Y, Onaga C, Ozaki A, Tamori S, Shiina TA, Kanai S, Ohira C, Hara Y, Harada Y, Takasawa R, Hanawa T, Tanuma SI, Mano Y, Sato T, Sato K, Akimoto K. High Expression of c-Met, PKClambda and ALDH1A3 Predicts a Poor Prognosis in Late-stage Breast Cancer. *Anticancer Res*. 2020;40(1):35-52.
 61. Wei D, Peng JJ, Gao H, Zhang T, Tan Y, Hu YH. ALDH1 Expression and the Prognosis of Lung Cancer: A Systematic Review and Meta-Analysis. *Heart Lung Circ*. 2015;24(8):780-788.
 62. Marcato P, Dean CA, Liu RZ, Coyle KM, Bydoun M, Wallace M, Clements D, Turner C, Mathenge EG, Gujar SA, Giacomantonio CA, Mackey JR, Godbout R, Lee PW. Aldehyde dehydrogenase 1A3 influences breast cancer progression via differential retinoic acid signaling. *Mol Oncol*. 2015;9(1):17-31.
 63. Chen MH, Weng JJ, Cheng CT, Wu RC, Huang SC, Wu CE, Chung YH, Liu CY, Chang MH, Chen MH, Chiang KC, Yeh TS, Su Y, Yeh CN. ALDH1A3, the Major Aldehyde Dehydrogenase Isoform in Human Cholangiocarcinoma Cells, Affects Prognosis and Gemcitabine Resistance in Cholangiocarcinoma Patients. *Clin Cancer Res*. 2016;22(16):4225-4235.
 64. Li G, Li Y, Liu X, Wang Z, Zhang C, Wu F, Jiang H, Zhang W, Bao Z, Wang Y, Cai J, Zhao L, Kahlert UD, Jiang T, Zhang W. ALDH1A3 induces mesenchymal differentiation and serves as a predictor for survival in glioblastoma. *Cell Death Dis*. 2018;9(12):1190.
 65. Wakimoto H. Deubiquitinating ALDH1A3 key to maintaining the culprit of aggressive brain cancer. *J Clin Invest*. 2019;129(5):1833-1835.
 66. Chen Z, Wang HW, Wang S, Fan L, Feng S, Cai X, Peng C, Wu X, Lu J, Chen D, Chen Y, Wu W, Lu D, Liu N, You Y, Wang H. USP9X deubiquitinates ALDH1A3 and maintains mesenchymal identity in glioblastoma stem cells. *J Clin Invest*. 2019;129(5):2043-2055.
 67. Yu H, Li X, Li Y, Wang T, Wang M, Mao P. MiR-4524b-5p-targeting ALDH1A3 attenuates the proliferation and radioresistance of glioblastoma via PI3K/AKT/mTOR signaling. *CNS Neurosci Ther*. 2023.
 68. Ganser K, Eckert F, Riedel A, Stransky N, Paulsen F, Noell S, Krueger M, Schittenhelm J, Beck-Wodl S, Zips D, Ruth P, Huber SM, Klumpp L. Patient-individual phenotypes of glioblastoma stem cells are conserved in culture and associate with radioresistance, brain infiltration and patient prognosis. *Int J Cancer*. 2022;150(10):1722-1733.
 69. Nie S, Qian X, Shi M, Li H, Peng C, Ding X, Zhang S, Zhang B, Xu G, Lv Y, Wang L, Friess H, Kong B, Zou X, Shen S. ALDH1A3 Accelerates Pancreatic Cancer Metastasis by Promoting Glucose Metabolism. *Front Oncol*. 2020;10:915.
 70. Canino C, Luo Y, Marcato P, Blandino G, Pass HI, Cioce M. A STAT3-NFkB/DDIT3/CEBPbeta axis modulates ALDH1A3 expression in chemoresistant cell subpopulations. *Oncotarget*. 2015;6(14):12637-12653.

71. Zhang W, Yan W, You G, Bao Z, Wang Y, Liu Y, You Y, Jiang T. Genome-wide DNA methylation profiling identifies ALDH1A3 promoter methylation as a prognostic predictor in G-CIMP- primary glioblastoma. *Cancer Lett.* 2013;328(1):120-125.
72. Sharma M, Barravecchia I, Magnuson B, Ferris SF, Apfelbaum A, Mbah NE, Cruz J, Krishnamoorthy V, Teis R, Kauss M, Koschmann C, Lyssiotis CA, Ljungman M, Galban S. Histone H3 K27M-mediated regulation of cancer cell stemness and differentiation in diffuse midline glioma. *Neoplasia.* 2023;44:100931.
73. Mao P, Wang T, Gao K, Li Y, Du C, Wang M. MiR-320b aberrant expression enhances the radioresistance of human glioma via upregulated expression of ALDH1A3. *Aging (Albany NY).* 2023;15(6):2347-2357.
74. Li S, He Y, Chen K, Sun J, Zhang L, He Y, Yu H, Li Q. RSL3 Drives Ferroptosis through NF-kappaB Pathway Activation and GPX4 Depletion in Glioblastoma. *Oxid Med Cell Longev.* 2021;2021:2915019.
75. Song Q, Peng S, Sun Z, Heng X, Zhu X. Temozolomide Drives Ferroptosis via a DMT1-Dependent Pathway in Glioblastoma Cells. *Yonsei Med J.* 2021;62(9):843-849.
76. Wei J, Wang L, Zhang Y, Sun T, Zhang C, Hu Z, Zhou L, Liu X, Wan J, Ma L. TRIM25 promotes temozolomide resistance in glioma by regulating oxidative stress and ferroptotic cell death via the ubiquitination of keap1. *Oncogene.* 2023;42(26):2103-2112.
77. Buccarelli M, Marconi M, Pacioni S, De Pascalis I, D'Alessandris QG, Martini M, Ascione B, Malorni W, Larocca LM, Pallini R, Ricci-Vitiani L, Matarrese P. Inhibition of autophagy increases susceptibility of glioblastoma stem cells to temozolomide by igniting ferroptosis. *Cell Death Dis.* 2018;9(8):841.
78. Wu W, Wu Y, Mayer K, von Rosenstiel C, Schecker J, Baur S, Wurstle S, Liesche-Starnecker F, Gempt J, Schlegel J. Lipid Peroxidation Plays an Important Role in Chemotherapeutic Effects of Temozolomide and the Development of Therapy Resistance in Human Glioblastoma. *Transl Oncol.* 2020;13(3):100748.
79. Sui X, Zhang R, Liu S, Duan T, Zhai L, Zhang M, Han X, Xiang Y, Huang X, Lin H, Xie T. RSL3 Drives Ferroptosis Through GPX4 Inactivation and ROS Production in Colorectal Cancer. *Front Pharmacol.* 2018;9:1371.
80. Yang J, Mo J, Dai J, Ye C, Cen W, Zheng X, Jiang L, Ye L. Cetuximab promotes RSL3-induced ferroptosis by suppressing the Nrf2/HO-1 signalling pathway in KRAS mutant colorectal cancer. *Cell Death Dis.* 2021;12(11):1079.
81. Shintoku R, Takigawa Y, Yamada K, Kubota C, Yoshimoto Y, Takeuchi T, Koshiishi I, Torii S. Lipoxygenase-mediated generation of lipid peroxides enhances ferroptosis induced by erastin and RSL3. *Cancer Sci.* 2017;108(11):2187-2194.
82. Kram H, Prokop G, Haller B, Gempt J, Wu Y, Schmidt-Graf F, Schlegel J, Conrad M, Liesche-Starnecker F. Glioblastoma Relapses Show Increased Markers of Vulnerability to Ferroptosis. *Front Oncol.* 2022;12:841418.
83. Schonberg DL, Miller TE, Wu Q, Flavahan WA, Das NK, Hale JS, Hubert CG, Mack SC, Jarrar AM, Karl RT, Rosager AM, Nixon AM, Tesar PJ, Hamerlik P, Kristensen BW, Horbinski C, Connor JR, Fox PL, Lathia JD, Rich JN. Preferential Iron Trafficking Characterizes Glioblastoma Stem-like Cells. *Cancer Cell.* 2015;28(4):441-455.
84. Viswanathan VS, Ryan MJ, Dhruv HD, Gill S, Eichhoff OM, Seashore-Ludlow B, Kaffenberger SD, Eaton JK, Shimada K, Aguirre AJ, Viswanathan SR, Chattopadhyay S,

- Tamayo P, Yang WS, Rees MG, Chen S, Boskovic ZV, Javaid S, Huang C, Wu X, Tseng YY, Roider EM, Gao D, Cleary JM, Wolpin BM, Mesirov JP, Haber DA, Engelman JA, Boehm JS, Kotz JD, Hon CS, Chen Y, Hahn WC, Levesque MP, Doench JG, Berens ME, Shamji AF, Clemons PA, Stockwell BR, Schreiber SL. Dependency of a therapy-resistant state of cancer cells on a lipid peroxidase pathway. *Nature*. 2017;547(7664):453-457.
85. Piao S, Ojha R, Rebecca VW, Samanta A, Ma XH, McAfee Q, Nicastrì MC, Buckley M, Brown E, Winkler JD, Gimotty PA, Amaravadi RK. ALDH1A1 and HLTF modulate the activity of lysosomal autophagy inhibitors in cancer cells. *Autophagy*. 2017;13(12):2056-2071.
86. Yang MC, Wang HC, Hou YC, Tung HL, Chiu TJ, Shan YS. Blockade of autophagy reduces pancreatic cancer stem cell activity and potentiates the tumoricidal effect of gemcitabine. *Mol Cancer*. 2015;14:179.
87. Wu W. The role of Aldehyde dehydrogenase 1 A3 in chemoresistance regulation in human glioblastoma. 2018.
88. Felsberg J, Hentschel B, Kaulich K, Gramatzki D, Zacher A, Malzkorn B, Kamp M, Sabel M, Simon M, Westphal M, Schackert G, Tonn JC, Pietsch T, von Deimling A, Loeffler M, Reifenberger G, Weller M, German Glioma N. Epidermal Growth Factor Receptor Variant III (EGFRvIII) Positivity in EGFR-Amplified Glioblastomas: Prognostic Role and Comparison between Primary and Recurrent Tumors. *Clin Cancer Res*. 2017;23(22):6846-6855.
89. INABA N, FUJIOKA K, SAITO H, KIMURA M, IKEDA K, INOUE Y, ISHIZAWA S, MANOME Y. Down-regulation of EGFR Prolonged Cell Growth of Glioma but Did Not Increase the Sensitivity to Temozolomide. *Anticancer Research*. 2011;31(10):3253-3257.
90. Gong L, Yin Y, Chen C, Wan Q, Xia D, Wang M, Pu Z, Zhang B, Zou J. Characterization of EGFR-reprogrammable temozolomide-resistant cells in a model of glioblastoma. *Cell Death Discov*. 2022;8(1):438.
91. Kang L, Guo Y, Zhang X, Meng J, Wang ZY. A positive cross-regulation of HER2 and ER-alpha36 controls ALDH1 positive breast cancer cells. *J Steroid Biochem Mol Biol*. 2011;127(3-5):262-268.
92. Liebscher CA, Prinzler J, Sinn BV, Budczies J, Denkert C, Noske A, Sehouli J, Braicu EI, Dietel M, Darb-Esfahani S. Aldehyde dehydrogenase 1/epidermal growth factor receptor coexpression is characteristic of a highly aggressive, poor-prognosis subgroup of high-grade serous ovarian carcinoma. *Hum Pathol*. 2013;44(8):1465-1471.
93. Wu Y, Kram H, Gempt J, Liesche-Starnecker F, Wu W, Schlegel J. ALDH1-Mediated Autophagy Sensitizes Glioblastoma Cells to Ferroptosis. *Cells*. 2022;11(24).

Appendix:

- Publication 1:

“ALDH1-Mediated Autophagy Sensitizes Glioblastoma Cells to Ferroptosis” was published to *Cells* in 2022 December. In this publication, Yang et al. demonstrate that RSL3-induced Lipid Peroxidation and ferroptotic cell death distinguish RSL3-sensitive and -resistant malignant glioma cell lines. RSL3 sensitivity is linked to ALDH1a3 expression, where only cells with high ALDH1a3 expression appear susceptible to ferroptosis induction. Inhibiting ALDH1a3 enzymatic activity through chemical inhibition or genetic knockout shields tumor cells from RSL3-induced ferroptotic cell death. The interaction between RSL3 and ALDH1a3, as well as the autophagic downregulation of ferritin, can be thwarted by ALDH inhibition. Consequently, ALDH1a3 emerges as a key player in ferroptosis by facilitating the crucial release of iron through ferritinophagy.

In this publication, Yang Wu involved in the project design, performed experiments, investigated and analyzed the data, and wrote the first version of the manuscript.

- Publication 2:


“Enhanced Sensitivity to ALDH1A3-Dependent Ferroptosis in TMZ-Resistant Glioblastoma Cells” was published to *Cells* on 2023 October. In this paper, TMZ-resistant LN229 cell lines were treated with the ferroptosis inducer RSL3. RSL3 induced lipid peroxidation in glioblastoma and led to ferroptosis, however, the TMZ-resistant LN229 clones displayed resistance to ferroptosis induction. Interestingly, down-regulation of ALDH1A3 in TMZ-resistant LN229 cells were identified. The cell viability results revealed that only those clones which exhibited an up-regulation of ALDH1A3 following TMZ withdrawal became re-sensitized to ferroptosis induction. The resurgence of ALDH1A3 expression seemed to be under the regulation of EGFR-dependent PI3K pathway

activation, as Akt activation was observed exclusively in ALDH1A3-high clones. Inhibiting the EGFR signaling pathway with the EGFR inhibitor AG1498 led to a decrease in ALDH1A3 expression. These findings offer insights into the potential utilization of RSL3 in addressing glioblastoma relapse.

In this publication, Yang Wu designed the project, performed the experiments, and wrote the original manuscript.

Article

ALDH1-Mediated Autophagy Sensitizes Glioblastoma Cells to Ferroptosis

Yang Wu ¹, Helena Kram ¹, Jens Gempt ² , Friederike Liesche-Starnecker ³, Wei Wu ⁴ and Jürgen Schlegel ^{1,*} 

- ¹ Department of Neuropathology, Institute of Pathology, School of Medicine, Technical University Munich, 81675 Munich, Germany
- ² Department of Neurosurgery, Klinikum Rechts der Isar, School of Medicine, Technical University Munich, 81675 Munich, Germany
- ³ Institute of Pathology and Molecular Diagnostics, Medical Faculty, University of Augsburg, 86156 Augsburg, Germany
- ⁴ Department of Radiology, Molecular Imaging Program at Stanford, Stanford University, Stanford, CA 94305, USA
- * Correspondence: schlegel@tum.de

Abstract: The fatal clinical course of human glioblastoma (GBM) despite aggressive adjuvant therapies is due to high rates of recurrent tumor growth driven by tumor cells with stem-cell characteristics (glioma stem cells, GSCs). The aldehyde dehydrogenase 1 (ALDH1) family of enzymes has been shown to be a biomarker for GSCs, and ALDH1 seems to be involved in the biological processes causing therapy resistance. Ferroptosis is a recently discovered cell death mechanism, that depends on iron overload and lipid peroxidation, and it could, therefore, be a potential therapeutic target in various cancer types. Since both ALDH1 and ferroptosis interact with lipid peroxidation (LPO), we aimed to investigate a possible connection between ALDH1 and ferroptosis. Here, we show that RSL3-induced LPO and ferroptotic cell death revealed RSL3-sensitive and -resistant malignant glioma cell lines. Most interestingly, RSL3 sensitivity correlates with ALDH1a3 expression; only high ALDH1a3-expressing cells seem to be sensitive to ferroptosis induction. In accordance, inhibition of ALDH1a3 enzymatic activity by chemical inhibition or genetic knockout protects tumor cells from RSL3-induced ferroptotic cell death. Both RSL3-dependent binding of ALDH1a3 to LC3B and autophagic downregulation of ferritin could be completely blocked by ALDH inhibition. Therefore, ALDH1a3 seems to be involved in ferroptosis through the essential release of iron by ferritinophagy. Our results also indicate that ferroptosis induction might be a particularly interesting clinical approach for targeting the highly aggressive cell population of GSC.

Keywords: glioblastoma; cancer stem cells; ferroptosis; autophagy; therapy



Citation: Wu, Y.; Kram, H.; Gempt, J.; Liesche-Starnecker, F.; Wu, W.; Schlegel, J. ALDH1-Mediated Autophagy Sensitizes Glioblastoma Cells to Ferroptosis. *Cells* **2022**, *11*, 4015. <https://doi.org/10.3390/cells11244015>

Academic Editor: Swapan K. Ray

Received: 3 November 2022

Accepted: 9 December 2022

Published: 12 December 2022

Publisher's Note: MDPI stays neutral with regard to jurisdictional claims in published maps and institutional affiliations.



Copyright: © 2022 by the authors. Licensee MDPI, Basel, Switzerland. This article is an open access article distributed under the terms and conditions of the Creative Commons Attribution (CC BY) license (<https://creativecommons.org/licenses/by/4.0/>).

1. Introduction

The reason for the devastating clinical prognosis of human malignant gliomas despite aggressive adjuvant therapies is the high rate of recurrent tumor growth, most likely due to an extremely resistant tumor cell population with stem-cell characteristics [1]. Aldehyde dehydrogenase 1 (ALDH1) has been identified as a biomarker for cancer stem cells (CSCs) in different tumor types including human glioblastomas (GBMs) [2,3]. It has been shown that ALDH1 not only is a marker for this highly resistant cell population, but also contributes to the therapy resistance of GBMs [4].

ALDH1 seems to be involved in detoxification of aldehydes that result from lipid peroxidation (LPO) in glioma cells [5]. High levels of LPO are present in proliferating cells due to high rates of oxidative stress, and these levels dramatically increase due to therapy-induced oxidative stress. Interestingly, ferroptosis also relies on LPO. Ferroptosis is a recently discovered cell death mechanism independent from other forms of cell death including apoptosis or necrosis [6]. So far, no unique biomarker of ferroptosis has been

identified, but it has been demonstrated that glutathione peroxidase 4 (GPX4) and the reduction in reactive oxygen species is a central component of ferroptosis. Blockade of GPX4 by RAS-selective lethal (RSL3) or downregulation of glutathione by erastin-induced inhibition of the cystine–glutamate antiporter system Xc leads to this form of iron-dependent cell death [7,8].

The functional interrelationship between these two important regulators in tumor biology could be of interest in glioma CSCs since LPO seems to be functional in both ferroptosis and ALDH1. This could also have clinical implications. Inhibition of ALDH1-dependent resistance against chemotherapy and induction of ferroptosis could theoretically lead to more effective adjuvant therapies. Here, we investigated the functional role of ALDH1 in ferroptosis in human malignant glioma cell lines.

2. Materials and Methods

2.1. Cell Culture, Reagents, Antibodies, and Plasmid

Human glioblastoma cell lines U87MG (male, 69 years, GBM), LN229 (female, 60 years, GBM), and T98G (male, 61 years, GBM) were purchased from the American Type Culture Collection (ATCC, Manassas, VA, USA) and cultured in DMEM with 10% FBS (Gibco, Dreieich, Germany) under standard cell culture conditions (37 °C, 5% CO₂). Isolated primary cell lines were cultured in primary cell culture medium, which included 500 mL of RPMI-1640 (Gibco, Dreieich, Germany), 10 mL of B27 (Gibco, Dreieich, Germany), 5 mL of N2 Supplement (Gibco, Dreieich, Germany), 5 mL of nonessential amino acids (Gibco, Dreieich, Germany), 10 mL of L-glutamine (Gibco, Dreieich, Germany), 10 µg of fibroblast growth factor 2 (Peprotech, Hamburg, Germany), 150 ng of transforming growth factor beta 2 (Peprotech, Hamburg, Germany), and 1 µg of epidermal growth factor (Peprotech, Hamburg, Germany). GBM stem-like cell line X01 (female, 68 years, GBM) [9] was cultivated as previously described [10]. Bafilomycin (Sigma, Munich, Germany), deferoxamine (ChemScene, South Brunswick, NJ, USA), RSL3, and ferrostatin-1 (Sigma, Munich, Germany) were dissolved in dimethyl sulfoxide (DMSO) at 10 mmol/L stock concentration (except DFO, 100 mmol/L stock concentration) and stored at –20 °C. The following antibodies were used: anti-ALDH1A3 (ab129815, Berlin, Germany), anti-LC3B (NB100-2220, Abingdon, UK), anti-vinculin (abcam, ab129002), rabbit IgG for immunoprecipitation (7074P2, CST, Leiden, Germany), anti-GFAP (3670, CST, Leiden, the Netherlands), anti-MAP2 (MAB3418, Chemicon, Nürnberg, Germany), anti-Nestin (4760S, CST, Leiden, the Netherlands). Protein G sepharose was from GE Healthcare Life Science (Munich, Germany). ALDH1a3 plasmid (Aldh1a3 (NM_053080) Mouse-Tagged ORF Clone) was obtained from Origene (Herford, Germany).

2.2. CRISPR/Cas9 Knockout

LN229 and T98G cells were transfected with CRISPR/Cas9 plasmid pSpCas9(BB)-2A-GFP (PX458) (Addgene plasmid #48138) using ALDH1A3 single-guided RNA as previously described [10].

2.3. Glioblastoma Primary Cell Lines

Glioblastoma specimens (IDH wildtype, CNS WHO grade 4 according to the WHO classification of tumors of the central nervous system [11]) were collected from the Department of Neurosurgery, Klinikum rechts der Isar of Technical University of Munich with patients' informed consent. Collection and use of patient-derived tumor samples were approved by the regional ethics committee. Tissue specimens were washed in PBS containing 1% penicillin–streptomycin and separated into pieces by surgery blades. Tissue pieces were incubated with 5 mL of Papain (with 500 uL DNase) for 30 mins to be isolated into single cells or cell groups. To stop the digestion, 5 mL of Ovocuid (with 500 uL DNase) was added for 5 min. Isolated primary cells were collected and cultured in primary cell culture medium (PDCL#9 female, 86 years; PDCL#13 male, 67 years; PDCL#17 female, 63 years).

2.4. Cell Viability Assays

LN229, U87MG, and T98G cells were seeded in 96-well plates (5000 cells/well). Treatment was performed at different concentrations for 24 h, while controls received 0.5% DMSO, only. The proportion of viable cells was determined using the 3-(4,5-dimethylthiazol-2-yl)-2,5-diphenyltetrazolium bromide (MTT, Sigma, Munich, Germany) assay following the manufacturer's recommendations. Absorbance was examined using an Infinite F200 pro Microplate Absorbance Reader (Tecan, Maennedorf, Switzerland).

2.5. LDH Release Assay

For cell death detection, LDH release was quantified using a cytotoxicity detection (LDH) kit (Roche #11644793001, Darmstadt, Germany) and was conducted following the manufacturer's instructions. Absorbance was examined using an Infinite F200 pro Microplate Absorbance Reader at 490 nm.

2.6. Lipid Peroxidation Assays

Cells were seeded on cover slides and treated 24 h before performing the lipid peroxidation assays. Cells were stained by BODIPY[®] 581/591 C11-Reagent (Thermo Fisher, Bremen, Germany) for 30 min and washed with PBS. Cells were either fixed by 30% PFA to perform fluorescence imaging or trypsinized into single cells to perform fluorescence-activated cell sorting (FACS). Fluorescence images were taken by a Zeiss fluorescence microscope (Zeiss, Munich, Germany) and analyzed using software Image J (National Institutes of Health, Bethesda, MD, USA). FACS results were analyzed using FlowJo (FlowJo Inc., Ashland, OH, USA).

2.7. Immunoprecipitation Assays

Glioblastoma cell lines LN229 and T98G were treated and collected after 24 h in lysis buffer (50 mM HEPES, pH 7.5, 10% glycerol, 0.1% Triton X-100, 1 mM dithiothreitol, 150 mM NaCl, 2 mM MgCl₂, and protease inhibitor cocktail). Then, 30 µg of protein was taken out from the cell lysate as the input sample. Anti-ALDH1a3 (ab129815, abcam, Berlin, Germany) and anti-IgG (7074p2, CST, Leiden, Netherland) were added to the lysate for immunoprecipitation (containing 30 µg of protein), and then incubated at 4 °C overnight. Next, 2 mg of protein-G-Sepharose beads were added to each immunoprecipitation sample for 3 h in 4 °C. After washing, Sepharose beads were collected and diluted with SDS sample buffer (1 M Tris-HCl pH 6.8, SDS, 0.1% Bromophenol Blue, glycerol, and 14.3 M β-mercaptoethanol), and then heated at 100 °C in 5 min. Input samples and immunoprecipitation samples were fractionated by 10% SDS-page gels and read out by Western blotting with anti-LC3b (NB100-2220, Novus bio, Munich, Germany).

2.8. Sphere Formation Assays

Glioblastoma established cell lines U87 LN229, and T98G, as well as corresponding ALDH1a3 knockout cell lines, were investigated in sphere formation assays as previously described [10]. Briefly, cells were seeded in ultralow-attachment 12-well plates and cultured under primary cell medium. Pictures were taken after 7 days using a Nikon microscope (Melville, NY, USA).

2.9. ALDH1a3 Stable Transfection

ALDH1a3 plasmid was obtained from OriGENE (MG222097). Briefly, PDCL#9 cells (ALDH1a3 negative) were transfected with ALDH1a3 plasmid using lipofectamine 2000 (Invitrogen, Carlsbad, CA, USA). After 48 h, ALDH1a3-overexpressing clones were selected by G418 (Merck, Germany, Munich, 50 mg/mL in H₂O) treatment for 2 weeks.

2.10. Statistics

Three independent experiments of each assay were conducted to validate results. A *t*-test was used for normally distributed data of two unpaired groups. GraphPad Prism

8 (GraphPad Software Inc.; San Diego, CA, USA) was used to perform the analysis, and p -values < 0.05 were regarded as statistically significant.

3. Results

3.1. RSL3-Induced Ferroptosis-Like Cell Death in Glioblastoma Cell Lines

To discover RSL3-induced cell death in glioblastoma, we treated tumor cells of three established glioma cell lines (U87MG, LN229, and T98G), three primary GBM cell lines (PDCL#9, PDCL#13, and PDCL#17), and GSC-enriched glioma cell line X01 with different concentrations of RSL3. We observed the RSL3 dose-dependent loss of cell viability, but it was different between glioblastoma cell lines (Figure 1A). There was an RSL3-resistant group of cell lines (A1G1, PDCL#9, PDCL#13, T98G, and X01) that showed no cell loss at lower concentrations up to 0.8 μ M RSL3 and weak effects at higher concentrations (ca. 80% cell viability at 1.6–6.4 μ M RSL3). In contrast, a group of RSL3-sensitive cell lines (LN229, U87, and PDCL#17) demonstrated decreased cell viability even at lower concentrations and approximately 30% cell survival at higher concentrations.

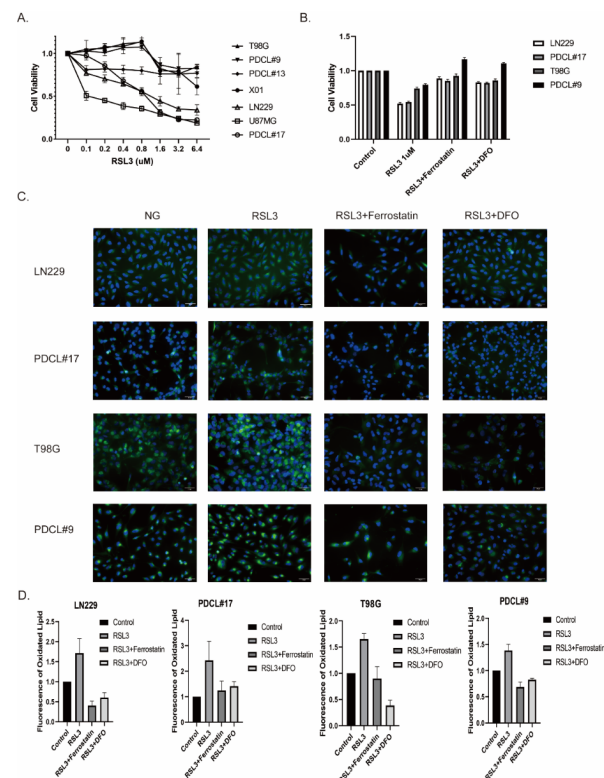


Figure 1. RSL3-induced ferroptosis-like cell death in glioblastoma cell lines. **(A)** Glioblastoma cell lines were treated with increasing doses of RSL3 (0 μ M, 0.1 μ M, 0.2 μ M, 0.4 μ M, 0.8 μ M, 1.6 μ M, 3.2 μ M, and 6.4 μ M), cell viability was assessed by MTT assays. Cell lines A1G1, T98G, PDCL#9, PDCL#13, and X01 showed only a mild reduction in cell viability, whereas LN229, U87MG, and PDCL#17 exhibited a significant reduction. **(B)** RSL3-sensitive LN229 and PDCL#17 cells, and RSL3-resistant T98G and PDCL#9 cells were treated with RSL3 combined with ferroptosis inhibitor ferrostatin and iron chelation DFO; cell viability was determined by MTT assays. Both ferrostatin and DFO completely abolished the RSL3-induced cell death. **(C,D)** RSL3-sensitive LN229 and PDCL#17 cells, and RSL3-resistant T98G and PDCL#9 cells were treated with RSL3, combined with ferrostatin and DFO, respectively; lipid peroxidation (LPO) induced by RSL3 treatment was determined using BODIPY C11-581/591 reagent, as shown by green fluorescence. Results are quantified in **(D)** (p -values: untreated control vs. RSL3 < 0.005, RSL3 vs. RSL3 + ferrostatin < 0.005, RSL3 vs. RSL3 + DFO < 0.005). All cell lines showed pronounced induction of LPO that could be completely blocked by ferroptosis inhibitors.

The type of RSL-3-induced cell loss was most likely ferroptosis, since concomitant treatment with ferrostatin-1, a specific ferroptosis inhibitor, and with deferoxamine (DFO), an iron chelator, completely abolished RSL3-induced cell death (Figure 1B).

Induction of lipid peroxidation (LPO) after RSL3 treatment was measured using BODIPY staining (Figure 1C). Using this approach, we observed an increase in LPO after RSL3 treatment at 1 μ M in all cell lines, which could be completely reverted by concomitant treatment with ferrostatin or DFO (Figure 1D).

These results indicate that the RSL3-induced cell death in glioma cell lines is a ferroptosis-like cell death.

3.2. The Sensitivity to RSL3-Induced Ferroptotic Cell Death in Glioblastoma Correlates with the Expression of ALDH1a3

We next verified cell death according to LDH release (Figure 2A). Most interestingly, sensitivity to RSL3-induced ferroptosis correlated with ALDH1a3 expression (Figure 2B). U87, LN229, and PDCL#17 cells exhibited high amounts of ALDH1a3 protein, T98G, PDCL#9, X01, and PDCL#13 showed no expression.

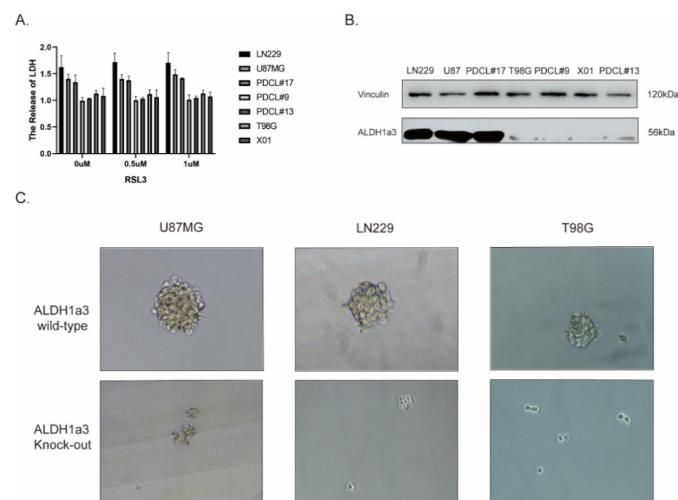


Figure 2. The sensitivity to RSL3-induced ferroptotic cell death in glioblastoma correlates with expression of ALDH1a3. **(A)** Relative LDH release (1.0 = untreated controls) after RSL3 treatment confirmed the cell viability results. RSL3 induced cell death in LN229, U87MG, and PDCL#17 cells, but not in T98G, PDCL#9, PDCL#13, and X01 cell lines. **(B)** Expression of ALDH1a3 protein was assessed in seven cell lines by Western blot analysis. RSL-3-sensitive LN229, U87MG, and PDCL#17 cells showed strong expression of ALDH1a3, whereas RSL3-resistant T98G, PDCL#9, PDCL#13, and X01 cells showed only weak expression. Vinculin served as a loading control. **(C)** ALDH1a3 high-expression U87MG and LN229 cells, and ALDH1a3 low-expression T98G cells, respectively, and their corresponding ALDH1a3 knockout cells were seeded into ultralow-attachment plates and were grown under primary cell culture conditions for 7 days. All three cell lines showed sphere formation with much smaller spheres in T98G cells under primary cell culture conditions. Sphere formation was completely abolished in knockout cells.

To prove the role of the ALDH1a3 subtype as a glioma stem cell (GSC) marker, we performed sphere formation assays of ALDH1a3 wildtype and corresponding knockout glioma cell lines. Our results showed that ALDH1a3 knockout cells lost their ability to form spheres or formed much smaller spheres compared to their ALDH1a3 wildtype counterparts (Figure 2C).

To further investigate the role of ALDH1a3 in RSL3-induced cell death, we tested the effect of inhibition of ALDH1 enzymatic activity by the specific inhibitor diethylaminobenzaldehyde (DEAB) in ALDH1a3 high-expression (LN229, PDCL#17) and low-expression cell lines (T98G and PDCL#9). DEAB at least partially reversed cell death induced by RSL3

(Figure 3A). These results were corroborated by ALDH1a3 knockout cells that showed similar effects compared with enzymatic inhibition (Figure 3C,D). Moreover, BODIPY staining demonstrated that DEAB treatment also decreased lipid peroxidation induced by RSL3 (Figure 3E,F). In line with these results, ALDH1a3 overexpression after stable transfection in ALDH1a3-negative PDCL#9 cells sensitized the cells to RSL3 treatment, an effect that could be reversed by DEAB treatment (Figure 3G).

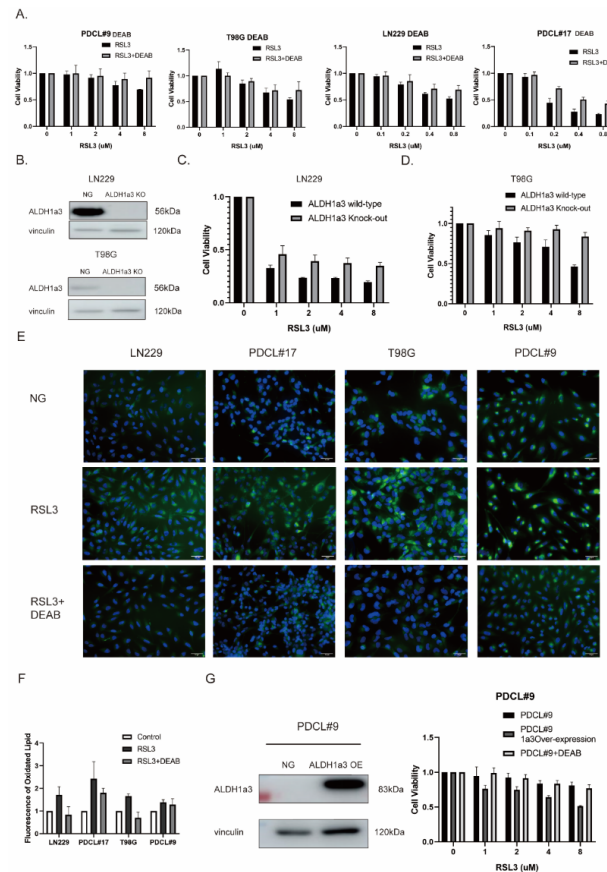


Figure 3. (A) RSL3 treatment with and without DEAB in T98G and PDCL#9 (0 μM, 1 μM, 2 μM, 4 μM, and 8 μM), and RSL-3 sensitive LN229 and PDCL#17 cells (0 μM, 0.1 μM, 0.2 μM, 0.4 μM, and 0.8 μM); cell viability was determined by MTT assays. All cell lines showed decreased cell viability (RSL-3-resistant cells at 10-fold higher concentrations), which could be partially reverted by ALDH1a3 inhibition using DEAB (*p*-values: PDCL#9 8 μM < 0.05; T98G 8 μM < 0.05; LN229 0.8 μM < 0.05; PDCL#17 0.2 μM < 0.01, 0.4 μM < 0.01, 0.8 μM < 0.05). (B) Western blot analysis in LN229 and T98G, demonstrating the results of ALDH1a3 knockout. (NG, negative control; KO, knockout). (C,D) RSL3 treatment (0 μM, 1 μM, 2 μM, 4 μM, and 8 μM) in RSL-3 sensitive LN229 and T98G ALDH1a3 wildtype and knockout cells showed partial reduction in cell death in ALDH1a3 knockout cells (*p*-values: LN229 each group < 0.05; T98G 4 μM < 0.05, 8 μM < 0.005). (E) BODIPY 581/591 C11 staining of lipid peroxidation after RSL3 with or without DEAB treatment demonstrated a significant reduction in LPO after concomitant DEAB treatment. (F) Quantification of BODIPY 581/591 C11 fluorescence staining (*p*-value: LN229 control vs. RSL3 < 0.005, RSL3 vs. RSL3 + DEAB < 0.05; PDCL#17 control vs. RSL3 < 0.05; T98G control vs. RSL3 < 0.001, RSL3 vs. RSL3 + DEAB < 0.05; PDCL#9 control vs. RSL# < 0.001). (G) Protein expression after stable ALDH1a3 transfection in ALDH1a3-negative PDCL#9 cells demonstrated strong ALDH1a3 overexpression in transfected cells. Cell viability was measured after RSL3 treatment with or without DEAB by MTT assays. ALDH1a3-overexpressing PDCL#9 cells demonstrated a reduction in cell viability after RSL-3 that could be reverted by DEAB treatment (*p*-values: PDCL#9 vs. PDCL#9-A3 OE in 4 μM < 0.001, in 8 μM < 0.001; PDCL#9A3-OE vs. PDCL#9A3-OE + DEAB in 1 μM < 0.05, in 2 μM < 0.05, in 4 μM < 0.01, in 8 μM < 0.01).

These results show that ALDH1a3 seems to be involved in RSL3-induced ferroptotic cell death, and that it might play a role upstream of LPO.

3.3. Autophagy Seems to Be Necessary for RSL3-Induced Cell Death

Autophagy is involved in the induction of ferroptosis, and ALDH1 also seems to play a role in autophagy. We, therefore, investigated the effect of autophagy inhibition on ferroptosis in glioma cell lines. The concomitant treatment with the specific autophagy inhibitor bafilomycin A1 rescued glioma cells from RSL3-induced LPO and ferroptotic cell death (Figure 4A–C). Moreover, autophagy by RSL3 treatment was more pronounced in ALDH1a3 wildtype cells than in ALDH1a3 knockout cells (Figure 4D). These results might indicate a role of ALDH1a3 in ferroptosis by autophagy activation. We, therefore, performed a coimmunoprecipitation assay to investigate the connection of ALDH1a3 protein to autophagosomes. After RSL3 treatment ALDH1a3 protein was complexed with LC3, while DEAB treatment eliminated the ALDH1a3–LC3 protein complex formation (Figure 4E). The binding of ALDH1a3 to LC3B-II seems to be relatively weak most likely due to the high autophagic flux in GBM cells and lysosomal degradation [12]. In addition, there seems to be also a binding to LC3B-I. Since it has been shown that ferroptosis depends on the release of iron from ferritin iron storage by autophagy (ferritinophagy), we investigated the ferritin content by Western analysis demonstrating downregulation of ferritin after RSL3 treatment that could be reversed by concomitant DEAB treatment (Figure 4F). These results were corroborated by experiments using ALDH1a3 knockout cell lines (Figure 4G) that showed higher ferritin levels and no decrease after RSL3 treatment.

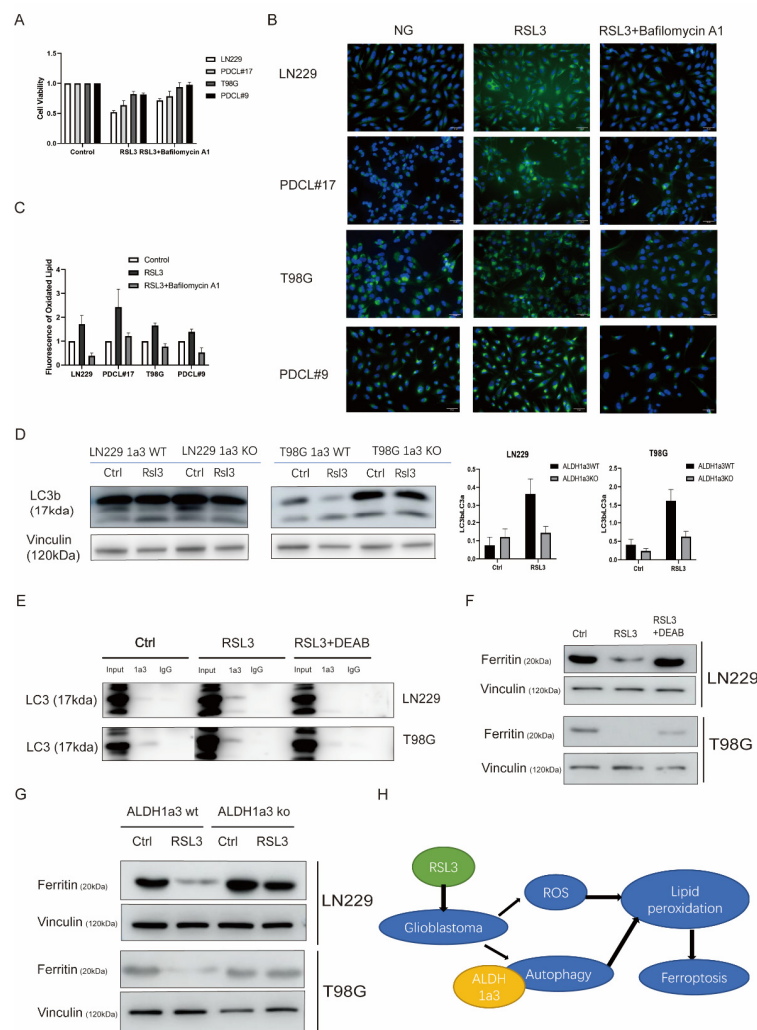


Figure 4. Autophagy in RSL3-induced cell death. **(A)** Cell viability after RSL3 with or without Bafilomycin A1 in LN229, PDCL#17, T98G, and PDCL#9 showed reversion of cell viability by autophagy inhibition by bafilomycin A1 (*p*-value: LN229 RSL3 vs. RSL3 + Bafilomycin A1 < 0.01; PDCL#17 RSL3 vs. RSL3 + Bafilomycin A1 < 0.01). **(B)** BODIPY 581/591 C11 staining of lipid peroxidation after RSL3 treatment with or without Bafilomycin A1 showed a significant reduction in fluorescence staining after autophagy inhibition. **(C)** Quantification of lipid peroxidation after RSL3 with or without Bafilomycin A1 treatment. **(D)** Western blot analysis and quantification of LC3B/LC3A ratio of ALDH1a3 wildtype and knockout cells showed a pronounced induction of autophagy in wildtype cells but not in ALDH1a3 knockout cells. Vinculin served as control. **(E)** Immunoprecipitation assays of LN229 and T98G cells; protein complexes were precipitated with ALDH1a3 antibodies after RSL3 treatment with or without DEAB. Immunoblots showed ALDH1a3 binding to LC3 after RSL3 treatment that could be reverted by concomitant DEAB treatment. **(F)** Western blot analysis of ferritin expression after RSL3 treatment with and without DEAB in LN229 and T98G cells. Ferritin iron storage was downregulated after RSL3 treatment, which could be reversed by concomitant DEAB treatment. Vinculin served as control. **(G)** Western blot analysis of ferritin expression after RSL3 treatment in LN229 and T98G ALDH1a3 wildtype or ALDH1a3 knockout cells. The results corroborated the results of (F), showing ferritin downregulation after RSL-3 treatment only in ALDH1a3 wildtype cells. **(H)** Schematic diagram: RSL3 treatment induces ROS accumulation and activates ALDH1a3-dependent autophagy in glioblastoma cells, leading to lipid peroxidation and finally to ferroptosis.

4. Discussion

The fatal clinical course of human glioblastoma despite aggressive adjuvant therapies is due to highly resistant tumor cells, i.e., glioma stem cells (GSC), which express ALDH1 [3], and ALDH1 seems to be involved in the biological processes that lead to therapy resistance by interacting with lipid peroxidation (LPO) [5]. Since ferroptosis is also LPO-dependent [13], we aimed to investigate a possible connection between ALDH1 and ferroptosis.

Here, we show that RSL3-induced ferroptotic cell death revealed RSL3-sensitive and -resistant malignant glioma cell lines. Most interestingly, the RSL3 sensitivity correlated with ALDH1a3 expression; only high-ALDH1a3-expressing cells seemed to be sensitive to ferroptosis induction. In accordance, inhibition of ALDH1a3 enzymatic activity by DEAB protected cells from RSL3-induced cell death.

Ferroptosis is a novel cell death mechanism distinct from necrosis or apoptosis [6]. So far, its role in normal cellular homeostasis is unclear, but it has been shown that ferroptosis induction could offer novel treatment options in aggressive tumor types including GBM [14]. Glioma stem cells (GSCs) characterized by ALDH1a3 expression seem to be the most resistant cell type in GBM, and ALDH1a3 enzymatic activity seems to be involved in the development of the resistant phenotype [10]. Therefore, we expected that combined treatment with an ALDH1 inhibitor (DEAB) and with a ferroptosis inducer (RSL3) should increase cell death in GBM cell lines. However, the contrary happened; ALDH1 inhibition by DEAB nearly completely reverted RSL3-induced ferroptotic cell death. So far, no direct involvement of ALDH1 family enzymes in ferroptosis has been shown.

Since autophagy is involved in both ferroptosis [15] and ALDH1a3 regulation [10], we next investigated the role of autophagy in glioma cell response. We showed previously that, in human GBM, ALDH1 is involved in therapy resistance against the standard chemotherapeutic agent temozolomide by detoxifying toxic aldehydes resulting from oxidative stress and consequent activation of LPO, and that this process seems to be mediated at least in part by autophagy [5]. The results of the present study also support the view that ALDH1 not only is involved in the regulatory processes of autophagy but could be an important regulator or sensor for autophagy. Here, we show that inhibition of ALDH1 enzymatic activity abolished autophagy, and this also was necessary for ferroptotic cell death.

Autophagy plays an important role in ferroptosis [16]. Ferroptosis is an iron-dependent cell death mechanism, and iron is released from ferritin storage by an NCOA4-dependent autophagic mechanism known as ferritinophagy [17]. Therefore, the critical biological process seems to be the release of iron by ferritinophagy. Consequently, ALDH1a3 high-expression cells exhibited high levels of autophagy and ferritin release compared with ALDH1a3 low-expression cells. These data indicate that ALDH1a3 is important in the ferroptosis of human malignant glioma cells by autophagy regulation.

These data are also relevant for clinical consequences, although our results do not support the hypothesis that ferroptosis and concomitant ALDH1 inhibition could increase tumor cell death under standard treatment conditions. However, tumor cells highly expressing ALDH1 represent the most aggressive subpopulation of GSC within GBM. Moreover, it has been shown that the number of ALDH1a3-expressing cells dramatically increases in recurrent tumor growth [18], eventually resulting in the high therapy resistance of recurrences. Our data show that ALDH1a3-positive GSCs that are highly resistant against standard therapy seem to be most susceptible to ferroptosis induction. Thus, ferroptosis could be a therapeutic option in recurrent tumors with high amounts of ALDH1-expressing cells. Therefore, our data might fuel the hope of overcoming resistance to therapy by ferroptosis induction in GBM.

Author Contributions: Data curation, Y.W.; funding acquisition, J.S.; investigation, Y.W.; methodology, W.W.; project administration, J.S.; resources, H.K., J.G. and F.L.-S.; writing—original draft, Y.W.; writing—review and editing, J.S. All authors have read and agreed to the published version of the manuscript.

Funding: This study was funded by the Deutsche Forschungsgemeinschaft, Collaborative Research Centre SFB 824 (Project B6) and the APC was funded by Technical University Munich.

Institutional Review Board Statement: The study was conducted in accordance with the Declaration of Helsinki, and approved by the Institutional Ethics Committee of Technical University of Munich (protocol code 2403/09).

Informed Consent Statement: Informed consent was obtained from all subjects involved in the study.

Acknowledgments: We are thankful to Sandra Baur for her excellent technical support, and to Gabriele Multhoff for offering the use of the FACS.

Conflicts of Interest: The authors declare no conflict of interest.

References

1. Cojoc, M.; Mabert, K.; Muders, M.H.; Dubrovskaya, A. A role for cancer stem cells in therapy resistance: Cellular and molecular mechanisms. *Semin Cancer Biol.* **2015**, *31*, 16–27. [[CrossRef](#)] [[PubMed](#)]
2. Marcato, P.; Dean, C.A.; Giacomantonio, C.A.; Lee, P.W. Aldehyde dehydrogenase: Its role as a cancer stem cell marker comes down to the specific isoform. *Cell Cycle.* **2011**, *10*, 1378–1384. [[CrossRef](#)] [[PubMed](#)]
3. Rasper, M.; Schafer, A.; Piontek, G.; Teufel, J.; Brockhoff, G.; Ringel, F.; Heindl, S.; Zimmer, C.; Schlegel, J. Aldehyde dehydrogenase 1 positive glioblastoma cells show brain tumor stem cell capacity. *Neuro Oncol.* **2010**, *12*, 1024–1033. [[CrossRef](#)] [[PubMed](#)]
4. Schafer, A.; Teufel, J.; Ringel, F.; Bettstetter, M.; Hoepner, I.; Rasper, M.; Gempt, J.; Koeritzer, J.; Schmidt-Graf, F.; Meyer, B.; et al. Aldehyde dehydrogenase 1A1—a new mediator of resistance to temozolomide in glioblastoma. *Neuro Oncol.* **2012**, *14*, 1452–1464. [[CrossRef](#)] [[PubMed](#)]
5. Wu, W.; Wu, Y.; Mayer, K.; von Rosenstiel, C.; Schecker, J.; Baur, S.; Wurstle, S.; Liesche-Starnecker, F.; Gempt, J.; Schlegel, J. Lipid Peroxidation Plays an Important Role in Chemotherapeutic Effects of Temozolomide and the Development of Therapy Resistance in Human Glioblastoma. *Transl. Oncol.* **2020**, *13*, 100748. [[CrossRef](#)] [[PubMed](#)]
6. Jiang, X.; Stockwell, B.R.; Conrad, M. Ferroptosis: Mechanisms, biology and role in disease. *Nat. Rev. Mol. Cell Biol.* **2021**, *22*, 266–282. [[CrossRef](#)]
7. Seibt, T.M.; Proneth, B.; Conrad, M. Role of GPX4 in ferroptosis and its pharmacological implication. *Free Radic. Biol. Med.* **2019**, *133*, 144–152. [[CrossRef](#)] [[PubMed](#)]
8. Zhao, Y.; Li, Y.; Zhang, R.; Wang, F.; Wang, T.; Jiao, Y. The Role of Erastin in Ferroptosis and Its Prospects in Cancer Therapy. *Oncotargets Ther.* **2020**, *13*, 5429–5441. [[CrossRef](#)] [[PubMed](#)]
9. Soeda, A.; Park, M.; Lee, D.; Mintz, A.; Androutsellis-Theotokis, A.; McKay, R.D.; Engh, J.; Iwama, T.; Kunisada, T.; Kassam, A.B.; et al. Hypoxia promotes expansion of the CD133-positive glioma stem cells through activation of HIF-1 α . *Oncogene* **2009**, *28*, 3949–3959. [[CrossRef](#)] [[PubMed](#)]
10. Wu, W.; Schecker, J.; Wurstle, S.; Schneider, F.; Schonfelder, M.; Schlegel, J. Aldehyde dehydrogenase 1A3 (ALDH1A3) is regulated by autophagy in human glioblastoma cells. *Cancer Lett.* **2018**, *417*, 112–123. [[CrossRef](#)]
11. Berger, T.R.; Wen, P.Y.; Lang-Orsini, M.; Chukwueke, U.N. World Health Organization 2021 Classification of Central Nervous System Tumors and Implications for Therapy for Adult-Type Gliomas: A Review. *JAMA Oncol.* **2022**. [[CrossRef](#)] [[PubMed](#)]
12. Klionsky, D.J.; Abdalla, F.C.; Abeliovich, H.; Abraham, R.T.; Acevedo-Arozena, A.; Adeli, K.; Agholme, L.; Agnello, M.; Agostinis, P.; Aguirre-Ghiso, J.A.; et al. Guidelines for the use and interpretation of assays for monitoring autophagy. *Autophagy.* **2012**, *8*, 445–544. [[CrossRef](#)]
13. Imai, H.; Matsuoka, M.; Kumagai, T.; Sakamoto, T.; Koumura, T. Lipid Peroxidation-Dependent Cell Death Regulated by GPX4 and Ferroptosis. *Curr. Top. Microbiol. Immunol.* **2017**, *403*, 143–170.
14. Yang, F.C.; Wang, C.; Zhu, J.; Gai, Q.J.; Mao, M.; He, J.; Qin, Y.; Yao, X.X.; Wang, Y.X.; Lu, H.M.; et al. Inhibitory effects of temozolomide on glioma cells is sensitized by RSL3-induced ferroptosis but negatively correlated with expression of ferritin heavy chain 1 and ferritin light chain. *Lab Invest.* **2022**, *102*, 741–752. [[CrossRef](#)] [[PubMed](#)]
15. Zhang, Y.; Kong, Y.; Ma, Y.; Ni, S.; Wikerholmen, T.; Xi, K.; Zhao, F.; Zhao, Z.; Wang, J.; Huang, B.; et al. Loss of COPZ1 induces NCOA4 mediated autophagy and ferroptosis in glioblastoma cell lines. *Oncogene* **2021**, *40*, 1425–1439. [[CrossRef](#)]
16. Liu, J.; Kuang, F.; Kroemer, G.; Klionsky, D.J.; Kang, R.; Tang, D. Autophagy-Dependent Ferroptosis: Machinery and Regulation. *Cell Chem. Biol.* **2020**, *27*, 420–435. [[CrossRef](#)] [[PubMed](#)]
17. Fang, Y.; Chen, X.; Tan, Q.; Zhou, H.; Xu, J.; Gu, Q. Inhibiting Ferroptosis through Disrupting the NCOA4-FTH1 Interaction: A New Mechanism of Action. *ACS Cent. Sci.* **2021**, *7*, 980–989. [[CrossRef](#)] [[PubMed](#)]
18. Kram, H.; Prokop, G.; Haller, B.; Gempt, J.; Wu, Y.; Schmidt-Graf, F.; Schlegel, J.; Conrad, M.; Liesche-Starnecker, F. Glioblastoma Relapses Show Increased Markers of Vulnerability to Ferroptosis. *Front. Oncol.* **2022**, *12*, 841418. [[CrossRef](#)] [[PubMed](#)]

Enhanced Sensitivity to ALDH1A3-Dependent Ferroptosis in TMZ-Resistant Glioblastoma Cells

Yang Wu ¹, Sophie Franzmeier ^{1,2} , Friederike Liesche-Starnecker ³  and Jürgen Schlegel ^{1,3,*} 

¹ Department of Neuropathology, Institute of Pathology, School of Medicine, Technical University Munich, 81675 Munich, Germany; ge46muc@tum.de (Y.W.)

² Department of Neuropathology, Institute for Animal Pathology, Ludwig-Maximilians-University Munich, 80539 Munich, Germany

³ Pathology, Medical Faculty, University of Augsburg, 81656 Augsburg, Germany

* Correspondence: schlegel@tum.de

Abstract: Temozolomide (TMZ) is standard treatment for glioblastoma (GBM); nonetheless, resistance and tumor recurrence are still major problems. In addition to its association with recurrent GBM and TMZ resistance, ALDH1A3 has a role in autophagy-dependent ferroptosis activation. In this study, we treated TMZ-resistant LN229 human GBM cells with the ferroptosis inducer RSL3. Remarkably, TMZ-resistant LN229 clones were also resistant to ferroptosis induction, although lipid peroxidation was induced by RSL3. By using Western blotting, we were able to determine that ALDH1A3 was down-regulated in TMZ-resistant LN229 cells. Most intriguingly, the cell viability results showed that only those clones that up-regulated ALDH1A3 after TMZ withdrawal became re-sensitized to ferroptosis induction. The recovery of ALDH1A3 expression appeared to be regulated by EGFR-dependent PI3K pathway activation since Akt was activated only in ALDH1A3 high clones. Blocking the EGFR signaling pathway with the EGFR inhibitor AG1498 decreased the expression of ALDH1A3. These findings shed light on the potential application of RSL3 in the treatment of glioblastoma relapse.

Keywords: therapy resistance; therapeutic interventions; glioblastoma; ferroptosis; ALDH1



Citation: Wu, Y.; Franzmeier, S.; Liesche-Starnecker, F.; Schlegel, J. Enhanced Sensitivity to ALDH1A3-Dependent Ferroptosis in TMZ-Resistant Glioblastoma Cells. *Cells* **2023**, *12*, 2522. <https://doi.org/10.3390/cells12212522>

Academic Editor: Kai Zheng

Received: 10 August 2023

Revised: 20 October 2023

Accepted: 24 October 2023

Published: 25 October 2023



Copyright: © 2023 by the authors. Licensee MDPI, Basel, Switzerland. This article is an open access article distributed under the terms and conditions of the Creative Commons Attribution (CC BY) license (<https://creativecommons.org/licenses/by/4.0/>).

1. Introduction

Glioblastoma (GBM) is characterized by its rapid and infiltrative growth and, consequently, its high rates of recurrence. Despite significant advancements in surgery, radiation therapy, and chemotherapy, the median survival rate remains discouragingly low, with an average survival of 12 to 15 months after diagnosis and a five-year survival rate of 7.2% [1]. The diffusely infiltrative nature of GBM makes complete removal by surgery nearly impossible, and the most disappointing aspect of GBM is its resistance to conventional therapies. Thus, the future of cutting-edge glioblastoma treatment approaches lies in precision medicine and customized medicines.

Temozolomide (TMZ) is part of the standard treatment regimen for GBM. It is usually given concomitantly with radiation therapy, followed by maintenance therapy with TMZ alone [2]. The methylation of the O-6-methylguanine-DNA methyltransferase (MGMT) promoter is a strong predictor of the therapeutic efficiency of TMZ treatment [3]. However, for reasons unrelated to their MGMT statuses, patients may undergo tumor relapse and develop resistance to TMZ [4,5]. TMZ generates reactive oxygen species (ROS) as byproducts of its metabolism and DNA-damaging effects, which contribute to oxidative stress in GBM cells [6]. Ferroptosis is an iron-dependent form of regulated cell death characterized by the accumulation of lipid peroxidation [7]. By inducing ROS generation, TMZ may potentially sensitize cancer cells to ferroptosis.

Aldehyde dehydrogenase (ALDH) 1A3 is a member of the ALDH enzyme family, and it plays a vital role in cellular detoxification and the oxidative stress response [8]. ALDH1

is primarily involved in the oxidation of retinaldehyde to retinoic acid, a crucial metabolite involved in various cellular processes, including differentiation and proliferation [9]. ALDH1A3 has been linked in recent studies to resistance to TMZ therapy [10] and to higher levels in recurrent GBM [11]. Moreover, the high expression of ALDH1A3 has been found to contribute to the maintenance of glioma stem-like cells (GSCs), a subpopulation of GBM cells with self-renewal capacities and enhanced resistance to therapies [12]. ALDH1A3 is regulated in many ways. In addition to direct or indirect transcriptional regulation mediated by different signaling pathways [13–15], the expression of ALDH1A3 is intricately regulated by histone epigenetic modifications at its promoter region [16]. Furthermore, post-transcriptional processes including autophagy or regulation by microRNA further contribute to its regulation [10,17].

The epidermal growth factor receptor (EGFR) plays an important role in the development and progression of GBM. EGFR activation triggers a cascade of signaling events, including the PI3K/AKT pathways, regulating cell growth, survival, and migration. The aberrant activation of AKT due to EGFR dysregulation contributes to the uncontrolled growth and aggressiveness of glioblastoma cells [18].

Emerging evidence has implicated the role of ALDH1A3 in conferring resistance to TMZ, accompanied by its influence on the autophagic process. Recent studies have placed significant emphasis on the association between ALDH1A3 and reactive oxygen species (ROS) metabolism, as well as its role in sensitizing glioblastoma cells to ferroptosis. The induction of ferroptosis appears to be a promising novel therapeutic strategy in the context of glioblastoma therapy.

Our previous results showed that TMZ induces ROS accumulation [8] and ALDH1a3 sensitizes GBM to ferroptosis [19]. Here, we demonstrated that TMZ-resistant (TMZ-res) LN229 clones were resistant to ferroptosis, although lipid peroxidation was induced by the ferroptosis inducer RSL3. We further discovered that ALDH1A3 was downregulated in TMZ-resistant LN229 clones in an EGFR-dependent PI3K-pathway-mediated manner. After the discontinuation of TMZ, cells up-regulated ALDH1A3 and became re-sensitized to ferroptosis induction. This might provide a glimpse into the potential future application of ferroptosis in glioblastoma treatment.

2. Materials and Methods

2.1. Cell Culture, Reagents, and Antibodies

The LN229 glioblastoma cell line (PTEN wild-type, p53 mutation, MGMT activity-deficient) (10.1111/jnc.14262) was obtained from American Type Culture Collection (ATCC, Manassas, VA, USA) and cultured in Dulbecco's Modified Eagle's Medium (DMEM) with 10% FBS (Gibco, Dreieich, Germany) under standard cell culture conditions (37 °C and 5% CO₂). The RSL3 (Sigma, Munich, Germany) was dissolved in dimethyl sulfoxide (DMSO) at a 10 mmol/L stock concentration and stored at –20 °C.

2.2. Cell Viability Assay

The LN229 cells were seeded in 96-well plates (5000 cells/well). Treatments were performed at different concentrations for 24 h, and the controls received 0.5% DMSO only. The proportion of viable cells was determined by 3-(4,5-dimethylthiazol-2-yl)-2,5-diphenyltetrazolium bromide (MTT, Sigma, Munich, Germany) assays following the manufacturer's recommendations. Absorbance was examined by an Infinite F200 pro Microplate Absorbance Reader (Tecan, Maennedorf, Switzerland).

2.3. Cell Migration Assay

Three thousand cells were cultured without serum for 24 h and then seeded onto a transwell chamber, which was subsequently placed in a 24-well plate for an additional 24 h. Following the incubation period, the cells on the bottom side of the chamber were stained with crystal violet to visualize and quantify cell attachment and migration. A total of five photographs were taken for each transwell chamber, capturing different areas of the

cells on the bottom side. The images were then used to count and analyze the number of cells in each photograph. This allowed for a comprehensive assessment of the cells' behavior and distribution under the specified experimental conditions.

2.4. Lipid Peroxidation Assay

Cells were seeded on the cover slides and treated 24 h before performing the lipid peroxidation assays. The cells were stained with BODIPY[®] 581/591 C11-Reagens (Thermo Fisher, Bremen, Germany) for 30 min and washed with PBS. The cells were either fixed by 30% PFA to perform fluorescence imaging or trypsinized into single cells to perform fluorescence-activated cell sorting (FACS). The FACS parameters were set according to the BODIPY[®] 581/591 C11-Reagens kit's guidance, and each group had 20,000 cells that went through the flow cytometer. The compensation was set as follows: FL1 −0.8% FL2; FL2 −29.8% FL1; FL2 −0.0% FL3; FL3 −19.3% FL2; FL3 −0.0% FL4; and FL4 −16.4% FL3. The FACS fluorescence images were taken using a Zeiss LSM780 fluorescence microscope (Zeiss, Munich, Germany) and analyzed using Image J software version 1.53k (National Institutes of Health, Bethesda, MD, USA). The FACS results were analyzed by FlowJo version 10.4 (FlowJo Inc., Ashland, OH, USA).

2.5. Oil Red O Staining Assay

The Oil Red O stain (1320-06-5, Sigma, Munich, Germany) was pre-prepared 10 min before the experiments. Cells were seeded into a 6-well plate for 24 h and received Oil Red staining for 1 min, and they were subsequently washed with 60% isopropanol for 15 s. Images were taken with a Nikon microscope (Melville, NY, USA).

2.6. RNA Isolation and Rt-PCR Assay

The RNA samples were isolated using Trizol Reagent (15596026, ThermoFisher, Waltham, MA, USA) and chloroform and subsequently purified by isopropanol and cleaned with 70% ethanol. The purified RNA was eluted in nuclease-free water. The RT-PCR assay utilized the following materials: the total RNA extracted from the LN229 parental and TMZ-resistant cell lines, and the reverse transcription was completed using a Takara reverse transcription kit (RR037B, Takara, Saint-Germain-en-Laye, France). The ALDH1A3 forward primer (CACCTTCCACGGCCCCGTTAGCGG) and reverse primer (AAACC-CGCTAACGGGGCCGTGGAA) were prepared for target amplification. A real-time PCR master mix (RR066A, Takara, Saint-Germain-en-Laye, France) was used and it contained all the necessary components for the PCR amplification. B-actin (Fw: GAGCTACGAGCT-GCCTGACG, Rev: GTAGTTTCGTGGATGCCACAGGAC) was used as the control. The instrument used for amplification and data analysis was a Zytomed.

2.7. Western Blotting

The cells were lysed in RIPA buffer with phosphatase inhibitors (5 mM sodium orthovanadate), and the protein lysates were separated using 10% SDS-PAGE and transferred onto a PVDF membrane. The membrane was blocked in 5% BSA and subsequently incubated with primary antibodies at 4 °C overnight. After washing three times, each for 5 min, in Tris-buffered saline containing 1% Tween-20 (TBST), the membrane was then incubated with peroxidase-conjugated goat anti-rabbit IgG (7074P2, CST, Leiden, Germany) and visualized using a super ECL detection reagent (GERPN2106, sigma, Munich, Germany). The anti-ALDH1A3 (1:2000, Rabbit polyclonal,) was obtained from Abcam (ab129815, Berlin, Germany), and the anti-p-AKT (#4060, 1:3000, Rabbit monoclonal) and anti-AKT (5112S, 1:3000, Rabbit) were obtained from Cell Signaling Technology (Leiden, Germany). Vinculin (abcam, ab129002) was used as the loading control. Quantification of the results was performed using ImageJ version 1.53k.

2.8. Colony Formation Assay

The LN229 glioblastoma cells were seeded in 10 cm dishes at a low density (500 cells per well) and incubated for 14 days. After the incubation period, the cells were washed with phosphate-buffered saline (PBS) and fixed with 4% paraformaldehyde for 15 min at room temperature. Following fixation, the cells were stained with crystal violet solution (0.5% crystal violet in 20% methanol) for 10 min. The excess stain was washed off with distilled water, and the plates were air-dried. Photos were taken with a smartphone (Lens: 26 mm; Pixel Pitch: 1.7 μm).

2.9. Cell Viability Assays

The LN229 cells were seeded in 96-well plates (5000 cells/well). Treatments were performed at different concentrations for 24 h, and the controls received 0.5% DMSO only. The proportion of viable cells was determined using a 3-(4,5-dimethylthiazol-2-yl)-2,5-diphenyltetrazolium bromide (MTT, Sigma, Munich, Germany) assay following the manufacturer's recommendations. Absorbance was examined by an Infinite F200 pro Microplate Absorbance Reader (Tecan, Maennedorf, Switzerland).

2.10. Statistical Analysis

Three independent experiments for each assay were conducted to validate the results. T-tests were used for the normally distributed data from the two unpaired groups. GraphPad Prism 8 (GraphPad Software Inc.; San Diego, CA, USA) was used to perform the analysis, and p -values of <0.05 were regarded as statistically significant.

3. Results

3.1. TMZ Long-Term Treated LN229 Cells

Ten clones of the LN229 cells were treated with gradually increasing concentrations of TMZ. Briefly, the cells were treated with TMZ for five days, followed by three weeks in a standard medium. The TMZ concentration was raised from 100 μM to 500 μM per cycle (Figure 1A). Five cell lines (TMZ-R#1, #2, #4, #7, and #8) survived the procedure and developed resistance to TMZ treatment (Figure 1B), and they were used for further experiments. The long-term treatment with TMZ resulted in morphological changes, with a transition from spindle-shaped to oval-shaped cells with cytopodia (Figure 1C). Additionally, the TMZ-resistant cells exhibited the formation of transparent vacuole structures.

Further investigation of their functional characteristics revealed that the TMZ long-term-treated cells exhibited enhanced migratory activity (Figure 2A,B). However, the colony formation assays and cell viability tests conducted over a period of 96 h demonstrated that their proliferation decreased compared to the parental LN229 cells (Figure 2C,D).

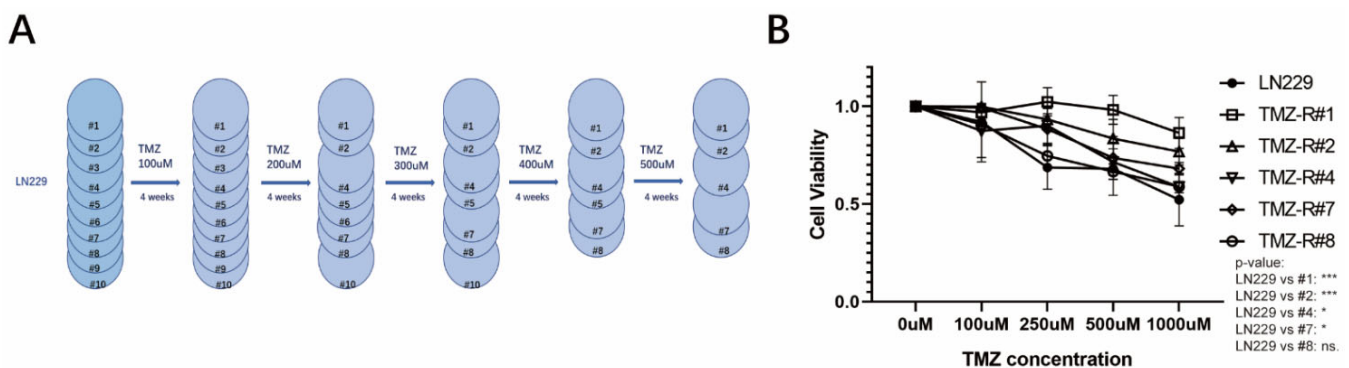


Figure 1. Cont.

C

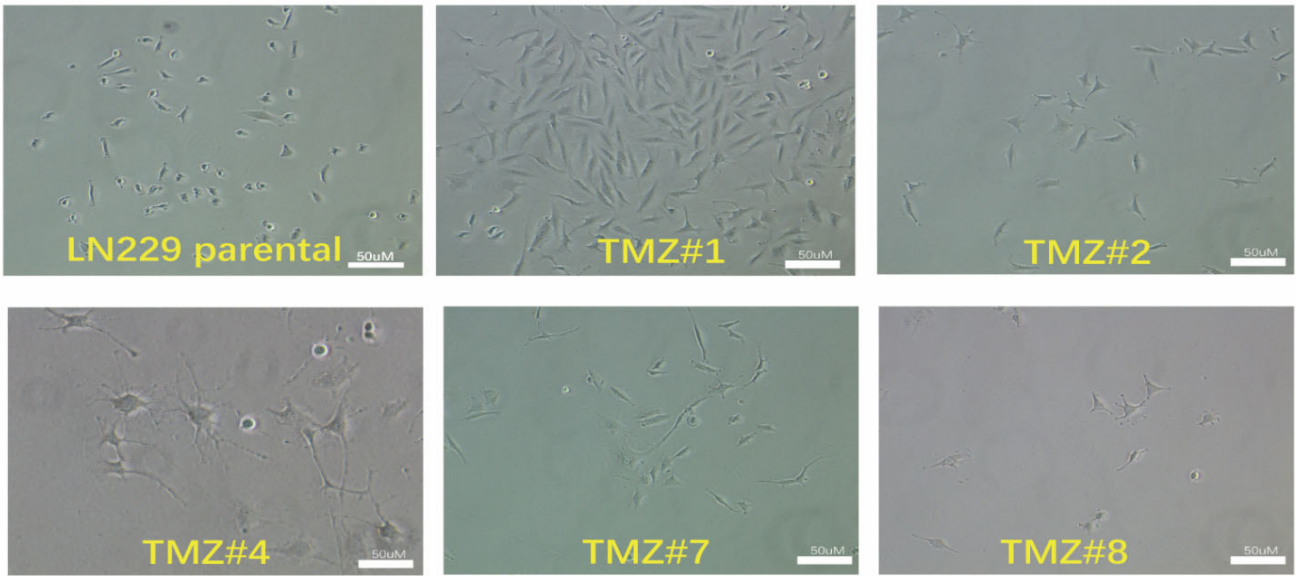


Figure 1. (A) The construction of the TMZ-resistant LN229 clones. (B) The cell viabilities of the LN229 cells and the five LN229 TMZ-resistant clones under increasing dosages of TMZ (100 µM, 250 µM, 500 µM, and 1000 µM) (* $p < 0.05$ and *** $p < 0.001$). (C) The cell morphologies of the LN229 cells and the five LN229 TMZ-resistant clones after 6 months of TMZ treatment.

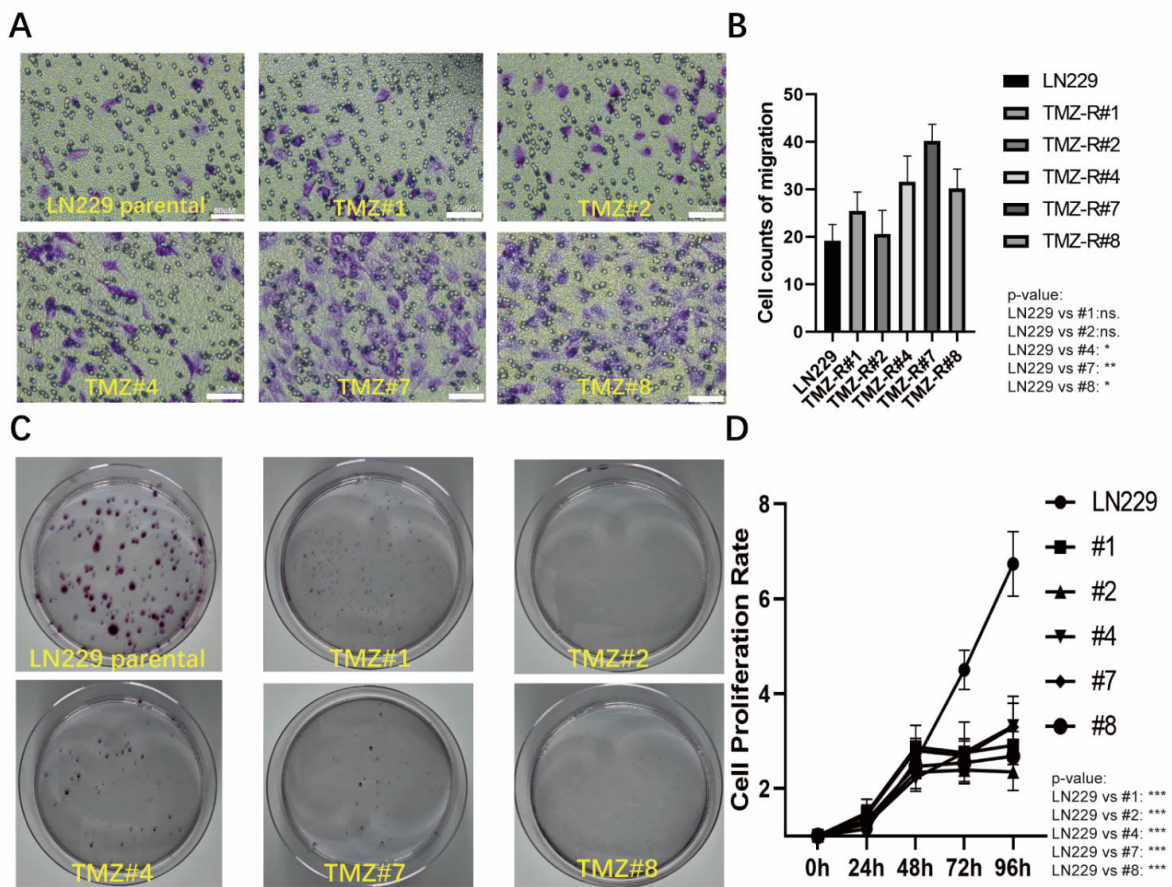


Figure 2. (A) The LN229 cells and the five LN229 TMZ-resistant clones were seeded into a Transwell chamber for the migration assay, and the cells on the bottom of chamber that were stained by the

crystal violet were considered to be migrated cells. (B) Quantification of A (* $p < 0.05$, ** $p < 0.01$, and *** $p < 0.001$). (C) Clone formation assay of the LN229 cells and the five LN229 TMZ-resistant clones under a normal medium (without TMZ). (D) Cell proliferation rates of the LN229 cells and the five clones (TMZ #1, TMZ #2, TMZ #4, TMZ #7, and TMZ #8) after 24 h, 48 h, 72 h, and 96 h, as measured by the MTT assay (* $p < 0.05$, ** $p < 0.01$, and *** $p < 0.001$).

3.2. The TMZ Long-Term Treated Cells Formed Higher Amounts of Lipid Droplets and Showed Elevated Lipid Peroxidation but Did Not Respond to RSL3-Induced Ferroptosis

Previously, we observed that TMZ treatment led to the accumulation of reactive oxygen species (ROS), indicating a potential therapeutic target for triggering ferroptosis. Building on this finding, we investigated lipid metabolism and lipid peroxidation in TMZ-resistant cell lines in further detail. Oil Red O staining of the TMZ long-term treated cells revealed a significant increase in the accumulation of lipid droplets as the cause for the cytoplasmic vacuoles in these cells (Figure 3A). To further investigate the lipid peroxidation (LPO) state in the TMZ long-term treated cells, we stained the cells with BODIPY 581/591 dye. The BODIPY staining results indicated that long-term TMZ treatment induced a higher level of LPO compared to the parental LN229 cells (Figure 3B,C). When we treated the cells with the ferroptosis inducer RSL3, the parental LN229 cells showed a pronounced ferroptotic response, whereas all the TMZ long-term treated cells did not show ferroptosis (Figure 3D). Using Western blotting analysis, we next verified the ALDH1a3 in the TMZ long-term treated cells and found a down-regulation of the protein compared with the parental LN229 cells (Figure 3E).

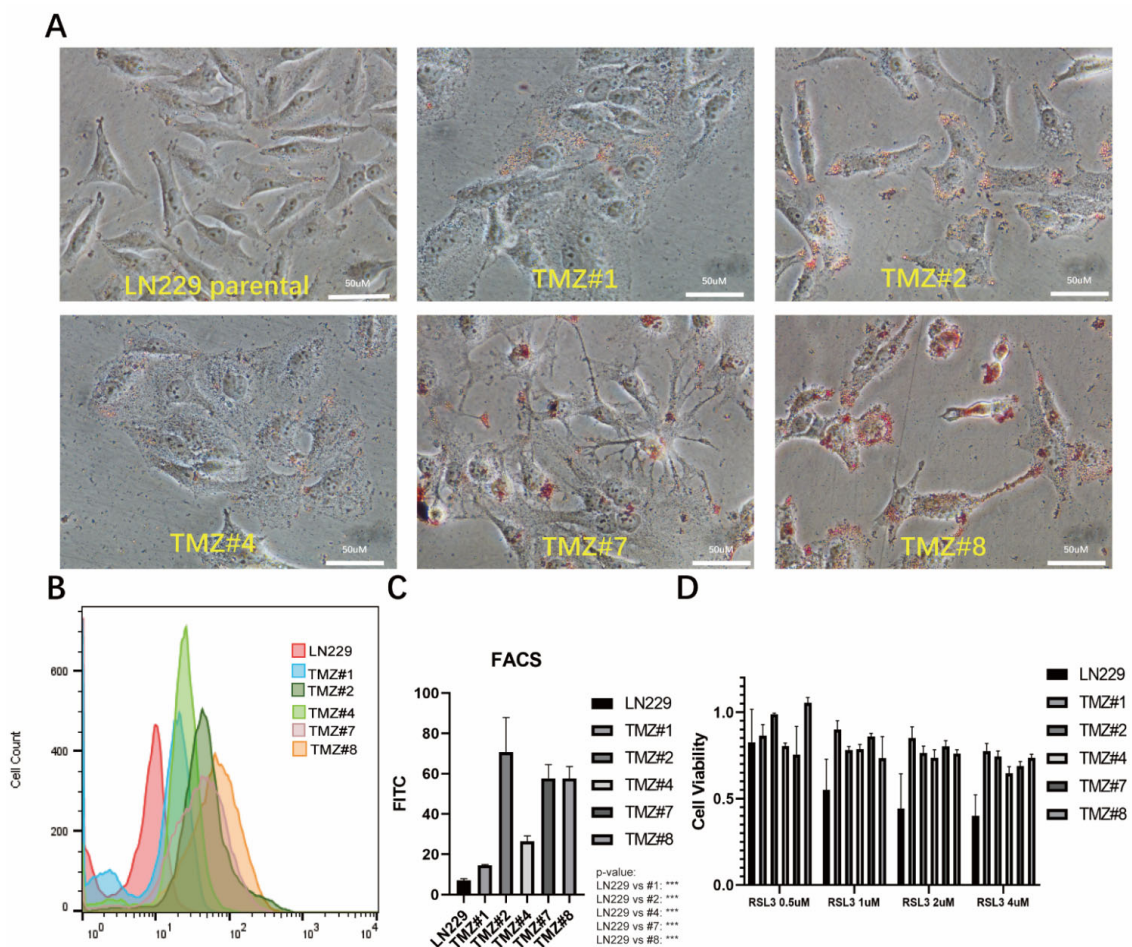


Figure 3. Cont.

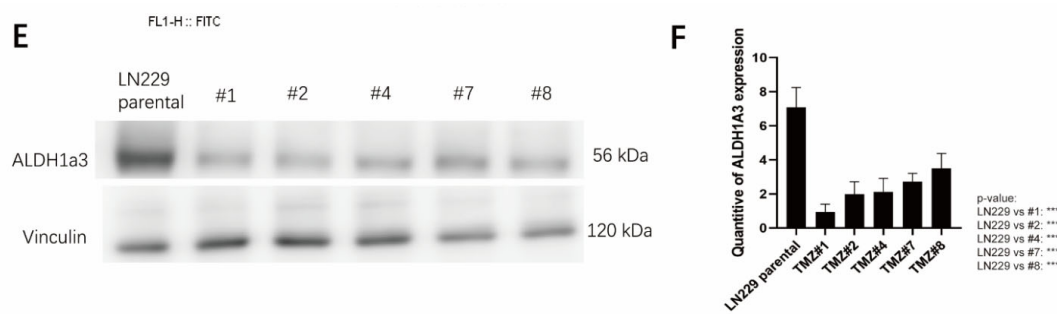


Figure 3. (A) The LN229 cells and the five LN229 TMZ-resistant clones were stained by Oil red O under a normal medium (TMZ removed before the cell seeding). After Oil Red O staining, the images showed bright red coloration in the lipid droplets. The lipid droplets were uniformly distributed and exhibited well-defined round shapes. (B) The BODIPY staining in the LN229 cells and the five LN229 TMZ-resistant clones as analyzed by FACS. X axis, density of fluorescence; Y axis, cell count of the fluorescent cells. (C) Quantification of B. (D) The cell viabilities of the LN229 cells and the five LN229 TMZ-resistant clones under the RSL3 treatments (0.5 uM, 1 uM, 2 uM, and 4 uM) (*p*-value: LN229 vs. TMZ #1, #2, #4, #7, and #8 in 4 uM: (***) $p < 0.001$). (E) The protein expression of ALDH1a3 in the LN229 cells and the five LN229 TMZ-resistant clones as analyzed by Western blotting. (F) Quantification of E, measured and analyzed using ImageJ version 1.53k. (***) $p < 0.001$.

3.3. TMZ Withdrawal Recovered ALDH1A3 Expression and Sensitivity to RSL3

After removal of the TMZ, the presence of the lipid droplets remained stable in all the TMZ long-term treated cells (Figure 4A). However, using Western blotting analysis, two out of the five clones (#4 and #8) showed re-expression of the ALDH1A3 protein (Figure 4B) that had been transcriptionally upregulated since the TMZ withdrawal (Figure 4C). Only these two clones also exhibited a reversal of the sensitivity to RSL3 (Figure 4D).

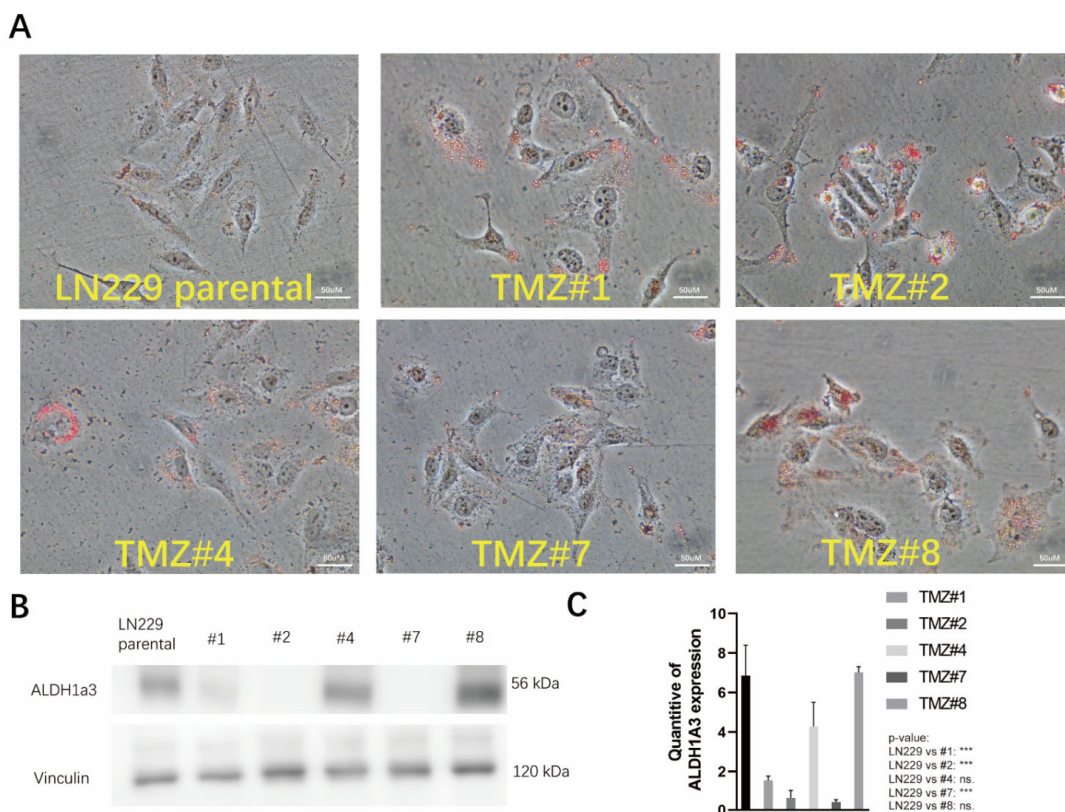


Figure 4. Cont.

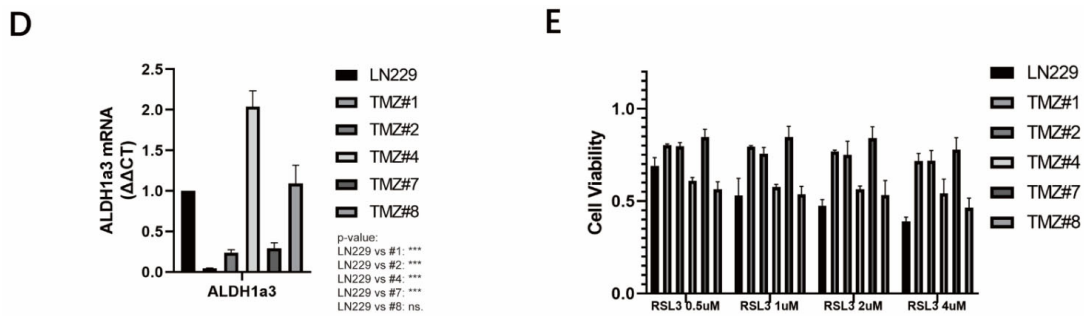


Figure 4. (A) After one-month of TMZ withdrawal, the LN229 cells and the five LN229 TMZ-resistant clones were stained with Oil red O. After Oil Red O staining, the images showed bright red coloration in the lipid droplets. (B) Protein expression of ALDH1a3 in the LN229 cells and the five LN229 TMZ-resistant clones after TMZ withdrawal, as analyzed by Western blotting. (C) Quantification of B, measured and analyzed using ImageJ version 1.53k (** $p < 0.001$). (D) Quantification of the ALDH1a3 mRNA in the LN229 cells and the five LN229 TMZ-resistant clones after TMZ withdrawal, as analyzed by RT-PCR (p -value: LN229 vs. TMZ #1, #2, and #7: ***, LN229 vs TMZ #4: *** (** $p < 0.001$)). (E) Cell viabilities of the LN229 cells and the five LN229 TMZ-resistant clones under the RSL3 treatments after TMZ withdrawal (0.5 uM, 1 uM, 2 uM, and 4 uM) (p -value: LN229 vs. TMZ #1, #2, and #7: *** (** $p < 0.001$)).

3.4. ALDH1A3 and Sensitivity to RSL3 Are Regulated by EGFR-Dependent Akt-Activation

We observed a down-regulation of Akt-phosphorylation in the TMZ long-term treated cells (Figure 5A). After TMZ withdrawal, Akt was phosphorylated, but only in two of the clones (#4 and #8) (Figure 5B) that exhibited ALDH1A3 re-expression and RSL3 sensitivity after TMZ removal. To learn more about the upstream regulation of ALDH1A3, the parental LN229 cells as well as the #4 and #8 cells were treated with and without AG1478, a specific EGFR tyrosine kinase inhibitor. With the AG1478 treatment, both Akt phosphorylation and ALDH1A3 expression were inhibited in the LN229 cells, as well as the #4 and #8 cells (Figure 5C), and ALDH1A3 was regulated at the transcriptional level (Figure 5D).

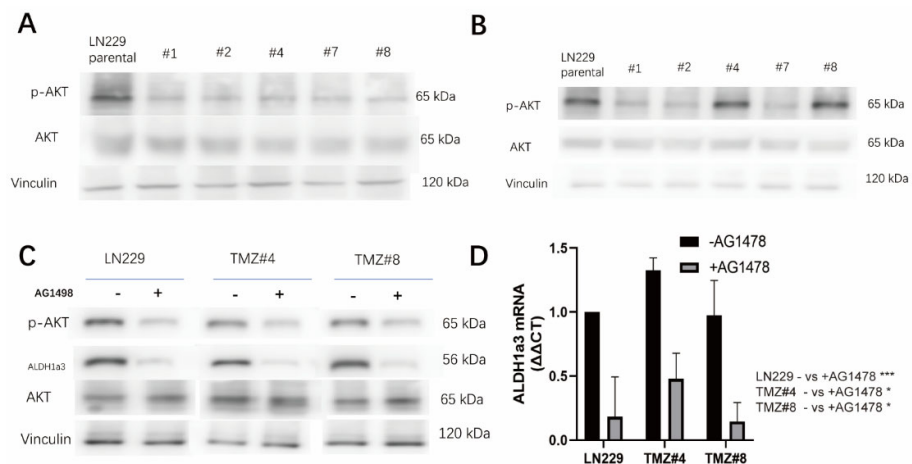


Figure 5. (A) The phosphorylation state of AKT in the LN229 cells and the five LN229 TMZ-resistant clones under the TMZ culture medium, as analyzed by Western blotting. (B) The phosphorylation state of AKT in the LN229 cells and the five LN229 TMZ-resistant clones after TMZ withdrawal, as analyzed by Western blotting. (C) The phosphorylation state of AKT and the protein expression of ALDH1a3 in the LN229 cells and the five LN229 TMZ-resistant clones after TMZ withdrawal, with/without AG1498 treatment, as analyzed by Western blotting. (D) Quantification of the ALDH1a3 mRNA in the LN229 cells and in the TMZ #4 and TMZ #8 cells with/without AG1478, as analyzed by RT-PCR (p -value: LN229: *, TMZ #4: *, and TMZ #8: * ($p < 0.05$ and *** $p < 0.001$)).

4. Discussion

Glioblastoma (GBM) is one of the most lethal brain tumors, with limited treatment approaches. Temozolomide (TMZ) is commonly used in the standard therapy for GBM, but its efficacy is often transient due to the development of resistance. A majority of patients experience recurrent GBM growth within two years [1]. Consequently, there is an urgent need to explore new treatment strategies to overcome therapy resistance.

Previously, we demonstrated that ALDH1a3 enhanced TMZ resistance in GBM and that this process was dependent on autophagy [10]. At the same time, we showed that ALDH1A3 sensitizes GBM cells to autophagy-dependent ferroptosis [19]. We could also show that ALDH1A3 and the ferroptosis elements were upregulated in relapsed GBMs [11]. By targeting the ALDH1A3-mediated autophagy-dependent ferroptosis pathway, we might be able to develop innovative and effective treatments to combat the therapy resistance in this devastating disease.

The aim of the present study was to investigate the potential of using the ferroptosis inducer RSL3 to generate ferroptotic cell death in GBM cells that were resistant to TMZ. Therefore, we generated several LN229 cell clones that were resistant to TMZ. Surprisingly, these TMZ-resistant LN229 clones also showed resistance to ferroptosis induction even though lipid peroxidation was evident. Upon further investigation, we identified the downregulation of the ALDH1a3 gene in the TMZ-resistant LN229 clones. Remarkably, when ALDH1A3 was up-regulated, these clones became re-sensitized to ferroptosis as induced by RSL3. Notably, this phenomenon appeared to be regulated by the EGFR-dependent PI3K pathway since the phosphorylation of Akt was EGFR-dependent and up-regulated specifically in the ALDH1a3-high clones.

Our previous results showed that ALDH1A3 is highly expressed in GBM cells, leading to resistance against TMZ treatment, but it is degraded by TMZ-induced autophagy [10]. Additionally, we observed that TMZ treatment induced the accumulation of reactive oxygen species (ROS) in GBM cells [8]. However, the expression of ALDH1A3 sensitized the GBM cells to ferroptosis, and this process required autophagy [19]. Therefore, the expression of ALDH1A3 appeared to be a key target in the crosstalk between TMZ-treatment and the induction ferroptosis in GBM. Here, we further proved that ALDH1A3 played an important role in therapy resistance and presented a new therapy approach to GBM. We showed that TMZ-resistant clones with low ALDH1A3 expression were resistant to RSL3, despite the presence of LDs and ROS accumulation. Furthermore, we could also demonstrate that when the expression of ALDH1A3 was reversed, the LDs accumulated TMZ-resistant clones and became sensitive to RSL3. These findings revealed the possibility of inducing ferroptosis in relapsed GBMs.

In GBM, the presence of lipid droplets (LDs) has been found to be closely linked to prognosis and treatment outcomes. Feng Gend et al. [20] demonstrated that LDs are highly accumulated in GBM cells but not in normal brain tissues or low-grade gliomas. GBM cells appear to utilize LDs to store excess fatty acids and cholesterol, thereby protecting themselves from lipotoxicity and endoplasmic reticulum (ER) stress. Furthermore, it has been shown that oxidative stress can induce the accumulation of LDs [21]. These results indicated that the TMZ treatment induced LD formation in GBM, and it potentially could be a therapy target for the ferroptosis inducer RSL3. However, our TMZ-resistant clones showed resistance to RSL3, which could be attributed to the significant role of LDs in cancer cells. These LDs act as scavengers for reactive oxygen species (ROS), offering protection to cancer cells against oxidative-stress-induced damage [22]. This protective mechanism enables cancer cells to survive and resist the oxidative stress induced by therapeutic treatments. These findings could indicate an alternative mechanism to explain RSL3 resistance in TMZ-resistant clones.

In our previous results, a five-day TMZ treatment suppressed the expression of ALDH1A3, followed by a rebound to higher levels after TMZ withdrawal. In this study, a similar pattern emerged, with ALDH1A3 expression being suppressed following TMZ treatment, and notably, two out of five TMZ-resistant cell lines showed a substantial re-

covery of ALDH1A3 expression within one month of TMZ withdrawal. These findings indicated that the recovery of ALDH1A3 could depend on the duration of TMZ withdrawal. During prolonged TMZ exposure, there is a drastic reduction in cell numbers, leading to the survival of TMZ-resistant clones through selective single-cell-like proliferation. In this case, the intrinsic heterogeneity within glioblastoma cells was a crucial consideration as it could have significantly impacted the experimental reproducibility and the interpretation of our results. Therefore, acknowledging the existence of heterogeneity is imperative when drawing conclusions from our findings.

Interestingly, we observed a correlation between the EGFR pathway activation and the recovered expression of ALDH1A3. Two ALDH1A3-recovered, TMZ-resistant clones exhibited activated Akt signaling, and the expression of ALDH1A3 could be down-regulated by EGFR-inhibition using the highly specific EGFR pathway inhibitor AG1478. The EGFR pathway promotes cell proliferation and metastasis and drives tumor recurrence. Aberrant EGFR signaling, often caused by overexpression, gene mutations, or amplification, is frequently observed in various cancer types, including GBM. The EGFR pathway exhibits abnormal activation in approximately 30% of glioblastoma patients, and it is associated with poor prognosis and tumor invasion. A study conducted by Nobuharu Inaba revealed that inhibiting the EGFR pathway led to a deceleration in cell proliferation and did not enhance sensitivity to TMZ treatment [23]. Gong et al. provided evidence that EGFR deficiency is associated with chemotherapy resistance in glioblastoma [24]. These studies support our findings, suggesting that the EGFR pathway may indeed be suppressed in TMZ-resistant cell lines. Moreover, phosphorylated AKT triggers the production of nitric oxide (NO), thus mediating cell proliferation, migration, ROS metabolism, and therapy resistance [25]. Additionally, based on our previous results, we found ALDH1A3 to be highly expressed in relapsed GBM, further supporting its role in tumor recurrence. These compelling findings collectively suggest a hidden connection between an activated EGFR pathway and ALDH1A3 expression in relapsed GBM, making them potential targets for ferroptosis. However, due to our limited findings, confirming EGFR's regulation of ALDH1A3 at the transcriptional level remains challenging. Additional experiments are necessary to unravel the underlying mechanism linking an activated EGFR pathway and the regulation of ALDH1A3. Targeting these pathways could offer a novel therapeutic strategy to combat treatment-resistant and recurrent GBM. Further research and exploration of these pathways might lead to the development of innovative therapies aimed at improving outcomes for patients with recurrent GBM.

In conclusion, our study sheds light on the complex interplay between lipid metabolism, ALDH1A3 expression, and TMZ resistance in glioblastoma. Nevertheless, our findings were constrained by the *in vitro* experiments conducted in an established cell line and the limited insights. Further investigations are essential for exploring the hidden mechanisms related to manipulating the EGFR pathway, therapy resistance, and the induction of ferroptosis in glioblastoma. Understanding these mechanisms may lead to the development of novel therapeutic strategies to overcome TMZ resistance and improve treatment outcomes in relapsed glioblastoma patients.

Author Contributions: Conceptualization, Y.W. and J.S.; investigation, Y.W.; methodology, Y.W. and S.F.; project administration, J.S.; supervision, F.L.-S. and J.S.; writing—review and editing, Y.W., J.S., S.F. and F.L.-S. All authors have read and agreed to the published version of the manuscript.

Funding: This research received no external funding.

Institutional Review Board Statement: Not applicable.

Informed Consent Statement: Not applicable.

Data Availability Statement: There's no sharing data.

Acknowledgments: The authors are thankful to Sandra Baur for her excellent technical support and to Gabriele Multhoff and Fei Wang for offering the use of the FACS.

Conflicts of Interest: The authors declare no conflict of interest.

References

1. Ostrom, Q.T.; Patil, N.; Cioffi, G.; Waite, K.; Kruchko, C.; Barnholtz-Sloan, J.S. CBTRUS Statistical Report: Primary Brain and Other Central Nervous System Tumors Diagnosed in the United States in 2013–2017. *Neuro Oncol.* **2020**, *22* (Suppl. S2), iv1–iv96. [[CrossRef](#)] [[PubMed](#)]
2. Rodriguez-Camacho, A.; Flores-Vazquez, J.G.; Moscardini-Martelli, J.; Torres-Rios, J.A.; Olmos-Guzman, A.; Ortiz-Arce, C.S.; Cid-Sanchez, D.R.; Perez, S.R.; Macias-Gonzalez, M.D.S.; Hernandez-Sanchez, L.C.; et al. Glioblastoma Treatment: State-of-the-Art and Future Perspectives. *Int. J. Mol. Sci.* **2022**, *23*, 7207. [[CrossRef](#)] [[PubMed](#)]
3. Kitange, G.J.; Carlson, B.L.; Schroeder, M.A.; Grogan, P.T.; Lamont, J.D.; Decker, P.A.; Wu, W.; James, C.D.; Sarkaria, J.N. Induction of MGMT expression is associated with temozolomide resistance in glioblastoma xenografts. *Neuro Oncol.* **2009**, *11*, 281–291. [[CrossRef](#)] [[PubMed](#)]
4. Wu, W.; Klockow, J.L.; Zhang, M.; Lafortune, F.; Chang, E.; Jin, L.; Wu, Y.; Daldrop-Link, H.E. Glioblastoma multiforme (GBM): An overview of current therapies and mechanisms of resistance. *Pharmacol. Res.* **2021**, *171*, 105780. [[CrossRef](#)] [[PubMed](#)]
5. Chien, C.H.; Hsueh, W.T.; Chuang, J.Y.; Chang, K.Y. Dissecting the mechanism of temozolomide resistance and its association with the regulatory roles of intracellular reactive oxygen species in glioblastoma. *J. Biomed. Sci.* **2021**, *28*, 18. [[CrossRef](#)] [[PubMed](#)]
6. Song, Q.; Peng, S.; Sun, Z.; Heng, X.; Zhu, X. Temozolomide Drives Ferroptosis via a DMT1-Dependent Pathway in Glioblastoma Cells. *Yonsei Med. J.* **2021**, *62*, 843–849. [[CrossRef](#)] [[PubMed](#)]
7. Dixon, S.J.; Lemberg, K.M.; Lamprecht, M.R.; Skouta, R.; Zaitsev, E.M.; Gleason, C.E.; Patel, D.N.; Bauer, A.J.; Cantley, A.M.; Yang, W.S.; et al. Ferroptosis: An iron-dependent form of nonapoptotic cell death. *Cell* **2012**, *149*, 1060–1072. [[CrossRef](#)] [[PubMed](#)]
8. Wu, W.; Wu, Y.; Mayer, K.; von Rosenstiel, C.; Schecker, J.; Baur, S.; Wurstle, S.; Liesche-Starnecker, F.; Gempt, J.; Schlegel, J. Lipid Peroxidation Plays an Important Role in Chemotherapeutic Effects of Temozolomide and the Development of Therapy Resistance in Human Glioblastoma. *Transl. Oncol.* **2020**, *13*, 100748. [[CrossRef](#)]
9. McLean, M.E.; MacLean, M.R.; Cahill, H.F.; Arun, R.P.; Walker, O.L.; Wasson, M.D.; Fernando, W.; Venkatesh, J.; Marcato, P. The Expanding Role of Cancer Stem Cell Marker ALDH1A3 in Cancer and Beyond. *Cancers* **2023**, *15*, 492. [[CrossRef](#)]
10. Wu, W.; Schecker, J.; Wurstle, S.; Schneider, F.; Schonfelder, M.; Schlegel, J. Aldehyde dehydrogenase 1A3 (ALDH1A3) is regulated by autophagy in human glioblastoma cells. *Cancer Lett.* **2018**, *417*, 112–123. [[CrossRef](#)]
11. Kram, H.; Prokop, G.; Haller, B.; Gempt, J.; Wu, Y.; Schmidt-Graf, F.; Schlegel, J.; Conrad, M.; Liesche-Starnecker, F. Glioblastoma Relapses Show Increased Markers of Vulnerability to Ferroptosis. *Front. Oncol.* **2022**, *12*, 841418. [[CrossRef](#)] [[PubMed](#)]
12. Rasper, M.; Schafer, A.; Piontek, G.; Teufel, J.; Brockhoff, G.; Ringel, F.; Heindl, S.; Zimmer, C.; Schlegel, J. Aldehyde dehydrogenase 1 positive glioblastoma cells show brain tumor stem cell capacity. *Neuro Oncol.* **2010**, *12*, 1024–1033. [[CrossRef](#)] [[PubMed](#)]
13. Corominas-Faja, B.; Oliveras-Ferraros, C.; Cuyas, E.; Segura-Carretero, A.; Joven, J.; Martin-Castillo, B.; Barrajon-Catalan, E.; Micol, V.; Bosch-Barrera, J.; Menendez, J.A. Stem cell-like ALDH(bright) cellular states in EGFR-mutant non-small cell lung cancer: A novel mechanism of acquired resistance to erlotinib targetable with the natural polyphenol silibinin. *Cell Cycle.* **2013**, *12*, 3390–3404. [[CrossRef](#)] [[PubMed](#)]
14. Canino, C.; Luo, Y.; Marcato, P.; Blandino, G.; Pass, H.I.; Cioce, M. A STAT3-NFkB/DDIT3/CEBPbeta axis modulates ALDH1A3 expression in chemoresistant cell subpopulations. *Oncotarget* **2015**, *6*, 12637–12653. [[CrossRef](#)] [[PubMed](#)]
15. Cheng, P.; Wang, J.; Waghmare, I.; Sartini, S.; Coviello, V.; Zhang, Z.; Kim, S.H.; Mohyeldin, A.; Pavlyukov, M.S.; Minata, M.; et al. FOXD1-ALDH1A3 Signaling Is a Determinant for the Self-Renewal and Tumorigenicity of Mesenchymal Glioma Stem Cells. *Cancer Res.* **2016**, *76*, 7219–7230. [[CrossRef](#)] [[PubMed](#)]
16. Lang, T.; Xu, J.; Zhou, L.; Zhang, Z.; Ma, X.; Gu, J.; Liu, J.; Li, Y.; Ding, D.; Qiu, J. Disruption of KDM4C-ALDH1A3 feed-forward loop inhibits stemness, tumorigenesis and chemoresistance of gastric cancer stem cells. *Signal Transduct. Target. Ther.* **2021**, *6*, 336. [[CrossRef](#)] [[PubMed](#)]
17. Pan, M.; Li, M.; You, C.; Zhao, F.; Guo, M.; Xu, H.; Li, L.; Wang, L.; Dou, J. Inhibition of breast cancer growth via miR-7 suppressing ALDH1A3 activity concomitant with decreasing breast cancer stem cell subpopulation. *J. Cell Physiol.* **2020**, *235*, 1405–1416. [[CrossRef](#)] [[PubMed](#)]
18. Ayuso-Sacido, A.; Moliterno, J.A.; Kratovac, S.; Kapoor, G.S.; O'Rourke, D.M.; Holland, E.C.; Garcia-Verdugo, J.M.; Roy, N.S.; Boockvar, J.A. Activated EGFR signaling increases proliferation, survival, and migration and blocks neuronal differentiation in post-natal neural stem cells. *J. Neurooncol.* **2010**, *97*, 323–337. [[CrossRef](#)]
19. Wu, Y.; Kram, H.; Gempt, J.; Liesche-Starnecker, F.; Wu, W.; Schlegel, J. ALDH1-Mediated Autophagy Sensitizes Glioblastoma Cells to Ferroptosis. *Cells* **2022**, *11*, 4015. [[CrossRef](#)]
20. Geng, F.; Cheng, X.; Wu, X.; Yoo, J.Y.; Cheng, C.; Guo, J.Y.; Mo, X.; Ru, P.; Hurwitz, B.; Kim, S.H.; et al. Inhibition of SOAT1 Suppresses Glioblastoma Growth via Blocking SREBP-1-Mediated Lipogenesis. *Clin. Cancer Res.* **2016**, *22*, 5337–5348. [[CrossRef](#)]
21. Lee, J.; Homma, T.; Kurahashi, T.; Kang, E.S.; Fujii, J. Oxidative stress triggers lipid droplet accumulation in primary cultured hepatocytes by activating fatty acid synthesis. *Biochem. Biophys. Res. Commun.* **2015**, *464*, 229–235. [[CrossRef](#)]
22. Jarc, E.; Kump, A.; Malavasic, P.; Eichmann, T.O.; Zimmermann, R.; Petan, T. Lipid droplets induced by secreted phospholipase A(2) and unsaturated fatty acids protect breast cancer cells from nutrient and lipotoxic stress. *Biochim. Biophys. Acta Mol. Cell Biol. Lipids.* **2018**, *1863*, 247–265. [[CrossRef](#)]

23. Inaba, N.; Fujioka, K.; Saito, H.; Kimura, M.; Ikeda, K.; Inoue, Y.; Ishizawa, S.; Manome, Y. Down-regulation of EGFR prolonged cell growth of glioma but did not increase the sensitivity to temozolomide. *Anticancer. Res.* **2011**, *31*, 3253–3257.
24. Gong, L.; Yin, Y.; Chen, C.; Wan, Q.; Xia, D.; Wang, M.; Pu, Z.; Zhang, B.; Zou, J. Characterization of EGFR-reprogrammable temozolomide-resistant cells in a model of glioblastoma. *Cell Death Discov.* **2022**, *8*, 438. [[CrossRef](#)]
25. Thomas, D.D.; Ridnour, L.A.; Isenberg, J.S.; Flores-Santana, W.; Switzer, C.H.; Donzelli, S.; Hussain, P.; Vecoli, C.; Paolucci, N.; Ams, S.; et al. The chemical biology of nitric oxide: Implications in cellular signaling. *Free Radic. Biol. Med.* **2008**, *45*, 18–31. [[CrossRef](#)] [[PubMed](#)]

Disclaimer/Publisher’s Note: The statements, opinions and data contained in all publications are solely those of the individual author(s) and contributor(s) and not of MDPI and/or the editor(s). MDPI and/or the editor(s) disclaim responsibility for any injury to people or property resulting from any ideas, methods, instructions or products referred to in the content.